Faculdade de Ciências e Tecnologia

Universidade de Coimbra

A disease model to understand neural mechanisms of visual perception: Neurofibromatosis type-1

Estudo de um modelo dos mecanismos neurais envolvidos na discriminação e percepção de contraste: Neurofibromatose tipo-1

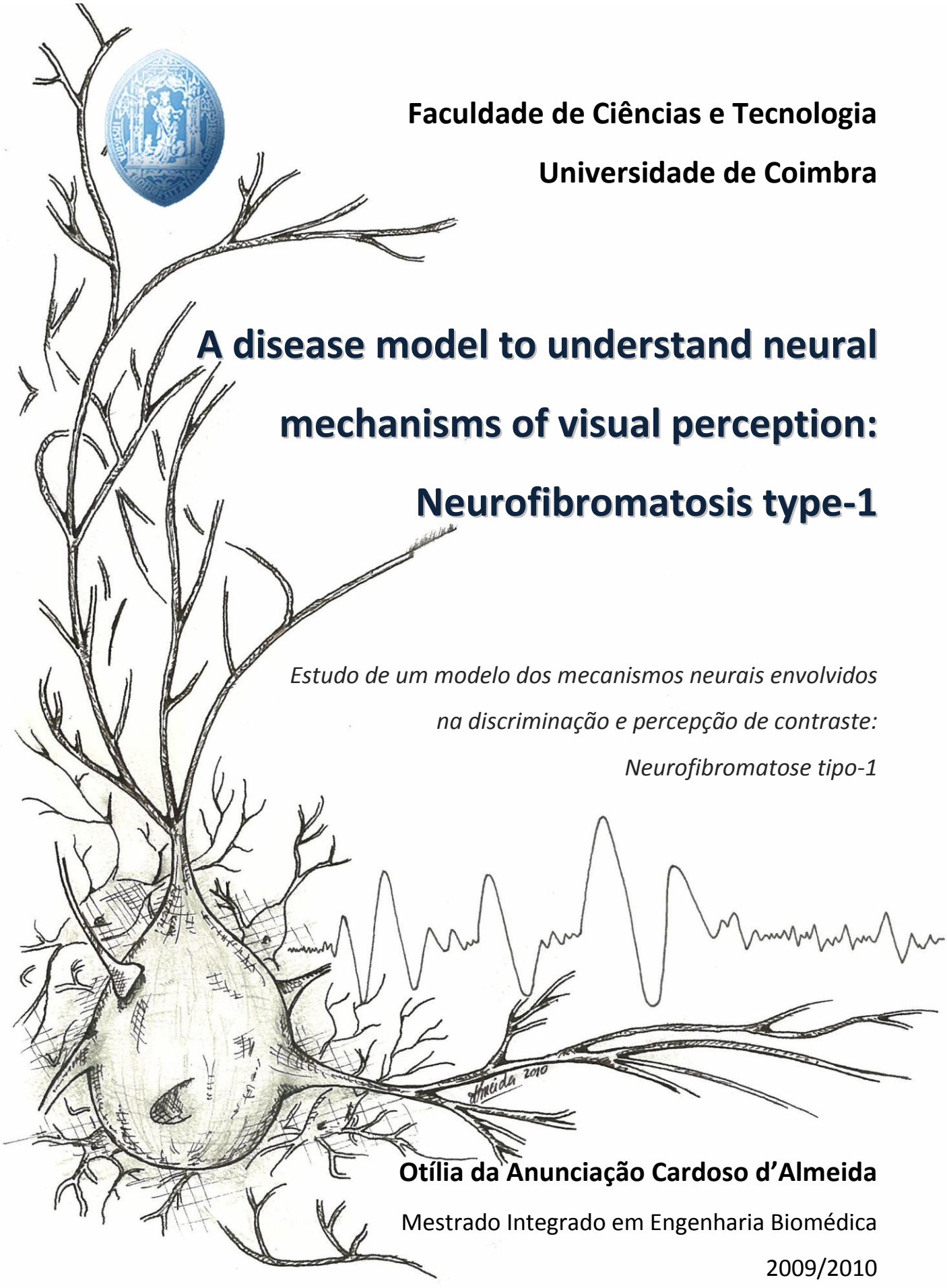

Otília da Anunciação Cardoso d'Almeida

Mestrado Integrado em Engenharia Biomédica

2009/2010

Faculdade de Ciências e Tecnologia

Universidade de Coimbra

A disease model to understand neural mechanisms of visual perception: Neurofibromatosis type-1

Estudo de um modelo dos mecanismos neurais envolvidos na discriminação e percepção de contraste: Neurofibromatose tipo-1

Otília da Anunciação Cardoso d'Almeida

Mestrado Integrado em Engenharia Biomédica

2009/2010

This dissertation is presented to the University of Coimbra with the purpose to conclude the Master Degree in Biomedical Engineering. All the work was done in IBILI – *Institute of Biomedical Research on Light and Image* –, Faculty of Medicine, University of Coimbra, with the scientific orientation of PhD Miguel Castelo-Branco, and PhD Maria Ribeiro.

THIS WORK CONTRIBUTED TO THE FOLLOWING PUBLISHED ABSTRACTS:

Ribeiro M. J., D'Almeida O. C., Duarte J. V. & Castelo-Branco M.

ABNORMALLY HIGH AMPLITUDE OF BRAIN OSCILLATIONS IN A NEURODEVELOPMENTAL DISORDER CHARACTERIZED BY ENHANCED GABAERGIC TRANSMISSION: NEUROFIBROMATOSIS TYPE 1

Accepted for poster presentation at 16th Annual Meeting of the Organization for Human Brain Mapping (June 6-10, 2010 in Barcelona, Spain)

Ribeiro M. J., D'Almeida O. C., Duarte J. V. & Castelo-Branco M.

ABNORMAL BRAIN OSCILLATIONS MIGHT UNDERLIE DEFICITS IN VISUAL ATTENTION AND MOTOR CONTROL, IN NEUROFIBROMATOSIS TYPE 1

Accepted for oral presentation at 14th Annual European Neurofibromatosis Meeting (September 9-12, 2010 in Oslo, Norway)

"The task of neural science is to explain behavior in terms of the activities of the brain. How does the brain marshal its millions of individual nerve cells to produce behavior, and how are these cells influenced by the environment...? The last frontier of the biological sciences – their ultimate challenge – is to understand the biological basis of consciousness and the mental process by which we perceive, act, learn, and remember."

Eric Kandel
(Kandel et al., 2000)

ACKNOWLEDGEMENTS

Ao Professor Dr. Miguel Castelo-Branco, pelo seu rigor científico e pelos conhecimentos transmitidos no mundo das Neurociências.

À Dr.ª Maria Ribeiro, pela supervisão do meu trabalho ao longo de todo o projecto, pelas discussões construtivas e pelo trabalho que desenvolvemos em equipa.

Ao Professor Miguel Morgado, pelo seu empenho e dedicação em promover os Engenheiros Biomédicos.

A todas as crianças e adolescentes que participaram neste projecto, e aos seus educadores, sem os quais este estudo não seria possível. Obrigada pela sua disponibilidade e colaboração.

Aos meus colegas do IBILI, que tão calorosamente me acolheram no seu grupo de trabalho. Pelo seu apoio, pelo convívio e bom ambiente criados.

Às meninas do Lar Nossa Senhora de Fátima e às Irmãs que me acolheram com ternura há 5 anos atrás. Pelos momentos divertidos, de alegria e pelo ambiente de companheirismo.

Aos meus grandes e bons amigos, pela sua lealdade e boa disposição.

Àqueles amigos especiais que me apoiaram incessantemente, especialmente neste ano mais marcante e laborioso, pela sua paciência nos momentos mais críticos, pelo seu incentivo e carinho. Pelos verdadeiros laços de amizade criados e por toda a força que me deram.

À minha família, pela sua preocupação, atenção e afecto. Em especial, aos meus queridos avós, os meus anjos-da-guarda, por me darem um exemplo de vida e me ensinarem desde pequena o sentido da responsabilidade, do trabalho e da luta.

Ao meu traquinas, o meu irmão Manuel que, apesar de me 'desencaminhar' para a brincadeira, sempre torceu pelo meu sucesso. Pelo seu carinho e energia pura e sadia. Obrigada por me fazeres sorrir!

Aos meus pais, Elisa e José Carlos, a minha fonte de inspiração e modelo de vida. Pelo apoio aos meus sonhos e aspirações, pelo amor, dedicação, ensinamentos e valores transmitidos. Obrigada por tudo o que são e por tudo o que fizeram por mim!

A todos, um sincero obrigada,

_____

(Otília da Anunciação Cardoso d'Almeida)

ABSTRACT

The present study aimed to investigate the physiological basis of the visual deficits associated with Neurofibromatosis type 1 (NF1). To achieve this goal, we used electrophysiological (using EEG/ERP (Electroencephalography/Event Related Potentials) techniques) and psychophysical techniques (visuo-motor task).

NF1 is one of the most common autosomal genetic disorders (prevalence rate of about 1 in 3500). NF1 patients have a variable clinical phenotype. Some of the physical characteristics of NF1 individuals include *café-au-lait* spots in the skin, macrocephaly and bone deformities. Furthermore, they are more prone to develop tumours, mainly neurofibromas and optic gliomas, and to show cognitive deficits. The cognitive deficits are characterized by learning, visuospatial, attentional, motor and language impairments. The visuospatial deficit has long been considered a hallmark feature of the disorder, especially in which concerns the Judgement of Line Orientation test. Interestingly, visuospatial performance represents a strong predictor of NF1 diagnosis, and there may be linkages between the deficits in visuospatial domains and the cognitive and language impairments in NF1. In addition, low-level visual impairments have also been described in NF1. In particular, NF1 individuals show decreased contrast sensitivity.

This disorder is caused by mutations in the NF1 gene that encodes a protein called neurofibromin, highly expressed all over the nervous system. The impairment of neurofibromin function prevents the inhibition of Ras (a protein subfamily of small GTPases that are involved in cellular signal transduction). Ras over-activation leads to an enhancement of the release of GABA (*γ-aminobutyric acid*), the canonical inhibitory neurotransmitter of the nervous system. Therefore, if over-released, GABA promotes enhanced inhibition of synapse function which may account for the visuospatial deficits and impaired sensitivity to visual contrast as well as the learning and other cognitive deficits seen in these patients. However, evidence that this mechanism identified in the animal model can be generalized to the human disorder is lacking.

This study focused on the visual deficits related to NF1, with the aim of determining if an excess of inhibition can explain the visual deficits of these patients. It is known that a balance between excitatory and inhibitory neurotransmission establishes the centre-surround antagonism in the receptive fields of visual neurons. Centre-surround antagonism ensures visual neurons responses to contrast. Indeed, pharmacological studies with the administration of lorazepam, a drug that enhances GABAergic transmission, showed that visual perception is affected, including alteration of contrast sensitivity, visual integration and visual binding.

EEG can provide significant information about the basis of the cognitive impairments on children. One great advantage is the capacity of providing precise temporal information of brain

activity. In this work, we measured the EEG responses in NF1 children and controls during visual stimulation and a simultaneous visuo-motor task to try to determine if the amplitude and latency of occipital VEPs (Visual Evoked Potentials) elicited by the visual stimuli were altered in NF1 children. At the cortical level, the detection and discrimination of low-level visual features like contrast involves early visual areas that receive input by three parallel processing pathways, magno-, parvo- and koniocellular, each one contributing differently to visual processing. The strength of the surround inhibition of the receptive fields of these pathways is significantly different and therefore alterations in GABAergic neurotransmission might alter them differently. In this study, we investigated the activation of these pathways separately.

We also performed a frequency domain analysis especially focused on the alpha rhythm. Alpha rhythm (8-13 Hz) has been related to conditions of physical relaxation and diminished mental activity. The amplitude of the alpha rhythm is related to thalamic GABAergic neurotransmission and therefore, might be affected in NF1 patients.

Unexpectedly, NF1 children showed VEPs with higher amplitude than controls. This difference was particularly significant for the koniocellular pathway. Furthermore, the amplitude of the evoked alpha oscillations was significantly higher in patients, for all tested pathways, suggesting a neural correlate for the visual deficits observed in these patients. High alpha might indicate enhanced inhibitory transmission supporting therefore the inhibition hypothesis. Alpha oscillations are known to be blocked or attenuated when the individual is paying attention, especially within the visual domain, thus abnormally high alpha in NF1 children might be associated to attention deficits.

Keywords: visual evoked potentials, inhibition, neurofibromatosis type 1, visual cortex, alpha rythms, time frequency analysis

RESUMO

Este estudo visou investigar as bases fisiológicas subjacentes aos défices visuais associados à Neurofibromatose tipo 1 (NF1, do inglês *Neurofibromatosis type 1*). Para atingir este objectivo, utilizamos técnicas electrofisiológicas (de EEG/ERP (EEG, do inglês *electroencephalography*; VEP, do inglês *Visual Evoked Potential*)) e psicofísicas (tarefa visuo-motora).

NF1 é uma das doenças genéticas autossómicas mais comuns (com taxa de prevalência de cerca de 1 em 3500). Os doentes com NF1 têm um fenótipo clínico variável. Algumas das características físicas dos indivíduos com NF1 incluem manchas *café-au-lait* na pele, macrocefalia e deformações dos ossos. Além disso, são mais susceptíveis a desenvolver tumores, principalmente neurofibromas e gliomas ópticos, e a apresentar défices cognitivos. Os défices cognitivos são caracterizados por défices de aprendizagem, visuoespaciais, de atenção, motores e de linguagem. Os problemas visuoespaciais têm sido considerados, desde há muito tempo, uma marca característica da doença, especialmente os défices observados no teste de *Judgement of Line Orientation* (JLO). Curiosamente, o desempenho visuoespacial representa um forte indicador do diagnóstico de NF1, e podem existir ligações entre os défices nos domínios visuoespaciais e os problemas cognitivos e de linguagem na NF1. Além disso, também foram descritos problemas visuais de baixo nível na NF1. Em particular, os indivíduos com NF1 têm sensibilidade ao contraste diminuída.

Este distúrbio é provocado por mutações no gene NF1 que codifica neurofibromina, expressa de forma ampla em todo o sistema nervoso. A diminuição da função da neurofibromina impede a inibição da Ras (uma subfamília de proteínas de pequenas GTPases que estão envolvidas na transdução de sinal a nível celular). A sobre-activação da Ras leva a um aumento da libertação de GABA (GABA, do inglês *γ-aminobutyric acid*), o neurotransmissor inibitório do sistema nervoso, por excelência. Portanto, se for libertado em excesso, o GABA promove o aumento da inibição da função sináptica, que pode influenciar nos défices visuoespaciais e na diminuição da sensibilidade ao contraste visual, bem como na aprendizagem e noutros défices cognitivos observados nestes doentes. Contudo, não está claro que este mecanismo, identificado no modelo animal, possa ser generalizado ao distúrbio nos humanos.

Este estudo focou-se nos défices visuais relacionados com a NF1, com o objectivo de determinar se um excesso de inibição pode explicar os défices visuais nestes doentes. Sabe-se que um balanço entre a neurotransmissão excitatória e inibitória estabelece o antagonismo centro-periferia nos campos receptores dos neurónios visuais. O antagonismo centro-periferia assegura a resposta dos neurónios visuais ao contraste. De facto, estudos farmacológicos com a administração de *lorazepam*, um fármaco que aumenta a transmissão GABAérgica, mostraram que a percepção visual é afectada, incluindo a alteração da sensibilidade ao contraste, integração e associação de elementos visuais.

A electroencefalografia pode fornecer informações significativas sobre as bases dos problemas cognitivos nas crianças. Uma grande vantagem é a capacidade em fornecer informações temporais precisas sobre a actividade cerebral. Neste trabalho, medimos as respostas do EEG em crianças com NF1 e em controlos durante a estimulação visual e, simultaneamente, efectuou-se uma tarefa visuo-motora para tentar determinar se a amplitude e latência dos VEPs occipitais, evocados pelos estímulos visuais estavam alterados nas crianças com NF1. A nível cortical, a detecção e discriminação de características visuais de baixo nível como o contraste, envolve áreas visuais primárias que recebem *input* de três vias de processamento paralelas, magno-, parvo- e coniocelular, cada uma contribuindo de modo diferente para o processamento visual. A força da inibição da componente periférica dos campos receptores destas vias é significativamente diferente e, portanto, as alterações na neurotransmissão GABAérgica poderão alterá-las de modo diferente. Neste estudo, investigamos a activação destas vias separadamente.

Também efectuámos a análise no domínio das frequências especialmente focada nas ondas alfa. As ondas alfa (8-13Hz) têm sido associadas a estados de relaxamento físico e a diminuição da actividade mental. A amplitude das ondas alfa está relacionada com a neurotransmissão talâmica GABAérgica e logo, poderá estar afectada nos doentes com NF1.

Inesperadamente, crianças com NF1 mostram VEPs com maior amplitude que os controlos. Esta diferença foi particularmente significativa na via coniocelular. Além disso, a amplitude das oscilações do alfa evocado foi significativamente maior nos pacientes, para todas as vias testadas, sugerindo uma correlação neuronal para os défices visuais observados nestes pacientes. Alfa elevado pode indicar transmissão inibitória aumentada apoiando, portanto, a hipótese de inibição. As oscilações do alfa são conhecidas por serem bloqueadas ou atenuadas quando o indivíduo presta atenção, especialmente dentro do domínio visual, pelo que alfa anormalmente elevado nas crianças NF1 poderá estar associado a défices de atenção.

Palavras-chave: potenciais evocados visuais, inibição, neurofibromatose tipo 1, córtex visual, ondas alfa, análise tempo-frequência

TABLE OF CONTENTS

ABBREVIATIONS

CNT - Control

cpd – cycles per degree

CRF – Contrast Response Function

CRT – Cathode Ray Tube

EEG – Electroencephalography

ERP – Event Related Potential

GABA – γ-aminobutyric acid

IBILI – Institute of Biomedical Research on Light and Image

JLO – Judgement of Line Orientation

LDR – Linear Derivation

LGN – Lateral Geniculate Nucleus

NF1 – Neurofibromatosis type-1

SC – Superior colliculus

se – Standard error

SNR – Signal-to-noise ratio

V1 – Primary Visual Cortex

VEP – Visual Evoked Potential

LIST OF FIGURES

LIST OF TABLES

1. INTRODUCTION / STATE-OF-THE-ART

1.1. COGNITIVE DEFICITS IN NEUROFIBROMATOSIS TYPE-1

Neurofibromatosis type-1 or von Recklinghausen's neurofibromatosis is the most common autosomal dominant neurocutaneous disorder with a prevalence rate of approximately 1 in 3.000 to 4.000 individuals, regardless of age, gender, or ethnic background (Levine et al., 2006;NINDS, 2010;NINDS, 2010).

Although there are traces from the 13th century, only in 1882 it was considered as a distinct disorder when the German doctor Friedrich Daniel von Recklinghausen published his landmark paper "On the multiple neurofibromas of the skin and their relationship to the multiple neuromas" (translated from the German) (Boyd et al., 2009). NF1 is characterized by a wide variable phenotypic expression among individuals, even within a given family, associated to a very strong genetic component (Levine et al., 2006;Pinson, 2002). The wide phenotypic variability led to the establishment of diagnostic criteria by NIDs (*National Institute of Health*) (**TABLE 1**). Nevertheless some diagnostic criteria may not manifest until later in life, being less manifest in very young children, especially those under 8 years of age (Boyd et al., 2009). Individuals with NF1, in addition to having several manifestations as café-au-lait spots, primarily plexiform neurofibromas and bone deformities, also have a high incidence of macrocephaly, optic pathway gliomas, T2-weighted hyperintensities in brain MRI scans (UBOs), and learning deficits.

TABLE 1. NIDs diagnostic criteria for NF1. An individual is considered to have NF1 when two or more of the below criteria features are met[1] (Kumar, 2004;NINDS, 2010;Levine et al., 2006).

• Six or more light brown macules on the skin (called *"café-au-lait spots"*) over 5 mm in greatest diameter in prepubertal individuals and over 15 mm across in postpubertal individuals ;
• Two or more neurofibromas of any type or one plexiform neurofibroma;
• Freckling in the axillary or inguinal regions;
• Two or more growths on the iris of the eye (known as *Lisch nodules* or iris hamartomas);
• A tumor on the optic nerve (known as optic (nerve) glioma);
• A distinctive osseous lesion such as sphenoid dysplasia, or abnormal development of the spine (scoliosis) or the tibia (thinning of long bone cortex with or without pseudoarthrosis);
• A first-degree relative (parent, sibling or offspring) with NF1 by the above criteria.

Although many cases are inherited between 30 and 50 percent of new cases result from a spontaneous genetic mutation of unknown cause (Levine et al., 2006). NF1 is thought to arise from a mutation in a gene located on the long arm of chromosome 17 and that encodes neurofibromin, a

[1] However, these diagnostic criteria are not sufficient for establishing the presence of NF1 in small children without a family history of the disease (Kumar, 2004).

220 kDa protein, highly expressed in the nervous system (Daston et al., 1992). The NF1 gene has been classified as a tumour suppressor; mutations in the NF1 gene lead to abnormal cell growth and differentiation, causing the development of neurofibromas, benign tumours of the peripheral nervous system, as well as malignant peripheral nerve sheath tumours (Costa and Silva, 2002;Kumar, 2004;Cichowski and Jacks, 2001).

Besides the increased predisposition for tumours, NF1 is associated to cognitive deficits in both language and visuospatial domains, and behavioural problems, leading to poor academic achievements. Indeed, the latest publications showed that nearly 50% of NF1 children are impaired in at least one area of cognitive functioning, namely learning domains, visual perception, motor/visuo-motor areas, and memory deficits (Levine et al., 2006). Interestingly, in spite of incidence of mental retardation[2] being higher than the general population, the overall cognitive functioning of the NF1 children is within normal range (Hyman et al., 2005;Hachon et al., 2010). Importantly, the brain tumours may not be linked to the cognitive deficit since the cognitive function of these patients can be affected even in the absence of brain tumours. Regarding the learning deficits, NF1 patients tend to show impairments on basic reading and/or reading comprehension domains, and substantial deficits in mathematical computation and in tests of executive function (problem-solving behaviour) (Levine et al., 2006). Motor deficiencies in both simple and complex motor tasks and in coordination have also been reported in NF1 (Levine et al., 2006). The visuospatial deficits have been taken as a hallmark feature of the cognitive profile of NF1 individuals. In particular, a high percentage of patients perform below average in the Judgment of Line Orientation[3] (Levine et al., 2006;Clements-Stephens et al., 2008;Hachon et al., 2010). Indeed, (Schrimsher et al., 2003) proved that visuospatial performance can be taken as a strong predictor of NF1 diagnosis. In their work, they performed a multivariate approach combining four visuospatial/motor tests that showed a particular pattern of performance on visuospatial measures in children with NF1. This strategy correctly identifyed nearly 90% of children and adolescents with NF1. Attention-Deficit Hyperactivity Disorder (ADHD) is other prevalent characteristic of the NF1 population, present in roughly 50% of NF1 individuals, suggesting that this may be linked to the NF1 phenotype (Levine et al., 2006). So, the presence of either factors, ADHD and visuospatial deficits, may be important contributing factors allied to the development of the cognitive/learning problems on NF1 children.

[2] The expression “mental retardation” is here defined as a full-scale IQ less than 70 on the Wechsler scale)

[3] Judgement of Line Orientation (JLO) Test is a relatively pure measure of visuospatial perception, analysis, and judgement. It evaluates visual-spatial skills by assessing the ability to judge the orientation and angles of lines in space (Mitrushina et al., 2005).

- ***Molecular basis of the behavioural and cognitive phenotype in NF1 disorder.***

The NF1 gene has been classified as a tumour suppressor factor. The protein coded by this gene, neurofibromin, contains a small conserved guanosine triphosphatase-activating (GTPase) domain that accelerates the inhibition of low molecular weight G proteins such as Ras, by stimulating their intrinsic GTPase activity (Cichowski and Jacks, 2001;Costa and Silva, 2002;Ho et al., 2007). Besides this function, neurofibromin has been shown to have a prominent role in the following biochemical functions, adenylate cyclase modulation, and microtubule binding, all them critical for neuronal physiology (Costa and Silva, 2002).

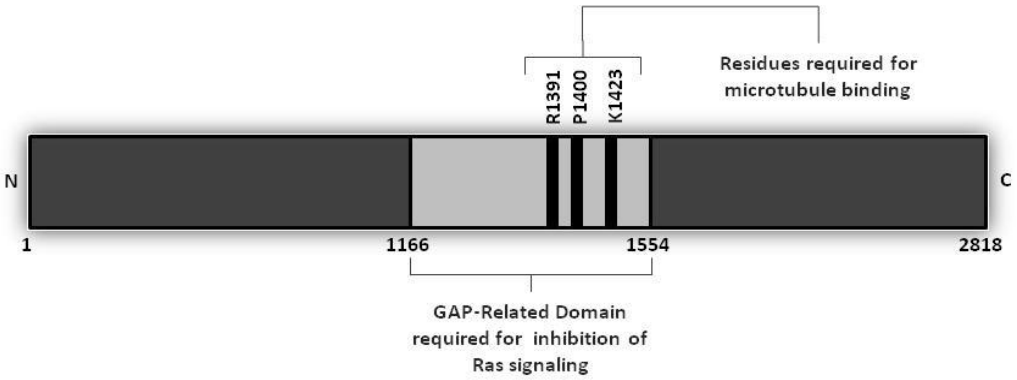

FIGURE 1. Schematic representation of the NF1 gene product, neurofibromin, depicting regions involved in Ras signalling pathway regulation, and residues required for proper microtubule binding.
(*Adapted from (Kumar, 2004)*).

Behavioural analysis on animal studies indicates that learning is disrupted in both *Drosophila* and mouse NF1 models. They suggest a link between the cognitive impairments observed and an increase of Ras activity due to a reduction in neurofibromin GAP activity. In a study with the fruit fly NF1 mutant, in addition to learning, it was verified the abolishment of long-term memory (LTM). Ho et al. (2007) showed that, when expressed in the fruit fly, human neurofibromin can rescue the learning and memory defects. Furthermore, in the same study, the GAP related domain was found to be important for long-term memory consolidation while a different domain in the C-terminal region was involved in immediate learning (Ho et al., 2007). Therefore, selective inactivation of different functional domains of this protein can cause different cognitive profiles. Consequently, when studying the cognitive function of these patients, the genotypic profile should be taken into account.

The mouse and human neurofibromins have 98% sequence similarity. Besides, not only there are similarities in the underlying mechanisms of tumourigenesis but also, in both species, NF1 mutations seem to impair similar brain functions such as visuospatial learning, attention and motor coordination (Costa and Silva, 2002). These evidences suggest that both biochemistry of the protein and the transcriptional regulation of the gene are conserved across species. Mice heterozygous for a

loss-of-function mutation in the NF1 gene display an impairment in a spatial memory task (Silva et al., 1997), suggesting a memory deficit associated with visuospatial perception. The deficits in spatial memory found in the mouse model of NF1, suggest hippocampal dysfunction. These mice show an up regulation of Ras and, consequently, present higher levels of GABA (**FIGURE 2**) that leads to over-inhibition. Indeed, NF1 mice have abnormally high levels of hippocampal neuronal inhibitory transmission and, as a consequence, impaired synaptic long-term potentiation (Costa et al., 2002). Surprisingly, genetic and pharmacological manipulations that decrease Ras function were found to reverse cognitive impairments in the NF1 heterozygotic mice (Costa et al., 2002). These findings imply that the behavioural deficiencies are more likely to be a consequence of a physiological defect rather than abnormal brain structure. These findings are particularly important for clinical investigation because they mean that the cognitive impairments can be treated.

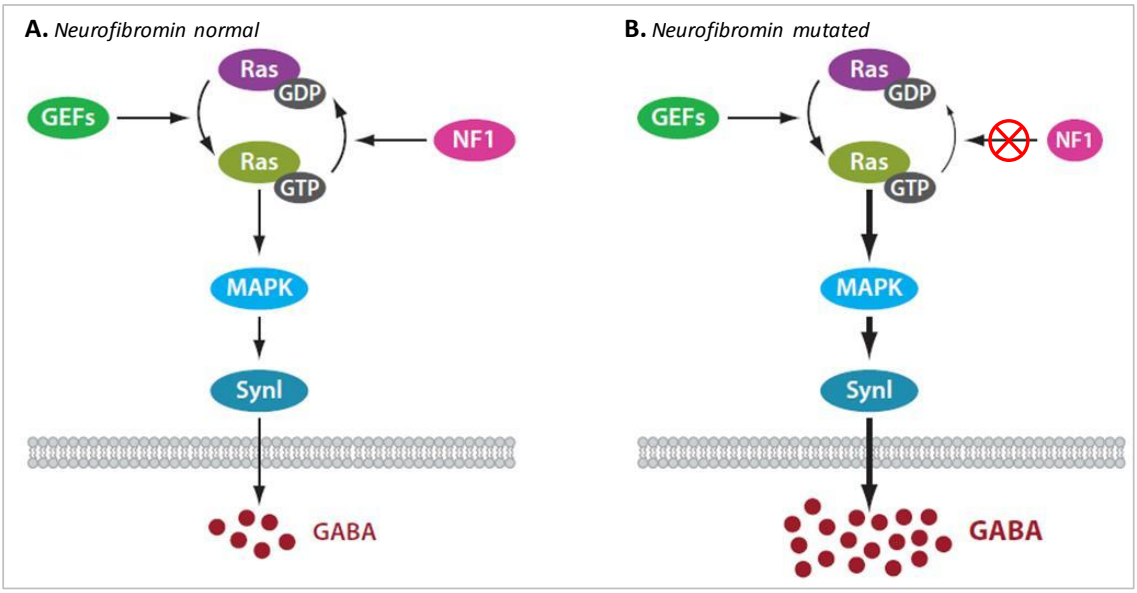

FIGURE 2. Proposed cellular mechanism underlying learning deficits of Nf1 mutant mice. (A) Learning triggers interneuronal Ras signaling leading to increased GABA release. (B) In Nf1 mutants, reduced NF1 activity leads to abnormal hyperactivation of Ras signaling in inhibitory interneurons during learning, resulting in abnormally high GABA release. This increased activity-dependent GABA release shifts the balance between excitatory and inhibitory processes in neural networks of the mutant mice and impairs synaptic plasticity needed for learning and memory.
(*Adapted from (Shilyansky et al., 2010)*).

1.2. FUNCTION AND ORGANIZATION OF RETINOCORTICAL PATHWAYS

Since we will be studying the visuospatial impairments in NF1 children, it is mandatory to know some aspects of the visual system machinery and how the visual information is processed.

- ***The brain as a coordinator of a multitude of signals and a neural network data integrator***

The visual cortex is a dynamic structure that receives local information from the visual image and integrates these signals into global percepts such as contours, surfaces, and three-dimensional shapes. There's growing evidence suggesting a meaningful role of the primary visual cortex (V1) on the integration process of all the visual features of the image (Kapadia et al., 2000).

Visual perception of low level features like contrast emerges from neuronal signals in early visual cortical areas (Boynton et al., 1999;Ress and Heeger, 2003). Importantly, the neuronal population responses are not determined by the knowledge of one single cell behaviour. Therefore, relating single cell activity to a population of cells is not straightforward. (Albrecht and Hamilton, 1982) measured the responses of 247 neurons from the striate cortex of monkey and cat as a function of contrast in order to describe and formulate the contrast response function (CRF). However, they realized that there's great variability from cell-to-cell, in which different cells respond over different ranges of contrast, enlarging the dynamic range of the CRF. As these authors reported in (Albrecht and Hamilton, 1982), *"Such range variation could be an important factor in behavioral contrast discrimination: in general, when considering the activation of a large population of cells, increasing the contrast of a grating produces an increase in both a) the overall number of action potentials produced as well as b) the overall number of cells responding."*.

- ***From the eye to the brain***

Visual processing begins in the retina and can be divided into two stages. First the light enters through the cornea, projecting onto the retina, on the back layer of the eye. There, the optic information is converted into an electric signal sent through the optic nerve to higher brain centres for further processing required to visual perception.

The axons of ganglion cells of the retina form the optic nerve that projects in an orderly way to four subcortical regions in the brain (**FIGURE 3.A**):

- The ***Lateral Geniculate Nucleus (LGN)*** – component of the thalamus, is the major subcortical center relaying visual information from both eyes to the primary visual cortex (**FIGURE 3.B**);
- The *superior colliculus* (SC) – controls eye movements;

- The *hypothalamus* – regulate the circadian rhythms;
- The *pretectum* – control the pupillary reflex.

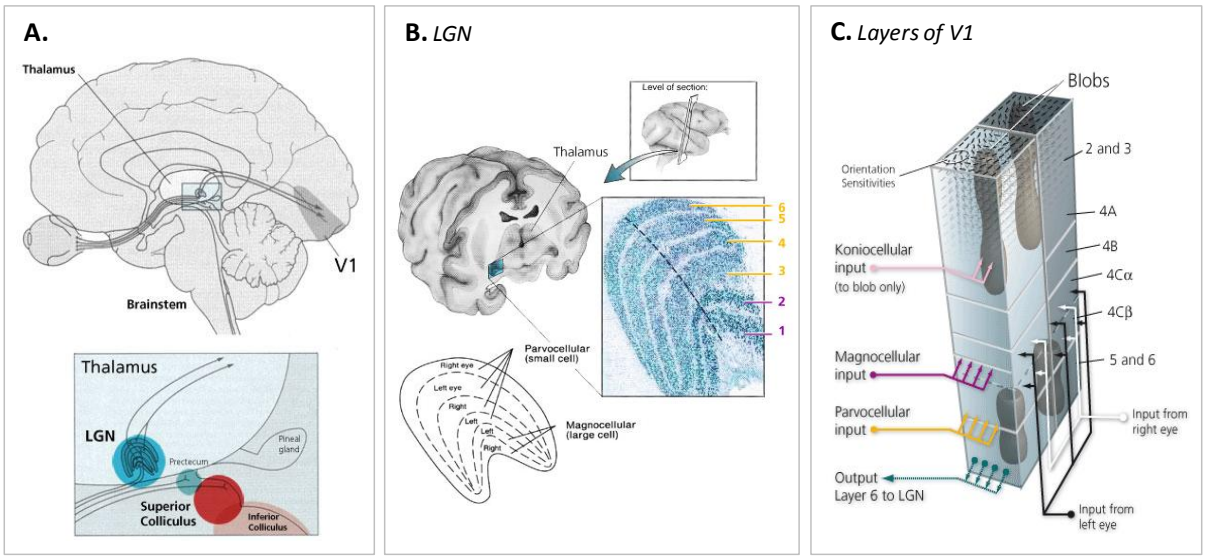

FIGURE 3. Organization of the retinocortical pathways (http://www.sharp-sighted.org/). **(A)** The light enters through the eye till the retina where patterns of light energy are converted into electric discharges – action potentials. These signals are conveyed along axons of retinal ganglion cells to mainly the LGN and the SC. Most of the output of the LGN are relayed directly to the Primary Visual Cortex (V1), and then to surrounding areas. **(B)** The LGN of the thalamus has a "knee-shaped" structure and it is built out of 6 layers. The LGN gets information from only 1 hemifield, but from 2 eyes and each layer receives inputs from only 1 eye. **(C)** V1 is divided into 6 layers which receive most visual input from the LGN from 3 parallel retinocortical pathways: parvocellular, koniocellular and magnocellular.

The LGN is the major target of the retinal ganglion cells. Regarding the circuitry retina-LGN-V1 (**FIGURE 3.A**), previous studies identified three principal types of relay cells: the parvocellular, the koniocellular and the magnocellular cells (**FIGURE 3.B**). These ganglion cells constitute the three major visual pathways that convey different types of visual attributes to V1 for further processing (**FIGURE 3.C**). These cells can be distinguished based on several criteria as laminar location, morphology, connections and neurochemistry (Xu et al., 2001) . The large ganglion cells (Alpha cells, in the cat) are phasic, i.e., transient and have fast conducting thick axons. They project to the magnocellular layers of the LGN. On the contrary, the small ganglion cells (Beta cells, in the cat) are tonic, i.e., sustained and have slow conducting axons. They project to the parvocellular layers of the LGN (Tobimatsu et al., 1995) (**FIGURE 3.B**). The smallest relay cells are, on average, the koniocellular cells of LGN that form thin layers lying below the magno- and parvocellular layers and constitute the koniocellular pathway that projects to V1 (Xu et al., 2001).

- ***Centre-surround antagonism of receptive fields ensures visual neurons respond to contrast; An alteration in inhibition predict changes in the perception of contrast***

One possible direction to take to inspect the excess of inhibition in NF1 individuals is by taking advantage of the well established role of inhibitory neurotransmission in visual processing.

The visual information projected onto the retina is conveyed to the ganglion cells. The axons of the ganglion cells form the optic nerve that transmits the information to the LGN as trains of action potentials. Each ganglion cell monitors a certain area of the retina, that in turn receives information from a certain region of the visual field, called the receptive field. The ganglion cell's receptive fields are circular areas divided into a central circular zone – the receptive field centre – and a peripheral area – the surround. There are two classes of ganglion cells, distinguished by their response to a small spot of light applied to the centre of their receptive field. The *ON-centre ganglion cells* (**FIGURE 4.A**) are excited when light falls directly on the centre of the receptive field. By contrast, *OFF-centre ganglion cells* (**FIGURE 4.B**) are inhibited by light applied to the centre of their receptive field. The stimulation of the centre of an *ON-centre ganglion cell* receptive field promotes depolarization and an increase in the firing of the ganglion cell, while the stimulation of the surround of the same cell promotes its hyperpolarization and a decrease in the firing of the cell. The opposite is verified for the *OFF-centre ganglion cells*. The stimulation of both the center and surround produces only a mild response, due to mutual stimulation/inhibition of centre and surround. Therefore the balance between the excitatory and inhibitory inputs dictates the neuronal firing frequency in response to the stimuli. The firing rate of the cells depends, thus, on the difference in stimulation of the centre and surround of the receptive fields, that is on the contrast of the stimulus (Kandel et al., 1995). The response to contrast is therefore dependent on the inhibitory inputs to visual neurons.

Indeed, previous studies with benzodiazepines[4] indicate an impairment of contrast sensitivity on the users, suggesting that this impairment is caused by the excess of the inhibitory transmission by GABA[5]. The intake of Midazolam (benzodiazepine), affected preferentially the parvocellular pathway, producing an overall decrease in visual sensitivity (Blin et al., 1993). Lorazepam (benzodiazepine), also alters contrast sensitivity both in healthy volunteers (Harris and Phillipson, 1995) and in long-term users (Giersch et al., 2006).

[4] Benzodiazepines are drugs that enhance the GABAergic effect (enhancement of inhibition).

[5] GABA (γ-Amino butyric acid) is the predominant inhibitory neurotransmitter in the mammalian brain (Whiting, 2006)

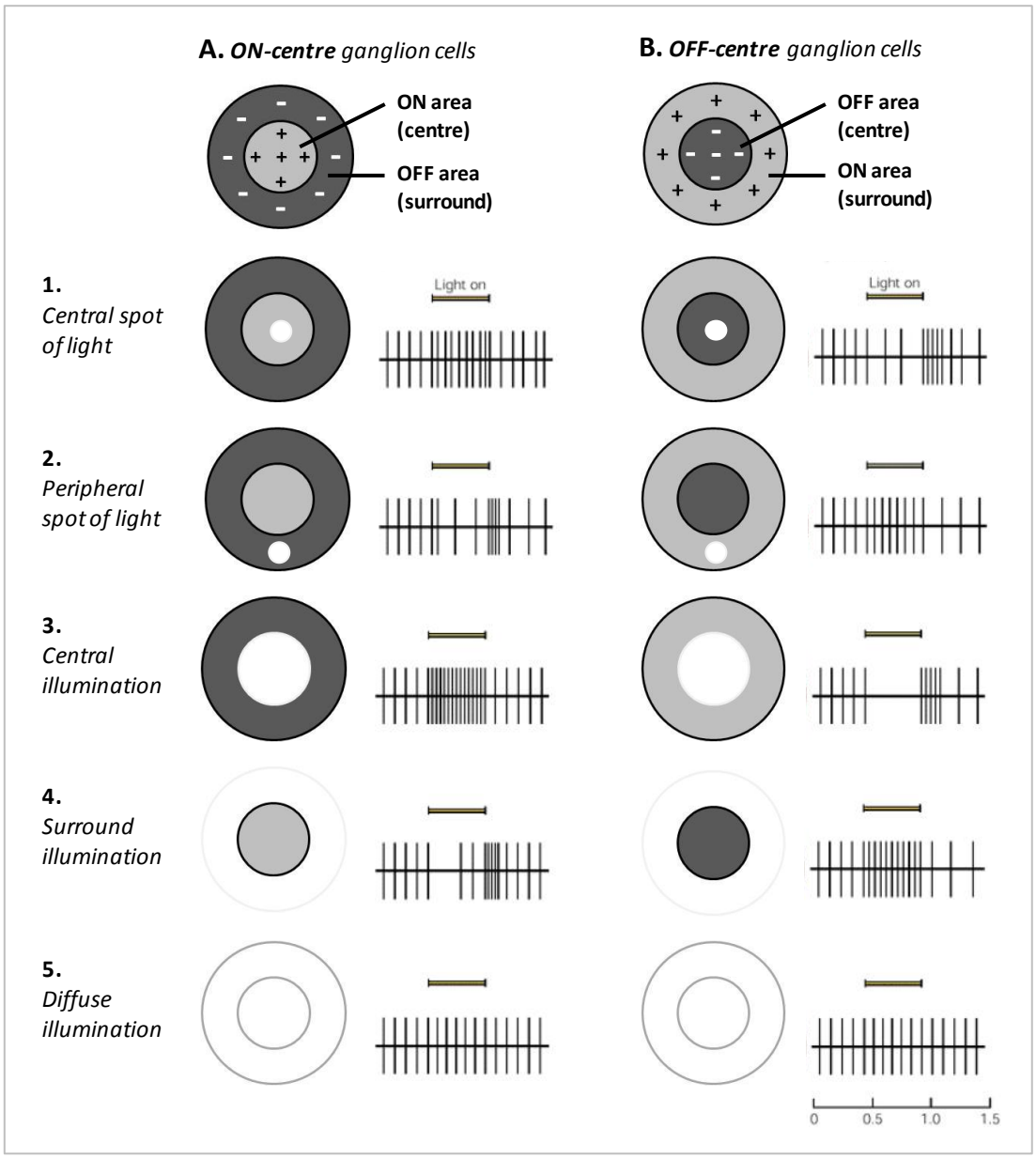

FIGURE 4. Retinal ganglion cells respond optimally to contrast in their receptive fields. Ganglion cells have circular receptive fields, with specialized center (light grey) and surround (dark gray) regions. On-center cells are excited when stimulated by light in the center and inhibited when stimulated in the surround; offcenter cells have the opposite responses. Both types of cells respond differently regarding the type of light stimuli (the stimulated portion of the receptive field is shown in white). The pattern of action potentials fired by the ganglion cell in response to each stimulus is also shown in extracellular recordings. Duration of illumination is indicated by a bar above each record. **(A)** On-center cells respond best when the entire central part of the receptive field is stimulated **(3)**. These cells also respond well, but less vigorously, when only a portion of the central field is stimulated by a spot of light **(1)**. Illumination of the surround with a spot of light **(2)** or ring of light **(4)** reduces or suppresses the cell firing, which resumes more vigorously for a short period after the light is turned off. Diffuse illumination of the entire receptive field **(5)** elicits a relatively weak discharge because the center and surround oppose each other's effects. **(B)** The spontaneous firing of off-center cells is suppressed when the central area of the receptive field is illuminated **(1, 3)** but accelerates for a short period after the stimulus is turned off. Light shone onto the surround of the receptive field excites the cell **(2, 4)**.
(*Adapted from (Kandel et al., 2000)*).

1.3. Relation between L, M, and S Cone response to the R, G, and B Incident Spectrum

Colour perception is only possible by the stimulation of three classes of light-sensitive cones in the retina: long-, middle- and short-wavelength-sensitive cones (referred to as L, M, and S cones, respectively), according to the selective sensitivity to the visible spectrum. The response of each class of cones to the incident light relies on the photon absorption rate of the cone pigment. Photons absorption may be computed via the spectral sensitivity of that class of cones. The LGN communicates to V1 by three visual streams responsible for the transmission of different properties of the visual input. These three streams are colour sensitive and are modulated selectively by cone-type activation. We aim to isolate and analyze separately these pathways. To establish the bridge between the stimulus and colour perception, we need to appeal to basic colorimetry techniques.

- ***Basic Colorimetry***

The main objective of colorimetry is to bind the properties of human colour vision into the measurement and numerical specification of visible light. The goal of the image processing is to obtain an image with the same colour appearance at each image location as the original. Thence, its crucial to understand how to represent the spectral properties of light, and the relationship between the colour camera, the monitor and how the human visual system encodes this spectral properties of light (Brainard and Stockman, 2010;Brainard and Stockman, 2010).

The Cathode Ray Tube (CRT) is basically a vacuum tube with an electron gun that sends streams of high speed electrons from a heated cathode into a fluorescent screen after deflection by a magnetic field. When an electron beam excites a phosphor coating at the front of the monitor, from each location on the monitor is emitted light. In a raster pattern, the electron beam quickly scans the monitor faceplate (left to right, top to bottom), so that the intensity of the beam is modulated during the scan. Colour CRT monitors comprise three interleaved phosphor types (red, green and blue) periodically arranged as dots or stripes across the face of the monitor. There are three electron beams and a shadow mask disposed so that each beam illuminates only one of the three phosphor types.

The light from each pixel is pictured as a mixture of light emitted by the red, green and blue phosphors. The spectrum of the light emitted from a single monitor pixel C(λ) can be described mathematically as,

$$C(\lambda) = rR(\lambda) + gG(\lambda) + bB(\lambda) + A(\lambda). \quad \text{(Eq. 1)}$$

where λ represents wavelength; R(λ), G(λ), and B(λ) are the spectra of light emitted by each of the monitors phosphors when maximally excited by the electron beam; r, g and b – the *phosphor light intensities* - are real numbers ranging from 0 to 1; and A(λ) is the ambient light emitted (or reflected) by the monitor when the video voltage input to the monitor is zero for each phosphor[6]. Therefore, spectrally, Eq.(1) says that the light can be represented by a linear combination of contributions from the three phosphors (Brainard et al., 2002).

From Eq.(1) we can be aware of the very limited set of spectra C(λ) these monitors produce (gamut), which consist of a weighted sum of the three fixed primaries. However, it is largely enough (although natural scenes contain colours outside the gamut) because human colour vision is mediated by three classes of light-sensitive cones: long-, middle- and short-wavelength-sensitive cones (referred to as L, M, and S cones, respectively), according to the part of the visible spectrum to which they are most sensitive. The response of each class of cones to a spectrum incident at the eye depends on the rate at which the cone pigment absorbs photons and this absorption rate may be computed via the spectral sensitivity of that class of cones (Brainard and Stockman, 2010).

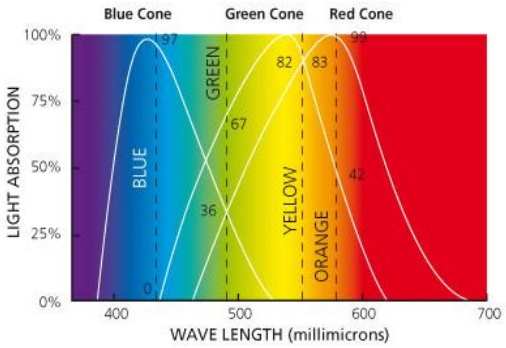

FIGURE 5. For human vision, the visible spectrum extends roughly between 400 and 700 nm. Colour and colour perception are limited at the first stage of vision by the spectral properties of the layer of light-sensitive photoreceptors that cover the backside of the eye – the retina. The opsin molecules in the three types of cones (L-,M-, and S-cones) are slightly different allowing the colour differentiation (*http://www.sharp-sighted.org/*).

Denoting the spectral sensitivity of the L, M, and S cones as L(λ), M(λ) and S(λ), respectively, the quantal absorption rates - *cone coordinates* of the spectrum C(λ) - l, m, and s of the L, M and S cones for a colour stimulus whose spectrum is C(λ), are given by the integrals,

$$l = \int_{380\,\mathrm{nm}}^{780\,\mathrm{nm}} L(\lambda)C(\lambda)d\lambda \;;\; m = \int_{380\,\mathrm{nm}}^{780\,\mathrm{nm}} M(\lambda)C(\lambda)d\lambda \;;\; s = \int_{380\,\mathrm{nm}}^{780\,\mathrm{nm}} S(\lambda)C(\lambda)d\lambda \qquad \text{(Eqs. 2)}$$

where each integral is taken across the visible spectrum[7].

The integrals of Eq.(2) may be approximated by the sums

[6] To simplify the main development, with a very good approximation, we may assume that A(λ)=0.

[7] The CIE (from the french, *Commission Internationale de l'Éclairage*) recommends sampling from 380 nm and 780 nm at 5 nm intervals, making n=81.

$$l = \sum_{i=1}^{n} L(\lambda_i)C(\lambda_i)\Delta\lambda \;;\; m = \sum_{i=1}^{n} M(\lambda_i)C(\lambda_i)\Delta\lambda \;;\; s = \sum_{i=1}^{n} S(\lambda_i)C(\lambda_i)\Delta\lambda \qquad \text{(Eqs. 3)}$$

Using matrix notation,

$$\mathbf{s} = \begin{bmatrix} l \\ m \\ s \end{bmatrix} \;;\; \mathbf{S} = \begin{bmatrix} L(\lambda_1) & L(\lambda_2) & \cdots \\ M(\lambda_1) & M(\lambda_2) & \cdots \\ S(\lambda_1) & S(\lambda_2) & \cdots \end{bmatrix}\Delta\lambda \;;\; \mathbf{c} = \begin{bmatrix} C(\lambda_1) \\ C(\lambda_2) \\ \vdots \end{bmatrix} \qquad \text{(Eqs. 4)}$$

we can rewrite Eq. (3) as

$$\mathbf{s} = \mathbf{S}\,\mathbf{c} \qquad \text{(Eqs. 5)}$$

Equation (5) computes cone coordinates **s** from the spectrum **c** of the colour stimulus.

When two physically distinct lights that have the same spatial structure result in the same quantal absorption rates for the L, M, and S cones, the lights are indistinguishable to cone-mediated vision[8]. Thus, accurate rendering a desired image on a characterized monitor means choosing R, G, and B values so that the spectrum **c** emmited by the monitor produces the same cone coordinates **s** as the desired image. Hence, to calculate the digital video values R, G and B required to provide a spectrum C(λ), we may use the standard CRT model, through the following computational steps:

1. Use Eq. (5) to compute cone coordinates l, m, and s corresponding to C(λ);

2. Compute the phosphor light intensities r, g, and b such that the mixture expressed on the right side of Eq. (1) produces the same quantal absorption rates, by the measurements of the phosphor spectra with a spectroradiometer[9].

3. Find DAC (*digital-to-analog* converter) values R, G, and B that will produce the desired phosphor intensities r, g, and b. This computation relies on measurements of the gamma functions but it is independent of the phosphor spectra. Because each intensity r, g, and b under the standard CRT model is a simple monotonic function of the corresponding digital video value (R,G, or B), it is straightforward to invert each *gamma function* to find the necessary digital video value to produce any desired output (Brainard et al., 2002), as explained below.

- ***Gamma Correction***

The gamma function of a CRT is used to describe the relationship between phosphor intensities (r, g, and b) and digital video values (R, G, and B) and is caused by a space charge effect in the neck of the tube.

[8] We neglet for now a possible effect of rod signals that can occur at light levels typical of many colour monitors.
[9] It was used SpectroCAL vision science meter from Cambridge Research Systems.

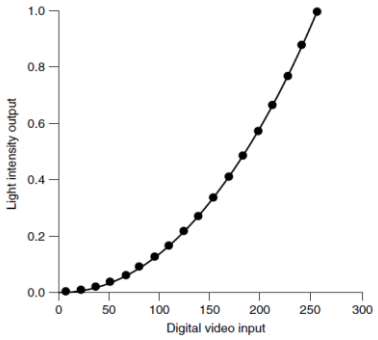

FIGURE 6. Representation of the typical gamma function. The plot shows the gamma function for a typical CRT monitor. The solid circles are the measured data. The intensity data were normalized to 1 for a digital video value of 255. The line express the best fit obtained using Eq. (6), with parameter estimates γ=2.11 and G_0=0.

To obtain a gamma curve similar as the above (**FIGURE 6**), the spectrum of light emitted by the green phosphor was measured for 17 values[10] (steps) of the G digital video value where R=B=0. A measurement of the ambient light (R=G=B=0) must be also measured to be subtracted from each individual measurement. These scalar values of intensity are then normalized to the maximum digital video value G=255. These scalars range between 0 and 1 and are the measured gamma function $f_{green}()$.

Given a desired value for the green-phosphor intensity g, gamma correction consists of using the measured gamma function to find the digital value G that produces the best approximation to g. For most CRT monitors, measured gamma functions are well fit by the functional form (e.g., for the green phosphor),

$$\begin{cases} g = f_{green}(G + e_{green}) = \left[\dfrac{(G - G_0)}{(255 - G_0)}\right]^{\gamma} & , \text{for } G > G_0 \\ g = 0 & , \text{otherwise} \end{cases} \qquad \text{(Eqs. 6)}$$

Where G_0 represents a cutoff digital video value below which no incremental light is emitted, and γ describes the nonlinear form of the typical gamma function. The error e_{green} is usually negligible. The Eq. (6) is easily inverted to determine, for example, G from g[11]:

$$G = (255 - G_0)g^{1/\gamma} + G_0 \qquad \text{(Eqs. 7)}$$

[10] In our procedure the spectrum of light emitted by each phosphor was measured for 17 values (steps) of the corresponding digital video value (increments of 5).

[11] The same protocol is used to the red and blue phosphors.

2. MOTIVATION

Several previous studies focused on NF1-related systematic impairments in visuospatial tasks. However, the neurophysiological causes behind these deficits are poorly understood.

Studies linking the genotype and functional phenotype essentially based on animal models of the disease. The development of NF1 mice models lead to the suggestion that the NF1 cognitive deficits are a consequence of enhanced levels of inhibitory transmission. The animal model can give us precious information and scientific knowledge about the intrinsic mechanisms but has some limitations. One crucial question is:

"How far can the animal model be related to the human phenotype?"

It is important to confirm that the disease mechanism identified in the animal model of NF1, excessive inhibition due to GABAergic transmission, is valid for the human disease and, thereby, amenable to therapeutic intervention. Thus, one main goal of this work is to establish the neural correlates of the visual deficits associated with NF1.

The molecular studies showed that in NF1 there is an abnormal excess of neuronal inhibition related to a pronounced enhancement of GABAergic neurotransmission. Visuospatial deficits and impaired sensitivity to visual contrast suggest abnormal visual processing that might be the consequence of this increase in GABAergic transmission in visual areas. This hypothesis raises other questions:

"How can we bridge the enormous gap from molecular processes to the human condition?"

and

"Can the GABAergic neurotransmission be related to the visuospatial deficits in NF1?"

Trying to answer these questions, we conducted our work through measurements of brain electrical activity elicited by visual stimulation. Hence, in this study, we investigate the underlying mechanisms of abnormal visual processing in NF1 children, using visual evoked potentials (VEP) recordings. VEPs are visual evoked electrophysiological signals extracted from the electroencephalographic activity in the visual cortex, recorded from the overlying scalp. They are a useful tool in diagnostic information regarding the functional integrity of the visual system. This technique allows the attainment of quantitative measures of the visual processing function elicited by chromatic and achromatic stimulation. It is known that the perception of contrast is possible by the balance between the excitatory and inhibitory inputs on the ganglion cells of the visual system. Therefore, we may establish a connection between the inhibitory inputs to different behaviours in response to visual contrast. So, the recording of the cortical electrical potentials from NF1 and controls (children without NF1 of same age range and without visuospatial deficits) allowed for a comparative data analysis between groups.

3. METHODS

3.1. ELECTROENCEPHALOGRAPHY – VISUAL EVOKED POTENTIALS

ELECTROENCEPHALOGRAPHY – AN OVERVIEW

The brain, the centre of the nervous system is an extremely complex structure, composed by knotty networks of excitable cells – neurons – and other supportive and protective cells – glial cells – tracing functional circuits, each one responsible for specific tasks at different levels, ranging from intellectual behaviour, cognition, emotion to physiological responses. The neuronal activation produces a current that leads to an electric field which can be measured directly on the brain tissue or even on the surface scalp of the head.

The first EEG records date from 1929, when Hans Berger reported a series of experiments in which he demonstrated to be possible to measure electrical activity of the human brain by placing an electrode over the scalp, and then plot the changes in voltage over time graphically on a strip of paper (Luck, 2005).

By placing electrodes on the scalp with a conductive media above the various regions of the brain, it is possible to detect the electrical activity associated with functioning neurons in that brain region. The investigators detected various patterns of electrical activity, denoted by "brain waves". Nowadays EEG is routinely used in medical practice. In medical and basic research, it is noticed that there is a correlation between particular brain rhythms and sleep phases, emotional states, psychological profiles, and mental activities.

A TYPE OF EVENT-RELATED POTENTIALS (ERPS) – VISUAL-EVOKED POTENTIALS (VEPS)

Evoked potentials are stimulus-locked EEG measures, i.e., they consist in a measurement of the brain activity by EEG phase-locked to the onset of external sensory stimuli. One can distinguish the spontaneous brain activity from responses to those stimuli. Most electroencephalographic studies of human perception are based on the averaged ERPs, evoked by brief visual stimulation – *visual evoked potentials* (VEP).

VEPs are non-invasive, simple approaches to analyze the sensory visual pathway, particularly in paediatric infants, who cannot communicate visual symptoms or cooperate for standard vision assessment. VEPs are sensitive indicators of subclinical lesions and can be used to differentiate visual impairment from visual inattention in young infants (Taylor and McCulloch, 1992) . Indeed, VEPs can confirm functional loss in disorders of the visual system. They are useful also to quantify visual impairment in patients with known visual disorders and monitoring patients who are at risk for visual

complications either from diseases (such as hydrocephalus or neurofibromatosis) or even as a complication of therapeutic intervention. Indeed, VEPs have become an valuable tool in pediatric ophthalmology and neurology and will probably play an increasingly important role in the future, essentially due to the difficulty in assessing visual system function in young or ill children and the VEP's sensitivity to subclinical damage (Taylor and McCulloch, 1992).

3.2. VISUAL TASK: CREATION AND PRESENTATION

VISUAL STIMULI CREATION

The stimuli used were adapted from (Ribeiro and Castelo-Branco, 2010). Stimuli were generated with MatLab® (R2008a, The MathWorks, USA). The ganglion cells connect to V1 by three distinct visual pathways that convey different types of visual attributes for further processing (more detailed on below section: "

Criteria to isolate the three parallel visual processing pathways"). Therefore we wanted to study their responses separately. Thus we used stimuli with different characteristics for each pathway. The stimuli consisted in phase-reversed circular horizontal Gabor[12] patterns of different chromaticities and spatial and temporal frequencies (detailed below in section: "

Spatiotemporal criteria and Chromatic contrast as a way to isolate the different pathways"; **TABLE 2**) and 5 different contrasts for each pathway stimulation (**TABLE 3**). Stimuli diameters[13] were 10.0 degrees of visual angle.

CRITERIA TO ISOLATE THE THREE PARALLEL VISUAL PROCESSING PATHWAYS

The three retinocortical streams, can be studied individually because each responds to stimuli with different characteristics. The three post-receptoral detection mechanisms, have already been defined psychophysically (Cole et al., 1993;Krauskopf et al., 1982;Sankeralli and Mullen, 1997), and are thought to process differently the visual information across space. Importantly, it is possible to stimulate selectively a specific population of cells, choosing an appropriate visual stimulus (Tobimatsu et al., 1995).

[12] Sinewave gratings modulated by a Gaussian window

[13] two times the standard deviation of the Gaussian aperture filter

The parvocellular pathway has colour selectivity being specially sensitive to modulation by L-M-cone contrast, that results in red-green chromatic contrast (Tobimatsu et al., 1995). It shows an excellent spatial resolution. Indeed, it is tuned to high spatial frequencies and low temporal frequencies (Kulikowski et al., 1997). Hence, it is thought to underlie fine discrimination of visual features in particular in the central visual field, and to play an important role in colour vision and form perception (Tobimatsu et al., 1995).

The koniocellular pathway was discovered more recently. Consequently its function is less understood (Hendry and Reid, 2000). As the parvocellular pathway, the koniocellular stream has colour sensitivity although it is sensitive to S-cone contrast that results in blue-yellow chromatic contrast (Xu et al., 2001). Therefore, it most certainly plays a role in colour vision. In addition, it might be involved in spatial processing, as suggested by its significant response to peripheral stimulation (Vanni et al., 2006;Mullen et al., 2007) Furthermore there are evidences that it might be involved in motion perception (Sincich et al., 2004;Wandell et al., 1999).

The magnocellular pathway is most sensitive to luminance stimuli, i.e., achromatic contrast and is thought to play an important role in spatial localization and motion processing and stereopsis (Xu et al., 2001;Merigan and Maunsell, 1993).

In conclusion, the best strategy to isolate the three pathways relies on chromatic properties and spatiotemporal criteria of the visual stimulus being presented. For parvo- and koniocellular isolation, the stimuli must be chromatic and have high spatial and low temporal frequency to minimize the response of the magnocellular pathway (Lee, 1996;Boon et al., 2005). The magnocellular pathway must be stimulated by achromatic stimuli (Boon et al., 2005) and, since it is most sensitive to high temporal frequencies, it should be used stimuli of high temporal and low spatial frequencies (Lee, 1996).

SPATIOTEMPORAL CRITERIA AND CHROMATIC CONTRAST AS A WAY TO ISOLATE THE DIFFERENT PATHWAYS

The three retino-cortical pathways were isolated by using three different types of visual stimuli, each stimulus type activating a single pathway. These stimuli differed by their chromaticity and spatial and temporal frequencies. To stimulate the magnocellular pathway, the gabors had spatial frequency of 0.5 cycles per degree (cpd) and temporal frequency of 5 Hz cycling rate; to the stimulate the parvocellular and koniocellular pathways we used Gabors with spatial frequency of 2 cpd and temporal frequency of 1 Hz cycling rate (**TABLE 2**).

The chromaticity of the stimuli was defined using a three-dimensional cone contrast space in which each axis represents the activation of the L-, M- and S-cone types, normalized with respect to

the background (i.e. cone contrast) (Cole and Hine, 1992;Derrington et al., 1984;MacLeod and Boynton, 1979). Stimulus chromaticity is given by vector direction, and contrast by vector length within the cone contrast space. Three cardinal stimuli (magno-, konio- and parvocellular) were determined within this space to isolate each of the three different retino-cortical pathways (based on (Cole et al., 1993;Sankeralli and Mullen, 1996;Sankeralli and Mullen, 1997)) which have the following directions in the cone contrast space: the magnocellular stimuli activates L-, M- and S-cones equally (weights of 1, 1 and 1, respectively); the koniocellular stimuli activates only the S-cones (weights of 0, 0 and 1); and the isoluminant parvocellular stimuli activates L- and M- cones opponently without S-cone activation (weights of 1, -3 and 0)[14]. Two vectors with same length but symmetric about the origin of the cone contrast coordinates represent the modulation of stimuli chromaticity (Ribeiro and Castelo-Branco, 2010) (**TABLE 2**).

TABLE 2. To isolate the three retino-cortical pathways we used three different types of visual stimuli of different chromaticity and spatial and temporal frequencies.

PATHWAYS	Chromaticities	Spatial Frequency	Temporal Frequency
	(-L,-M,-S)	(cpd)	(Hz cycling rate)
MAGNOCELLULAR	(1,1,1)	0.5	5
PARVOCELLULAR	(0,0,1)	2	1
KONIOCELLULAR	(1,-3,0)	2	1

Since the visual measure in study is the CRF, for each stimulus type, we studied the effect of contrast defining five different contrast levels (**TABLE 3**).

TABLE 3. Contrast levels used for each pathway stimulation.

PATHWAYS	CONTRASTS				
	1	2	3	4	5
MAGNOCELLULAR	0.120	0.240	0.480	0.720	0.960
PARVOCELLULAR	0.015	0.030	0.060	0.090	0.125
KONIOCELLULAR	0.150	0.325	0.500	0.675	0.850

[14] The value 3.0 represents the mean ratio L:M cone input, ranging from 2.1 to 4.9, measured by the individual isoluminant point for each subject in (Ribeiro and Castelo-Branco, 2010), and consistent with values obtained in previous studies.

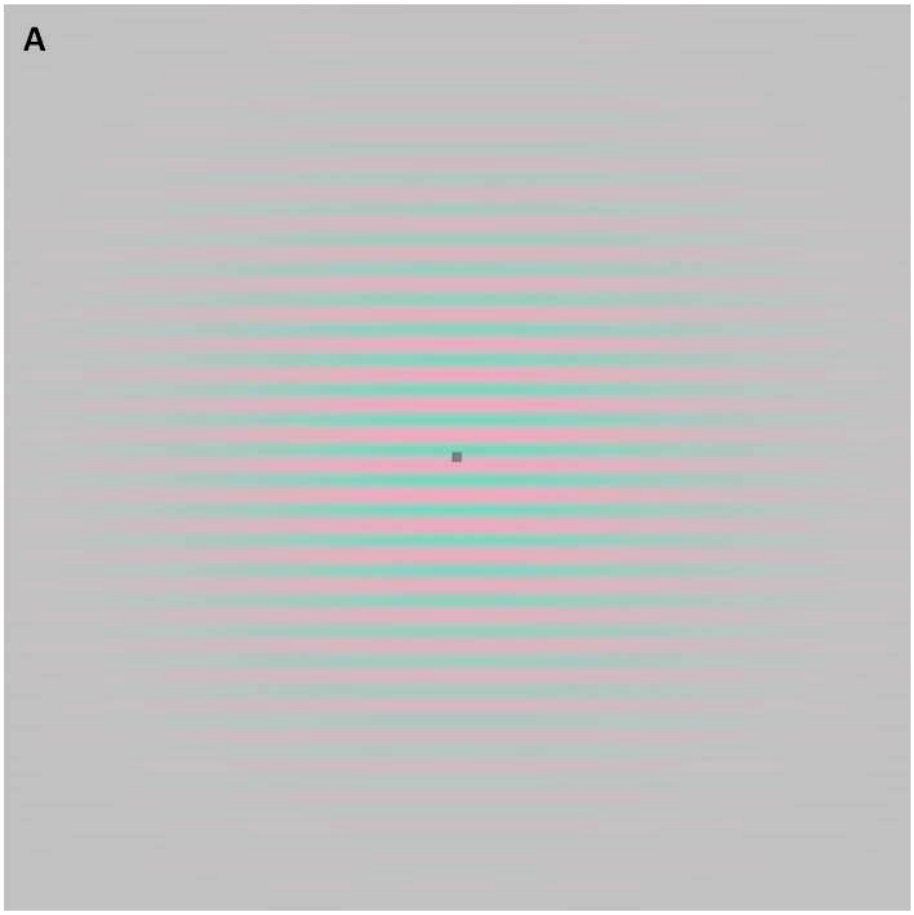
A

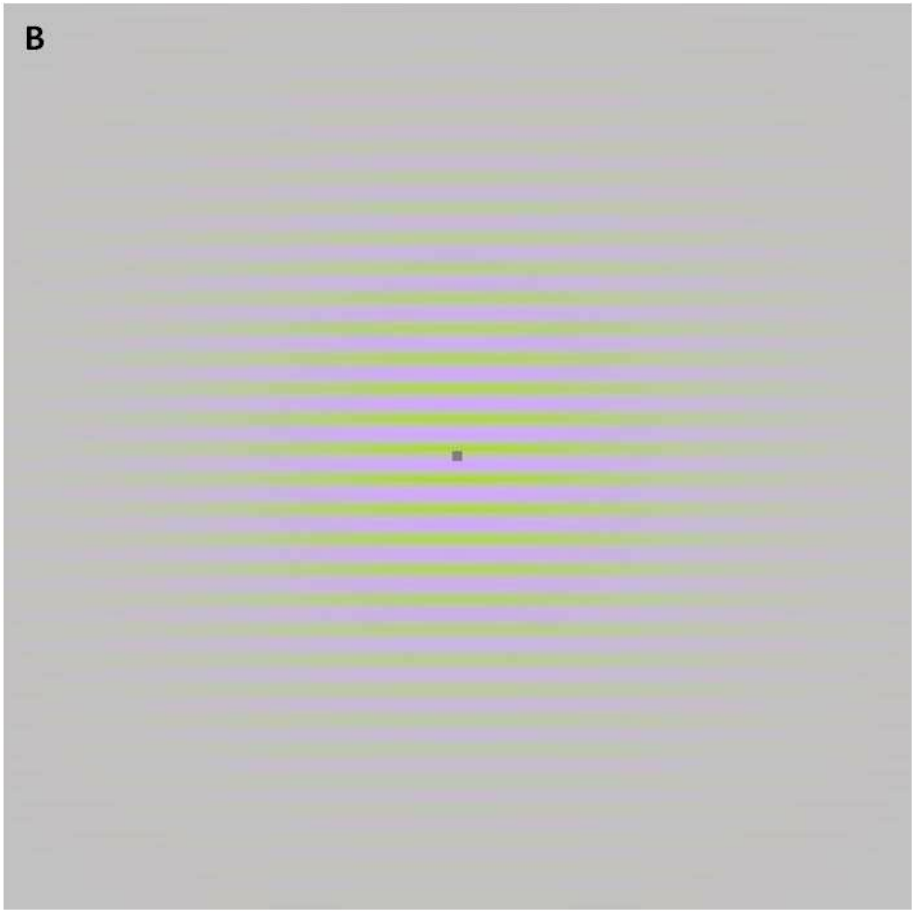
B

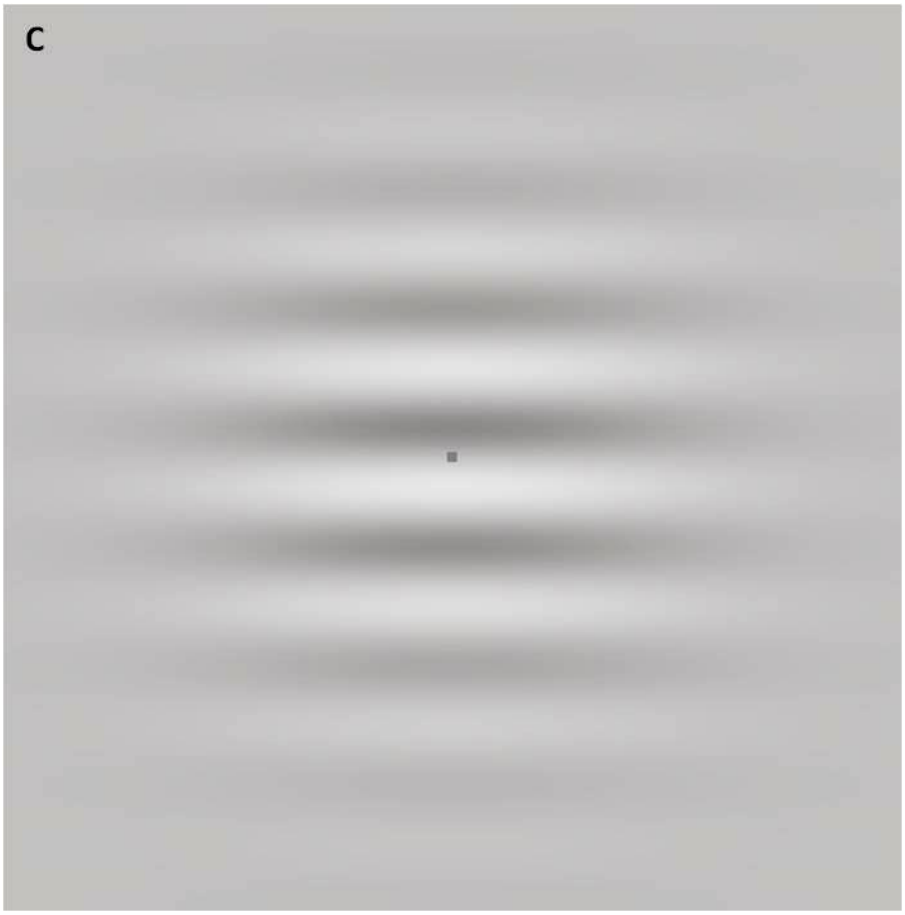

FIGURE 7. Examples of three types of stimuli used. CHROMATIC: **(A)** L-M cone stimulation (red-green) – Parvocellular stimulation (contrast: 12.5%); **(B)** S cone stimulation (blue-yellow) – Koniocellular stimulation (contrast: 85%); ACHROMATIC:**(C)** Magnocellular stimulation (contrast: 96%).

VISUAL STIMULI PRESENTATION

Stimuli was presented with the STIM stimulation software (version 4.0, NeuroScan, USA) with a display resolution of 1280x1024x32, over a grey background ([0.4 0.4 0.4] (rgb) → [182 179 178] (RGB)) (**FIGURE 8**).

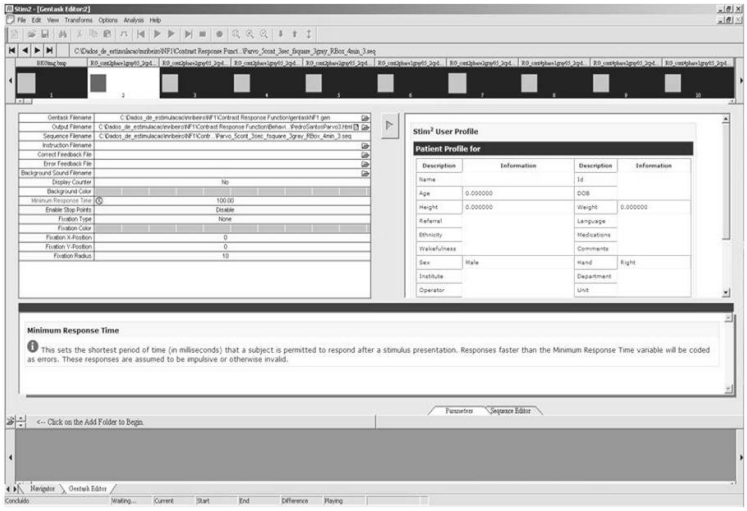

FIGURE 8. STIM layout - Gentask setup.

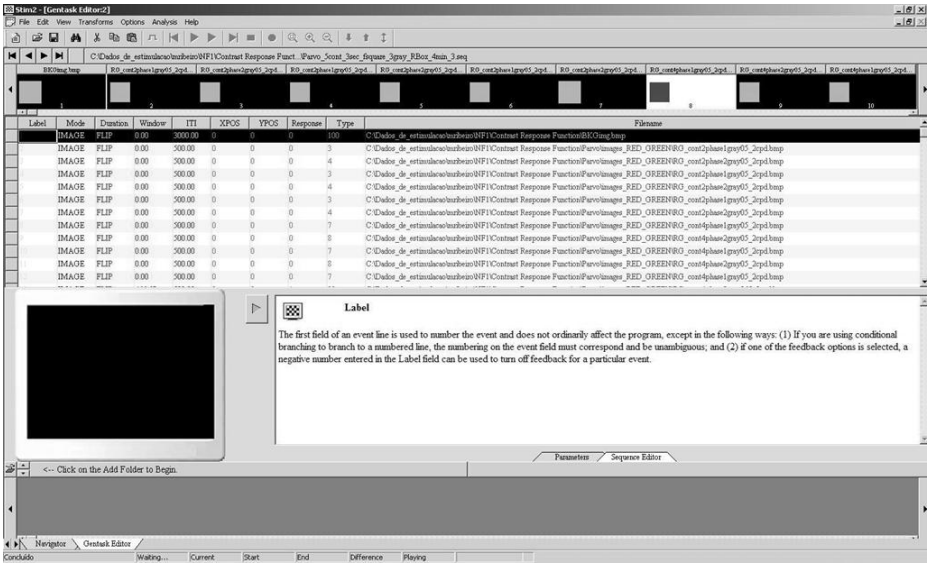

FIGURE 9. STIM stimulation software – Sequence file.

The sequence file was developed with MatLab® (R2008a, The MathWorks, USA) and then transferred to STIM (version 4.0, NeuroScan, USA) for display (**FIGURE 9**). The run for either pathway consisted into segments during which only one type of stimuli (L-S cone, S cone or achromatic) was presented. Within each run, the contrast was changed in a pseudo-random way every 3s. That is, in each 15s, all the 5 contrasts were randomly presented. This procedure minimized the likelihood of short-adaptation effects. To achieve the desired frequency rates, parvo- and koniocellular stimuli were set with a reversal rate of 2 reversals/s, and the magnocellular stimuli was set with a reversal rate of 10 reversals/s. In the very beginning of each run a blank image was presented on the CRT only with the background and fixation point for 3s, to allow an adaptation to the luminance of the stimulation.

The stimuli was presented at the centre of a CRT monitor (Philips) calibrated with a spectroradiometer (SpectroCAL, Cambridge Research Systems). The spectrum of each phosphor was measured at 1 nm intervals across the visible spectrum. The (Stockman and Sharpe, 2000) 2-deg cone fundamentals were used for the spectral absorptions of the L-, M-, and S- cones. From this data, a linear transform was calculated to specify the phosphor contrasts required for a given cone contrast ((Brainard et al., 2002),(Brainard and Stockman, 2010)). The "contrast" and "brightness" of the monitor were set at 100% and 25% respectively and these values were kept over the monitor characterization, calibration and tests to not affect the gamma function. Gamma correction of the monitor output was achieved via software look-up tables. The monitor refresh rate was set at 85 Hz. The mean luminance of the screen was 40 cd/m^2 (measured with ColorCAL colorimeter, Cambridge Research Systems).

3.3. BEHAVIOURAL TASK

Subjects were instructed to focus on a fixation square at the centre of the screen that changed luminance randomly within 3 to 10s. The subjects were instructed to indicate through button press when it became brighter or darker (**FIGURE 10**). This behavioural task aimed at maintaining the subject's attention during the EEG recording session.

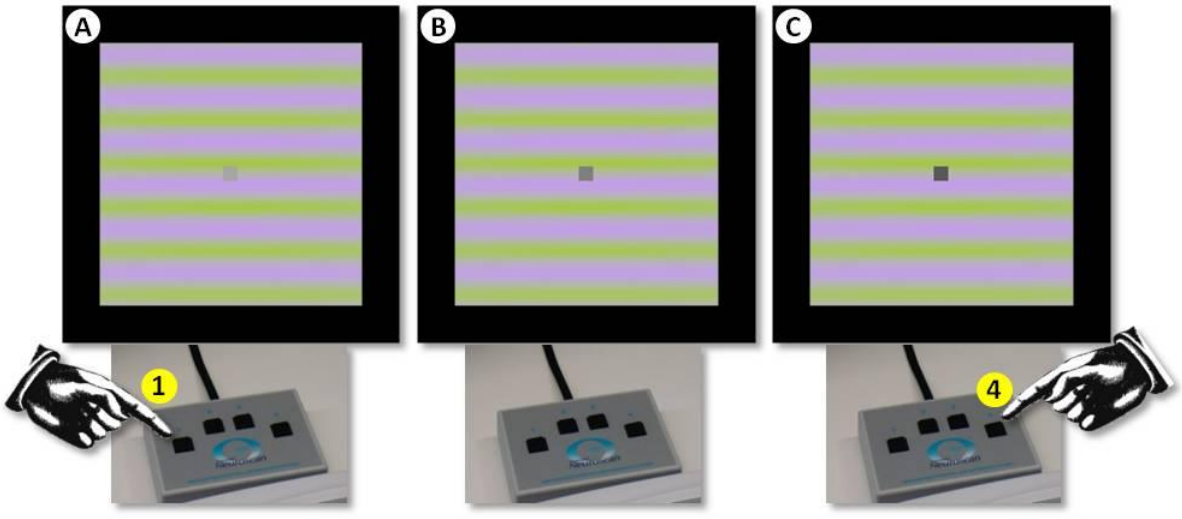

FIGURE 10. Behavioural task. The fixation square had a certain luminance value **(B)** and every time the luminance of the fixation square increased **(A)**, the participant should press the button 1 with the left thumb, and if the luminance decreased **(C)**, the participant should press the button 4 with the right thumb.EEG experimental procedures

Hansen's Axiom(Luck, 2005):

"There is no substitute for good data."

J.C.Hansen

PARTICIPANTS

In this study, we investigated deficits in visual processing in two groups: NF1 patients and controls. ERPs were recorded from 34 participants between 7 and 16 years-old.

The NF1 group was composed of children and adolescents aged 8 till 16 years-old: 5 boys (8-15 years); 12 girls (10-16 years) (**TABLE 4**). All patients were recruited from the Genetics Department of the Paediatric Hospital of Coimbra, in Portugal.

The control group was composed of children and adolescents aged 7 till 16 years-old: 5 boys (7-14 years); 12 girls (8-16 years) (**TABLE 4**). For this group, we recruited unaffected siblings (n=2) and healthy children and adolescents from a local school, Escola B.2,3 Martim de Freitas (n=15).

The participants have volunteered for psychophysical and electrophysiological measurements after a full description of the aims and methods of this study. All subjects had normal or corrected to normal visual acuity. Before the experiment an informed consent was obtained from family or caretakers of all participants.

Parents of children on stimulant medication for ADHD were requested not to give their children the medication on the days of testing (n=3 NF1 children). The study was conducted in accordance with the tenets of the Declaration of Helsinki, and with the approved guidelines of the Ethics Committee of the Faculty of Medicine of Coimbra.

TABLE 4. Participants characterization by gender and age[15] in years. (Age=mean age ± standard error).

	♂ Boys	♀ Girls	Total
CONTROLS	5	12	17
Age (y)	10.99± 1.180	13.32 ± 0.681	12.63 ± 0.631
NF1	5	12	17
Age (y)	11.48 ± 1.254	11.965 ± 0.632	11.82 ± 0.559
Total	10	24	34
Age (y)	11.23 ± 0.816	12.64 ± 0.476	12.23± 0.421

[15] The age value was calculated regarding the EEG recording day. To get the age in years rounded to the hundredths it was used the Microsoft Office Excel formula above:

=(DAYS360(DATE(D1,M1,Y1),DATE(D2,M2,Y2))/360

where D1, M1, Y1 refers to the date of the EEG recording (Day, Month, Year) and D2, M2, Y2 refers to the birth date of the participant. DATE function returns the Microsoft Office Excel serial number of a date and DAYS360 returns the number of days between two dates, based on a 360-day year (12 months of 30 days).

3.3.1. POSITIONING OF THE EEG CAP FOR THE 64-CHANNEL RECORDING PROCEDURE

During the whole procedure, one thing we kept in mind was that we were dealing with children who require special attention, because children usually do not sit quietly and calmly for long periods of time and get bored very easily. Therefore modifications to VEP recording methods and testing strategies were required to optimize the quality of the results of the visual assessment. Usually, two scientists/technicians participated in all stages of the experiment. It is beneficial to have two testers in the EEG Lab: one more focused on working with the child, because direct interaction with the child helps them to maintain attention and fixation, and other to control data acquisition (Odom et al., 2010).

- ***Materials***

To optimize testing procedures, we prepared, in advance, all the materials required to do the EEG test, checking its availability and minimizing the preparation time (**FIGURE 11**).

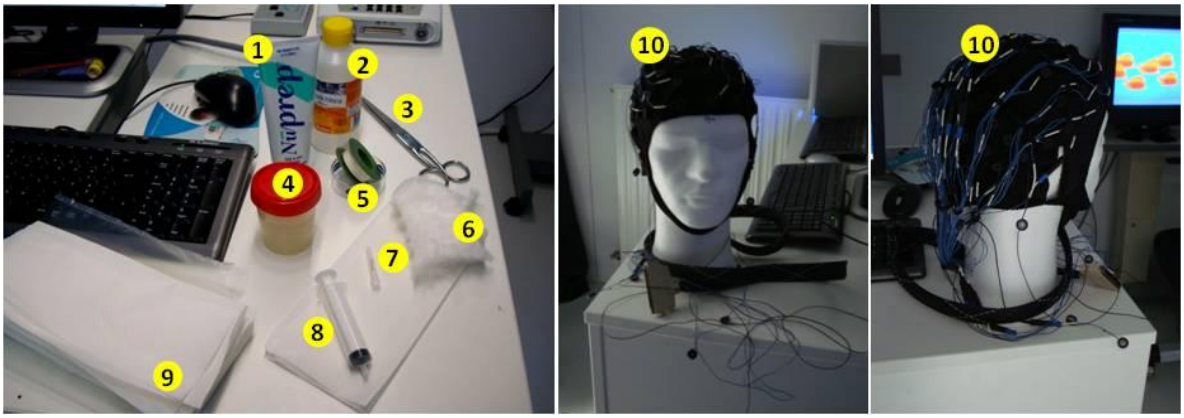

FIGURE 11. Materials required for the EEG recording. **(1)** Abrasive skin gel; **(2)** Alcohol; **(3)** Scissor; **(4)** Conductive gel (electro-gel – Quik-Gel); **(5)** Tape; **(6)** Cotton; **(7)** Blunt tip needles; **(8)** Syringe; **(9)** Cleaning paper; **(10)** Quik-Cap™ (small or medium with 64-channel).

- ***Positioning the cap***

Once arriving at the EEG lab for testing, the subject was prepared for the Quik-Cap™ [16] (**FIGURE 11.10**) application.

The procedure started by preparing the skin areas where the electrodes would be located:

[16] The Quik-CapTM (by Compumedics Neuroscan, NeuroMedical Supplies) are manufactured of highly elastic breathable lycra material with soft neoprene electrode gel reservoirs which enhance the subject comfort, and makes the preparation easier and faster. We utilized one of two different sizes of caps (small or medium) according to the children's head sizes, such that the inter-electrode distances were not variable (Taylor and Baldeweg, 2002).

First, gentle but firmly, cleaning these areas with cotton embedded in alcohol (**FIGURE 11.2,6**); Then, with an abrasive skin gel (**FIGURE 11.1**), exfoliating the scalp surface and reducing the need to abrade the scalp surface after loading the electrodes with gel.

Positioning the cap is a two-person process. Most of the times, the subjects were required to place their thumbs under the front edge of the cap, while the other person pulled the cap onto to the head slowly, carefully ensuring the proper electrode alignment on the head. The criterion for proper localization of the electrodes was based on their placement to bony landmarks (Odom et al., 2010). CZ should be located in the cross point of the anterior-posterior midline with the coronal plane that links the ears (**FIGURE 12.B**). The lowest occipital electrode should be approximately two fingers above inion, and Fpz approximately two fingers above the nasion (**FIGURE 12.A**). At this point, we start routinely inquiring the subject if he feels any kind of discomfort, like pressure, because the test is long and we want to avoid the need to change to other cap size, or stop the experiment caused by physical discomfort.

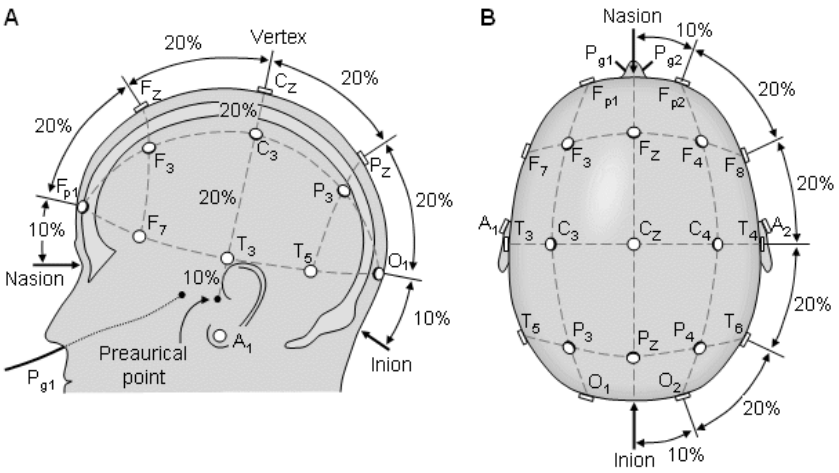

FIGURE 12. According to the International 10/20 system, scalp electrodes are located relative to bony landmarks, in proportion to the size of the head. **(A)** The international 10-20 system seen from sagittal plane (left) and **(B)** transversal plane (above the head). A=ear lobe; C=central; Pg=nasopharyngeal; P=parietal; F=frontal; Fp=frontal polar, O=occipital, T=temporal (Malmivuo and Plonsey, 1995).

With the cap correctly placed, we connected the cap connector to the amplifier, to check the impedances (see below section: "Testing impedances") while filling each electrode cup (see electrodes used on below section: "3.3.4. Data Analysis") with Quik-Gel[17] (**FIGURE 11.4**) using a syringe (**FIGURE 11.8**) and a blunt tip needle (**FIGURE 11.7**), pressing the electrode down with the fingers to ensure close contact with the skin. A similar procedure was followed to position the

[17] Quik-Gel is a Neuroscan electro-gel, a conductive paste that lowers impedance and acts as a conductive bridge between the scalp and the electrode.

The amount of electro-gel injected should be sufficient to obtain good impedances but so as not to form a bridge between neighbouring electrodes.

electrooculogram electrodes (to monitor eye movements) and the earlobe electrodes. These had to be fixed to skin with tape (**FIGURE 11.5**).

Testing impedances

High electrode-scalp impedance might induce distortions in the signal. Therefore, this parameter is one crucial aspect to take into account when performing an EEG exam (Teplan, 2002;Luck, 2005).

To obtain cleaner records, we took time to try to get all impedances, at least, lower than 10kOhm, and balanced across the electrodes.

The SCAN hardware/software acquisition system provides automatic impedance measurements and display (**FIGURE 13**), by a grading colour system (pink to black; black means impedance lower than 5 kOhm).

The first step to get good impedances is, when scheduling the EEG test, to ask the subjects to wash their hair the morning of testing or, at least, the night before it. They should wash it with a normal shampoo without conditioner. After shampooing, the subject should not use any kind of styling products, because they can coat the scalp, making it much more difficult to obtain low impedance connections.

When testing the impedances, if they were bad we repeated some of the previous steps, to reach the best condition, namely putting more gel and verifying that there weren't air bubbles. Many times, the impedances improved and stabilized during the experiment.

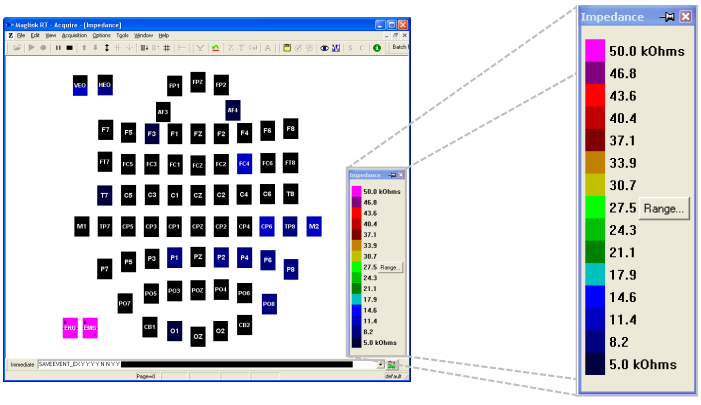

FIGURE 13. Monitoring the electrodes impedances while applying the electro-gel is a good principle to get the best recordings. SCAN hardware/software acquisition system provides automatic impedance measurements and display by a colour grading system (**Pink:** impedance higher than 50 kOhms, or no connection at all; **Black:** impedance lower than 5 kOhm).

Acquisition Setup

After preparing the subject, we verified our acquisition settings (gain, A/D rate, filters, sampling rate, etc.; see parameters on above section: "3.3.3. Data Acquisition"), and loaded the setup file (**FIGURE 14**) into the acquisition system.

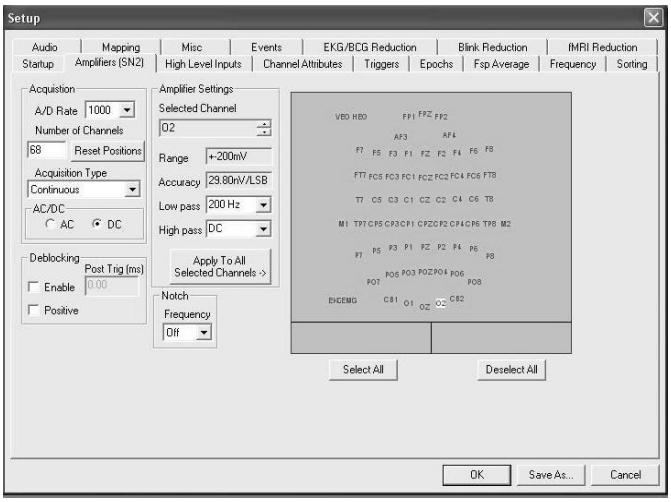

FIGURE 14. Acquire4.3 (Neuroscan) setup – Amplifiers tab.

In this phase we verified also the STIM Gentask (version 4.0, NeuroScan, USA) file in the stimulation computer and selected the first sequence to be presented into the monitor (**FIGURE 8**).

We subdued room lightning without bright sources visible to the subject (only the brightness of the stimulation CRT, and the low brightness of the acquisition monitor). Then we explained the task to the child (see above section: "3.3.2. Experimental Protocol"), and allowed each to practice the task for a few minutes before starting the recording session. When the participant was prepared to start, the EEG data was recorded continuously for each run. To prevent timing errors, there were separated acquisition and stimulation computers.

The behavioural task responses were recorded by Stim2 (version 4.0, NeuroScan, USA) and by Acquire Data Acquisition software (MagLink - SCAN4.3, version 4.3.1, NeuroScan, USA).

Between runs, during the experiment, we always tried to prevent other kind of artefacts and minimize the noise problem, improving conditions of cable/connectors locations.

Cleaning up

After the experiment, we unplugged the wire harness from the amplifier equipment and removed all the tape and the cap from the wearer. After washing the participant's scalp/hair, we took the cap to a sink and removed all the electro-gel with warm water running from the tap, cleaning each used electrode from both sides of the cap. The blunt tips were placed into a recipient with alcohol for disinfecting and re-use.

3.3.2. EXPERIMENTAL PROTOCOL

In the darkened room, subjects were sat in a comfortable chair at a viewing distance of around 100 cm from the monitor presenting the stimuli. We adjusted the height of the CRT table so that the centre of the monitor was at eyes level.

To avoid eye strain and tiredness due to long visual stimulation we divided the stimulus presentation into segments of around 4 minutes each allowing the subjects to rest in between runs, as necessary (**FIGURE 15**).

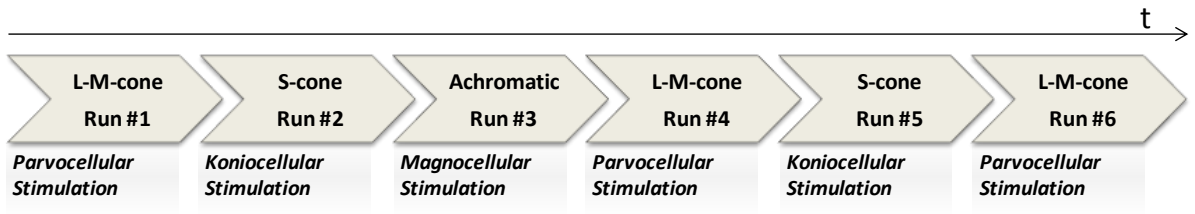

FIGURE 15. Scheme of the order of the runs followed in the experiment.

During each segment, only one type of stimulus was presented (L-M-cone, S-cone, achromatic stimuli) in which stimuli contrast changed randomly every 3 seconds. For each stimulus type there were 5 different contrasts, making a total of 5 stimuli per retino-cortical pathway. For further processing, continuous files of the same type of stimulation were concatenated using the Append function of SCAN 4.3 application (version 4.3.3, Compumedics NeuroScan, USA). Parvocellular stimulation elicited smaller responses, therefore the need for more trials for a good SNR.

To enhance participants motivation, before the experimental procedure *per se*, we showed them the EEG acquisition window with their EEG signal and informed about the problems of bioelectric artefacts (as talking, blinking, body movements, etc), encouraging them to minimize them without too heavy attentional burden. First, we ran run number six for practice before recording. When we noticed that the subject understood the task, we recorded EEG data starting with run number 1 (**FIGURE 15**).

3.3.3. DATA ACQUISITION

To acquire de bioelectric potential from the scalp, we used an electrode array of 9 occipital electrodes from a Neuroscan system of 64 Ag/AgCl electrodes (**9.** Appendix**.89C**) (Compumedics Quik-Cap™, NeuroScan, USA), according to the extended 10/20 system (American Clinical Neurophysiology Society (ACNS), 2006) interfaced through SynAmps2 (Compumedics NeuroScan, USA) signal amplifier.

The 9 occipital electrodes used ((P1, PZ, P2, PO3, POZ, PO4, O1, OZ, O2) with reference between CZ and CPZ. Vertical and horizontal electrooculograms were also recorded in order to reject artifacts caused by blinking and eye movements (**FIGURE 16**).

The amplifier fed the signal through the Acquire Data Acquisition software (version 4.3.1, Compumedics NeuroScan, USA) at a sampling rate of 1000 Hz with an active input range of ±200 mV per bit and on-line low-pass filter set at 200 Hz with DC correction. No notch filters were used (**FIGURE 14**) to avoid signal distortion (Luck, 2005).

During recordings, some electrodes were marked as bad and skipped from analysis due to high impedances, too much noise and interference or no reliable acquisition. However, these channels were recorded.

A trigger pulse was generated at the onset of each stimulus (at each phase reversal), to allow further processing procedures (see above section: "3.3.4. Data Analysis").

The digitized EEG was saved and processed off-line.

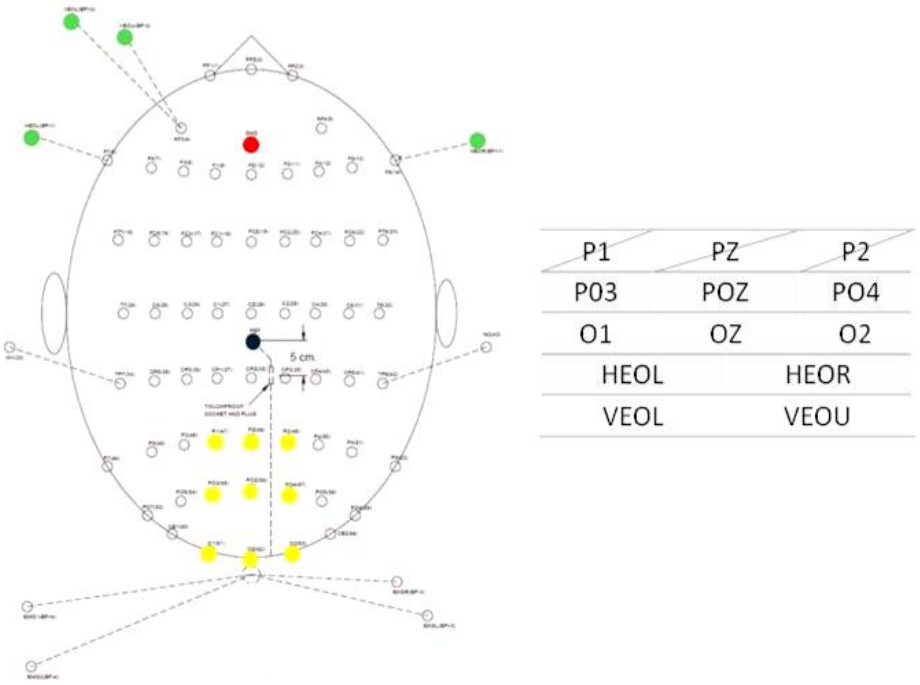

FIGURE 16. Schematization of the positions of the active electrodes (**yellow**), vertical and horizontal eye electrodes (**green**), reference (**blue**) and ground (**red**) electrodes. (To see 64-channel Quik-Cap™ design check 9. Appendix – *C.* EEG cap - **FIGURE 34**); P1, PZ and P2 were excluded from the analysis (see above section: "3.3.4. Data Analysis").

3.3.4. DATA ANALYSIS

All data analysis was performed with the EDIT Application (VERSION 4.3.1, Neuroscan, USA). To automatize the procedure, we wrote TCL[18] scripts using TCL Batch Editor (Version 1.0, Neuroscan 2003, USA) (9. Appendix A).

- *Analysis of the responses to **parvo- and koniocellular stimulation***

First, we applied a bandpass filter, without latency shifts[19], with cutoff frequencies of 0.5 and 100 Hz and attenuation of 12dB/oct. Then, the recording was cut into epochs defined from -100 ms till 400 ms post-stimulus. Baseline correction was performed on the period from 100 ms before stimulus onset till the onset of the stimulus (0 ms). In order to being able to compute the frequency spectra of the response using the FFT (*Fast Fourier Transform*) the number of points was reduced to a power of 2 (512 points). The artefact rejections were conducted automatically on the basis of deflections with amplitude higher than 50 µV. The epochs of each stimulus type and for each contrast were averaged in time domain[20] (9. Appendix A.1,4).

Since the reference channel was very close to P1, PZ and P2 channels, the signal was almost null, so it was decided to exclude these three channels from analysis. In order to increase signal-to-noise ratio we averaged the responses of the other 6 channels recorded using the Linear Derivation (LDR) Transform, with equal weights[21]. The time-domain analysis was based on the amplitudes and latencies of the main peaks of the averaged waves of each individual. They were calculated by programming the Scan 4.3 software (9. Appendix A.2,5) to find automatically the maximums and minimums of the waves within time windows defined by inspection of the grand average[22] VEPs (see below chapter: "4. Results" - **FIGURE 20**, **FIGURE 24**). We determined two positive peaks (P1 and P2) and one negative peak (N1) imposed by the time windows referred in **TABLE 5**.

TABLE 5. Inspecting the Grand Averages of each stimulus type, the following time windows were defined in which the software should automatically detect the maximums, P1 and P2 and minimum, N1, of the respective time range.

PATHWAYS	TIME WINDOW (ms)		
	P1	N1	P2
PARVOCELLULAR	50-90	60-120	100-170
KONIOCELLULAR	70-110	100-150	130-200

[18] TCL – *"Tool Command Language"*

[19] The *"Zero Phase Shift"* filtering command makes two "passes" through the filter, once in each direction. In spite of being slower than analog filtering, it has no effect on the latencies of the evoked potentials.

[20] Time domain averages were generated by creating a simple point-for-point averaged waveform.

[21] LDR is a process that enables the creation of a new channel (channels) as arbitrary linear combinations of existing channels.

[22] The grand averages are the means for all the individuals within each group for each contrast. For graphic presentation, the group averages were filtered with a lowpass filter of 30 Hz with 12 dB/oct of attenuation without latency shift.

To make the process quicker, I wrote a MatLab script that groups the amplitudes and latencies of each peak for each contrast for each subject into a table and calculates the mean amplitude and latency for that subject (9. Appendix B.1). This data was then copied to excel and SPSS files for statistical analysis.

In addition to time domain analysis, we may represent the same information in another way. We may present it in the frequency domain based on the principle that our stationary waveforms may be represented as a sum of sinusoidal waveforms, each one of a different frequency and having an associated amplitude and phase – *Fourier analysis*. Thus, to perform the frequency spectrum analysis, we computed the Fast Fourier Transform (FFT) of the averaged data. We obtained the amplitude files windowed with a 10% cosine taper (Appendix A.3,6).

The Fourier approach to analyzing a finite time series of length T (in seconds) is built around a sinewave of frequency 1/T (in Hz) and its harmonics (2/T, 3/T, etc.). In the output of the forward FFT, each such frequency is sometimes called a *frequency bin*[23]. To analyze the amplitude of the frequency spectrum, the amplitude was averaged in defined frequency bins of 2 Hz (T=0.5s; Δf_{bins}=2Hz).

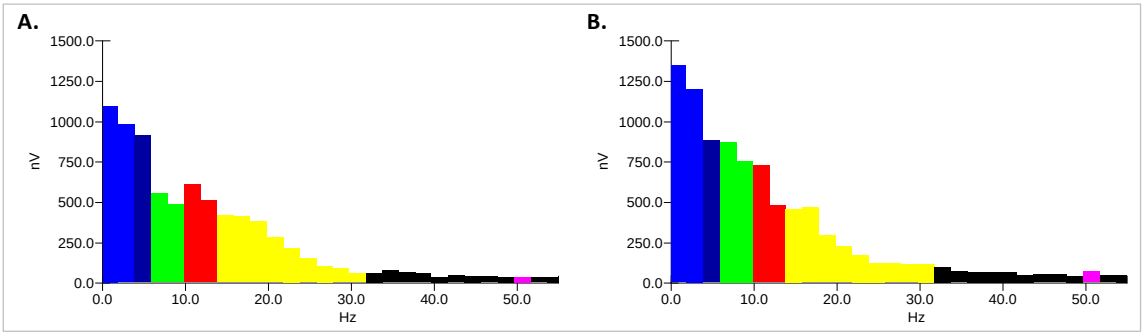

FIGURE 17. SCAN power spectrum of the LDR file. The frequency bands (delta, theta, alpha, beta, low gamma) are displayed as a series of colours. Amplitude of the frequency spectrum of the group average of the higher contrast in parvocellular stimulation: **(A)** CNT; **(B)** NF1. The koniocellular power spectrum has a similar appearance.

The analysis of the frequency response was based on the definition of frequency bands, chosen based on published reports (**FIGURE 17**,

TABLE 6), namely (Robert et al., 2009;Niedermeyer and Lopes da Silva, 1999;Taylor and Baldeweg, 2002). These values were computed by SCAN and saved into .xls files. An arithmetic mean of the amplitudes of the frequency bins inside the frequency band range was performed.

[23] The longer the duration of the epoch, the narrower the frequency bins (or the greater the frequency resolution).

TABLE 6. The frequency bands were ranged within defined frequency bins. Frequency bands for parvo- and koniocellular stimulation power spectra analysis.

PATHWAYS	FREQUENCY BAND (HZ)				
	Delta	Theta	Alpha	Beta	Low Gamma
PARVOCELLULAR KONIOCELLULAR	2:4	4:8	8:12	14:24	24:40

- *Analysis of the response to **magnocellular stimulation***

First, a bandpass filter was applied, without latency shifts (as described before in parvo- and koniocellular analysis), with cutoff frequencies of 1 and 100 Hz, and attenuation of 12dB/oct. Baseline was determined as the average value of the entire sweep ranging from stimulus onset till 200 ms after, the amplitude of one temporal cycle of the magnocellular visual stimulus. In order to being able to compute the frequency spectra of the response using FFT the number of points was reduced to a power of 2 (216 points). As in parvo- and koniocellular analysis, the artefact rejections were conducted automatically on the basis of deflections with amplitude higher than 50 μV. The epochs of each stimulus type were averaged in time domain (Appendix A.7).

For the same reasons as above, P1, PZ and P2 were excluded from the analysis and the other 6 channels were averaged to reduce noise ratios using LDR, with equal weights. The magnocellular stimulation produces a cyclic, steady state response (see grand averages[24] waves in chapter below: "4. Results" - **FIGURE 28**). For that reason, instead of peak amplitude analysis, the time-domain analysis was performed by measuring the signal strength of the magnocellular responses based on the mean amplitude of the rectified wave within a stimulus cycle (Appendix A.8). Due to the shape of the wave, the latency analysis was based on the phase of the wave, since there were no definable peaks, if one assumes component superposition.

To make the process quicker, I wrote a MatLab script that grouped the mean amplitude for each contrast for each subject into a table and calculates the mean of the mean amplitude for that subject (Appendix B.2). This data was then copied to excel and SPSS files for statistical analysis.

As in parvo- and koniocellular analysis we also made a "frequency domain" analysis. Thus, to perform the frequency spectrum analysis, we computed the Fast Fourier Transform (FFT) of the averaged data. We obtained the amplitude and phase files windowed with a 10% cosine taper (Appendix A.9).

To analyze the amplitude and phase of the frequency spectrum, the measures were averaged in defined frequency bins of 5 Hz (T=0.2s; Δf_{bins}=5Hz).

[24] See footnote 22 in page 3.

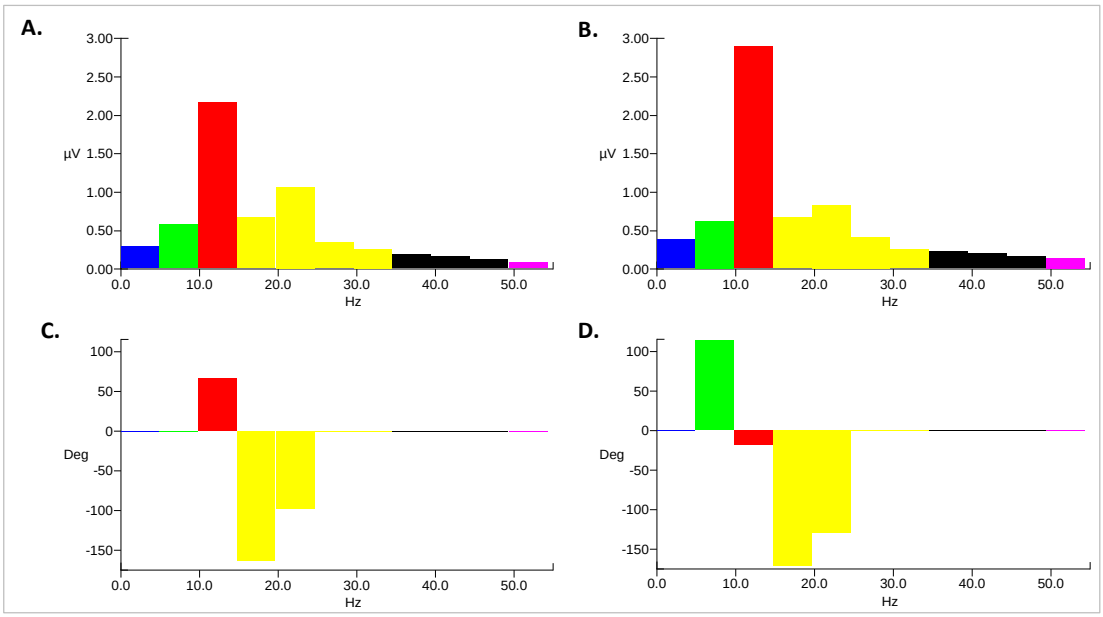

FIGURE 18. SCAN power spectrum of the LDR file. The frequency bands (delta, theta, alpha, beta, low gamma) are displayed as a series of colours. Amplitude of the power spectrum of the group average of the higher contrast in magnocellular stimulation: **(A)** CNT; **(B)** NF1. Phase of the power spectrum of the group average of the higher contrast in magnocellular stimulation: **(C)** CNT; **(D)** NF1.

The analysis of the frequency response was based on the definition of frequency bands, chosen based on published reports (**FIGURE 18**, **TABLE 7**), namely (Robert et al., 2009;Niedermeyer and Lopes da Silva, 1999;Taylor and Baldeweg, 2002). These values were computed by SCAN and saved into .xls files. We calculated an arithmetic mean of the amplitudes of the frequency bins inside the frequency band range. The phase analysis was performed only for the 10 Hz frequency - the frequency of the cortical response.

TABLE 7. The frequency bands were ranged within defined frequency bins. Frequency bands for magnocellular stimulation power spectra analysis.

PATHWAYS	FREQUENCY BAND (HZ)				
	Delta	Theta	Alpha	Beta	Low Gamma
MAGNOCELLULAR	-	5	10	15:20	25:35

- *Analysis of the **behavioural responses***

The button presses on the response pad (Compumedics Neuroscan, USA) were wired to the STIM® Audio System (Neuro Scan Labs) which allowed the recording of the button pressed and the time in which the participant pressed it. The matrix of these parameters could be taken out from the SCAN software.

The button press task aimed the gaze of the subjects on the fixation point. Therefore the VEP would be a consequence of the visual stimuli presented on the monitor rather than a consequence of other visual stimuli from the surroundings, and to avoid eye movements artifacts. However, importantly, we could also get performance measures. So, with a MatLab script (Appendix B.3), we got the percentage of right, wrong and no response relative to the number of the overall number of events (changes in luminance of the fixation square) and also the mean time they took to answer (latency to response) for right and wrong responses. The criteria took to classify the responses is explained below (**FIGURE 19**,

TABLE 8).

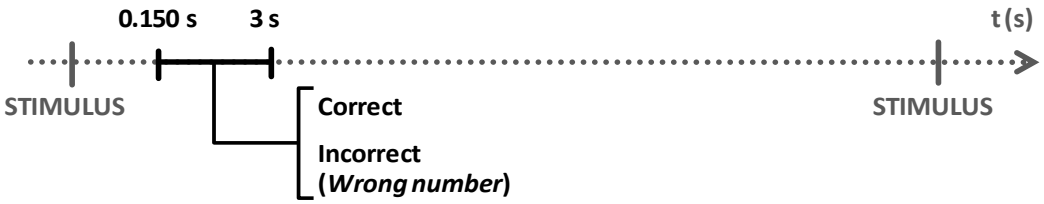

FIGURE 19. Conceptual diagram of the criteria to classify and count the motor responses.

TABLE 8. Criteria used to characterize the behavioural parameters.

• Correct Responses	The subject pressed the correct button within the time window of [0.150:3] seconds post-event;
• Incorrect Responses	The subject pressed a button within the time window of [0.150:3] seconds post-event;
• No Response	The subject pressed the wrong button before or after the time window of [0.150:3] seconds post-event or didn't press any button at all between two consecutive events;
• Latency	Elapsed time between the event and button press.

- ***Statistical Analysis***

The VEPs had several parameters as amplitude, latency and phase, that we wanted to analyse. In particular, we wanted to determine if they were modulated by contrast and if there was any significant difference between the two groups, CNT and NF1. Consequently, we performed ANOVA GLM (General Linear Model) Repeated Measures. First we checked the within-subject effects, i.e., if there was any significant difference of the measures with contrast for each group and if there was any interaction of contrast and group. If the significance level of the Mauchly's test was inferior to 0.05 ($p<0.05$), sphericity couldn't be assumed and we used the Greenhouse-Geisser correction. Then we analysed the between-subject effects, i.e, if there was any differences between groups.

Regarding the motor responses (called behavioural responses), we wanted to analyze the modulation of the percentage of answers, and latency within the runs for both groups, and if there was any significant difference between them. As in evoked potential analyses, we proceeded the same way, performing ANOVA GLM (General Linear Model) Repeated Measures.

For correlation statistics, we analysed the groups separately. Since the samples were relatively small (17 CNT; 17 NF1), we decided that it would be preferable to perform non parametric analysis. Therefore we computed the Spearman rho and the significance level, correlating all the parameters except the latencies of peaks (for parvo- and koniocellular measurements), age with mean amplitude (for magnocellular measurements), and latency for answer (in behaviour measurements for parvo- and koniocellular).

All the statistical tests were performed using SPSS Statistics 17.0 for Windows.

4. RESULTS

4.1. PARVOCELLULAR STIMULATION

4.1.1. GRAND AVERAGES

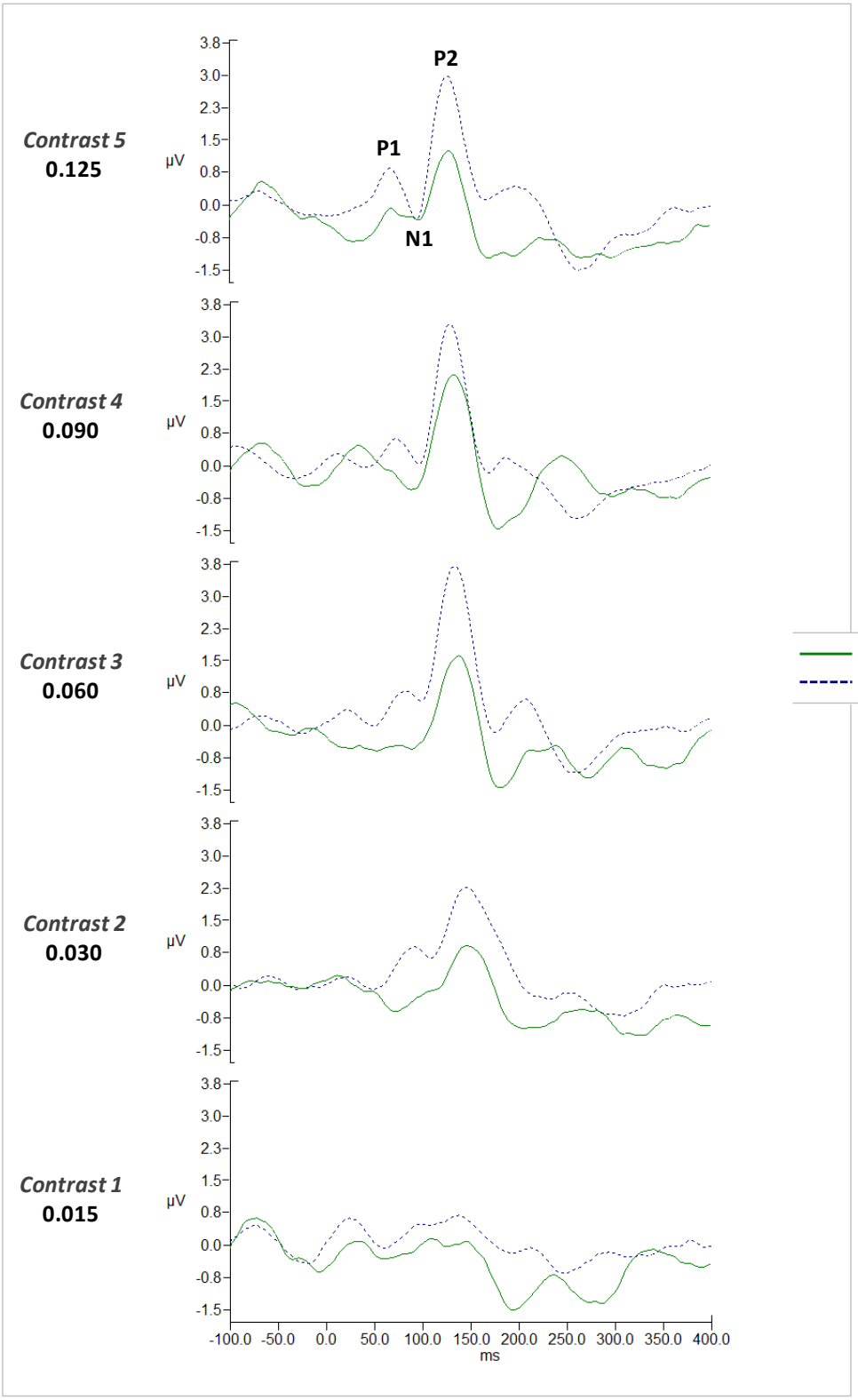

FIGURE 20. Grand averages of visual evoked potentials for parvocellular stimulation.

The parvocellular stimulation elicited transient VEPs as expected from temporal frequency of the stimuli (2 reversals per second). The low temporal frequency allows the response to each stimulus modulation to reset to baseline before the next modulation (Boon et al., 2005). The grand averages of the VEPs of both groups obtained with L-M cone stimulation, suggested the presence of one positive peak, P1, at [50:90]ms, followed by a negative peak, N1, at [60:120]ms, and a positive peak, P2, at [100:170]ms after the stimulus onset (**FIGURE 20**).

4.1.2. PEAK AMPLITUDE ANALYSIS

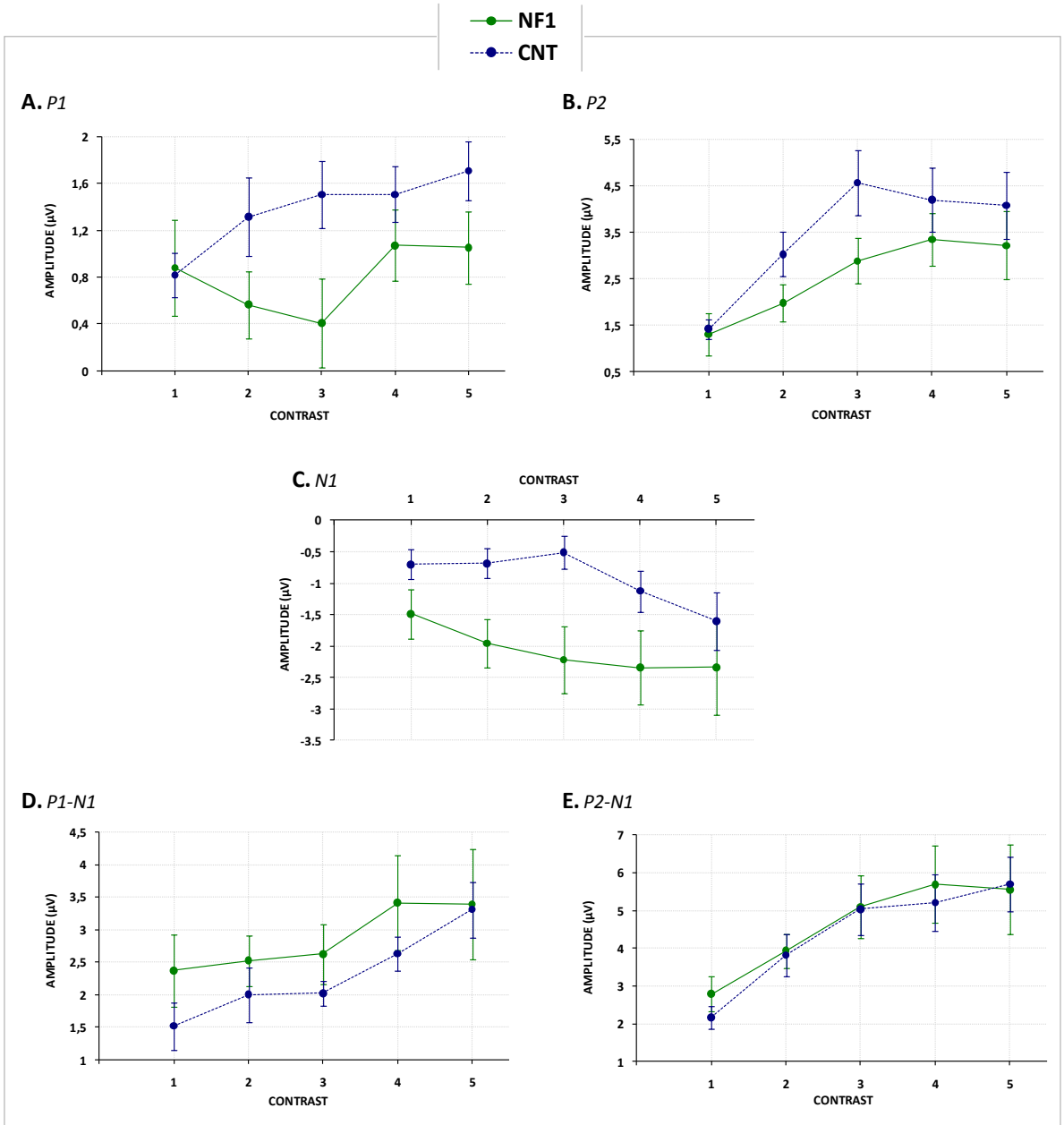

FIGURE 21. Average VEP peak amplitude as a function of contrast level for each group. **(A)** Mean amplitude of P1 – maximum amplitude in the time window of [50,90] ms; **(B)** Mean amplitude of P2 – maximum amplitude in the time window of [100,170] ms; **(C)** Mean amplitude of N1 – minimum amplitude in the time window of [60,120] ms; **(D)** Peak-to-peak amplitude: P1-N1; **(D)** Peak-to-peak amplitude: P2-N1;

Error bars represent ± standard error (SE).

TABLE 9. Statistical Analysis for parvocellular mean peak amplitude as a function of contrast.

	Effect of CONTRAST	Effect of GROUP	CONTRAST*GROUP interaction
P1	*F (4,128)=1.729* p = 0.147	*F (1,32)=3.922* p = 0.056	*F (4,128)=1.435* p = 0.226
P2	*F (2.626,84.042)=14.463* **p < 0.010****	*F (1,32)=2.115* p = 0.156	*F (2.626,84.042)=1.016* p = 0.383
N1	*F (1.942,62.129)=2.236* p = 0.117	*F (1,32)=5.805* **p < 0.050***	*F (1.942,62.129)=0.718* p = 0.488
P1-N1	*F (1.901,60.837)=5.377* **p < 0.010****	*F (1,32)=1.065* p = 0.310	*F (1.901,60.837)=0.361* p = 0.688
P2-N1	*F (1.809,57.897)=14.851* **p < 0.010****	*F (1,32)=0.072* p = 0.789	*F (1.809,57.897)=0.210* p = 0.790

Statistical analysis of the peak amplitudes revealed significant effects of contrast only for the second positive peak, P2. CNTs showed higher peak amplitudes for the positive peaks and lower amplitude for the negative peak (**FIGURE 20**). There was only group effect for N1. When we analysed the difference of the peak amplitudes, the group effect "disappeared". This evidence suggests that the group effect noticed on N1 (and on P1 is borderline) may be elicited by a baseline factor. P1 and N1 can be part of the same component and therefore it can be more accurate to analyse the peak difference as a measure of the response amplitude. This difference is independent of baseline correction. In spite of no group effect in the peak-to-peak analysis there's a significant and general increment of the amplitude with contrast that tends to saturate for higher contrast levels (**TABLE 9**).

4.1.3. PEAK LATENCY ANALYSIS

Regarding the **FIGURE 20**, for contrast 1, the peaks are not distinguishable from baseline. Therefore, it is not possible to accurately determine peak latency. Latencies should only be calculated from contrast 2 onwards.

Indeed, for peak latency analysis, we examined only the values of the latencies of each peak for the contrasts from 2 to 5.

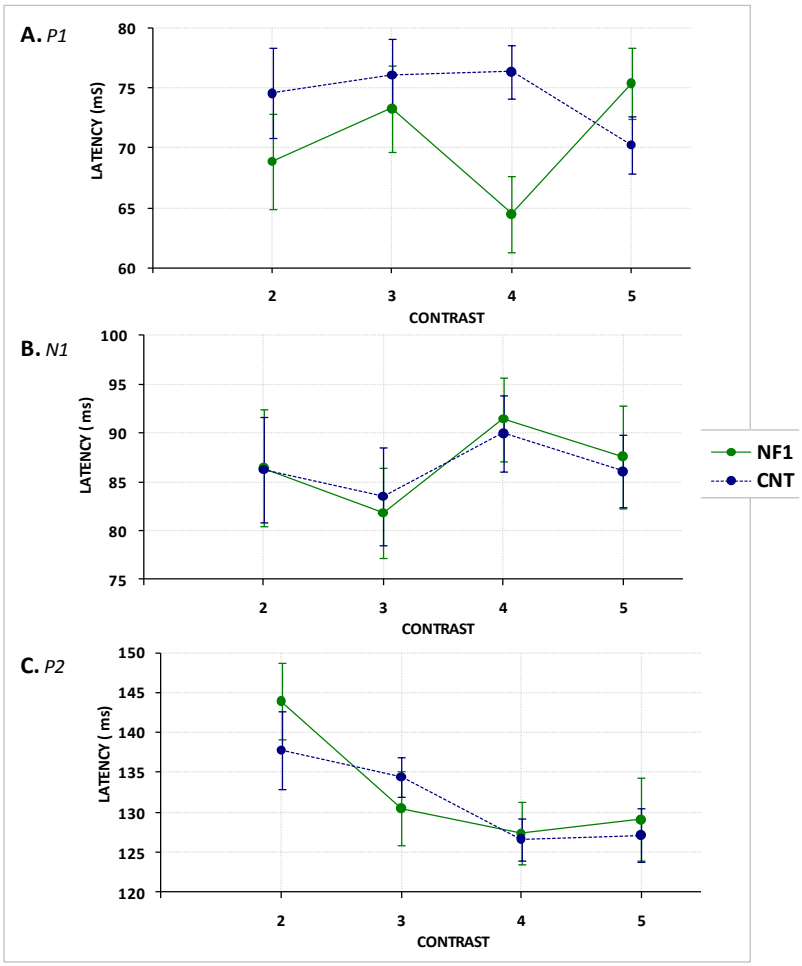

FIGURE 22. Mean peak latency for each group with stimulus contrast. **(A)** Mean latency of P1 – positive peak latency in the window of [50,90] ms; **(B)** Mean latency of N1 – negative peak latency in the time window of [100,170] ms; **(C)** Mean latency of P2 – positive peak latency in the time window of [60,120] ms.

Error bars represent ± SE.

TABLE 10. Statistical Analysis for parvocellular peak latency as a function of contrast.

	Effect of CONTRAST	Effect of GROUP	CONTRAST*GROUP interaction
P1	*F (3,96)=0.804* p = 0.495	*F (1,32)=1.763* p = 0.194	*F (3,96)=3.075* **p < 0.050***
N1	*F (3,96)=1.677* p = 0.177	*F (1,32)=0.005* p = 0.945	*F (3,96)=0.085* p = 0.968
P2	*F (1.824,58.362)=6.550* **p < 0.010****	*F (1,32)=0.097* p = 0.757	*F (1.824,58.362)=0.715* p = 0.481

Regarding the latency of the peaks, only P2 latency decreases significantly with stimulus contrast (**TABLE 10**). Indeed, as we may notice from **FIGURE 20**, P2 is the most prominent peak. P1 signal was so low that might not be distinguishable from background oscillations or noise. Therefore, the interaction between contrast and group verified by statistical analyses (**TABLE 10**) seems more likely to happen by chance. Both groups, CNTs and NF1, have a similar behaviour (**FIGURE 22**).

4.1.4. SPECTRAL ANALYSIS

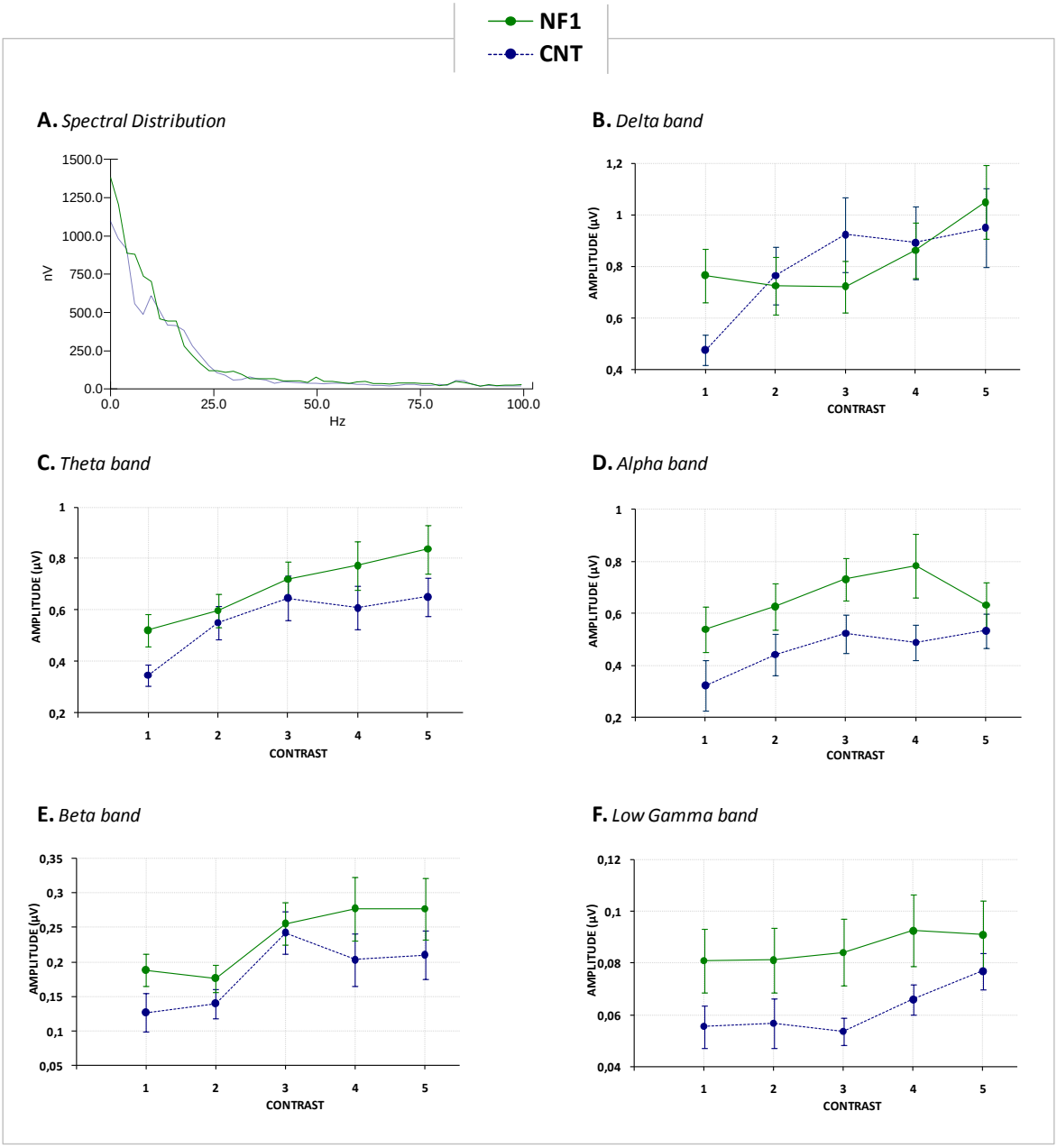

FIGURE 23. **(A)** Spectral distribution for each group. – Variation of the mean amplitude with the frequency of the waveform; Mean amplitude for each group with the contrast within each frequency band: **(B)** delta band [2-4]Hz; **(C)** theta band [4-8]Hz; **(D)** alpha band [8-12]Hz; **(E)** beta band [14-24]Hz; **(F)** low gamma band [24-40]Hz;

Error bars represent ± SE.

TABLE 11. Statistical Analysis for parvocellular mean amplitude as a function of contrast for each frequency band.

	Effect of CONTRAST	Effect of GROUP	CONTRAST*GROUP interaction
Delta	*F (4,128)=5.377* **p < 0.010****	*F (1,32)=0.032* p = 0.859	*F (4,128)=2.239* p = 0.068
Theta	*F (3.017,96.559)=11.602* **p < 0.010****	*F (1,32)=2.299* p = 0.139	*F (3.017,96.559)=0.786* p = 0.505
Alpha	*F (2.918,93.389)=3.787* **p < 0.050***	*F (1,32)=4.436* **p < 0.050***	*F (2.918,93.389)=0.670* p = 0.569
Beta	*F (1.680,53.756)=22.236* **p < 0.010****	*F (1,32)≈0.000* p = 0.996	*F (1.680,53.756)=1.554* p = 0.222
Low Gamma	*F (2.674,85.554)=6.217* **p < 0.010****	*F (1,32)=2.993* p = 0.093	*F (2.674,85.554)=6.217* p = 0.346

Since the temporal frequency of the stimulus is 2Hz and delta band includes this frequency within its range, we need to take care in its analysis because it may lead to misleading conclusions. We can't disentangle the reversal oscillation rate of the parvocellular stimulation from the ongoing 2Hz rhythm. Therefore the delta band defined might be potentiated by the partial synchronization with the frequency of the stimulation.

For all the rhythms analyzed there is a significant effect of contrast in the amplitude (**TABLE 11**), NF1 children having higher amplitudes than CNTs (**FIGURE 23**).

One curious aspect is the alpha band analysis result which is the only one that shows a significant effect of group (**TABLE 11**), with the NF1 having higher amplitude than CNTs.

4.2. KONIOCELLULAR STIMULATION

4.2.1. GRAND AVERAGES

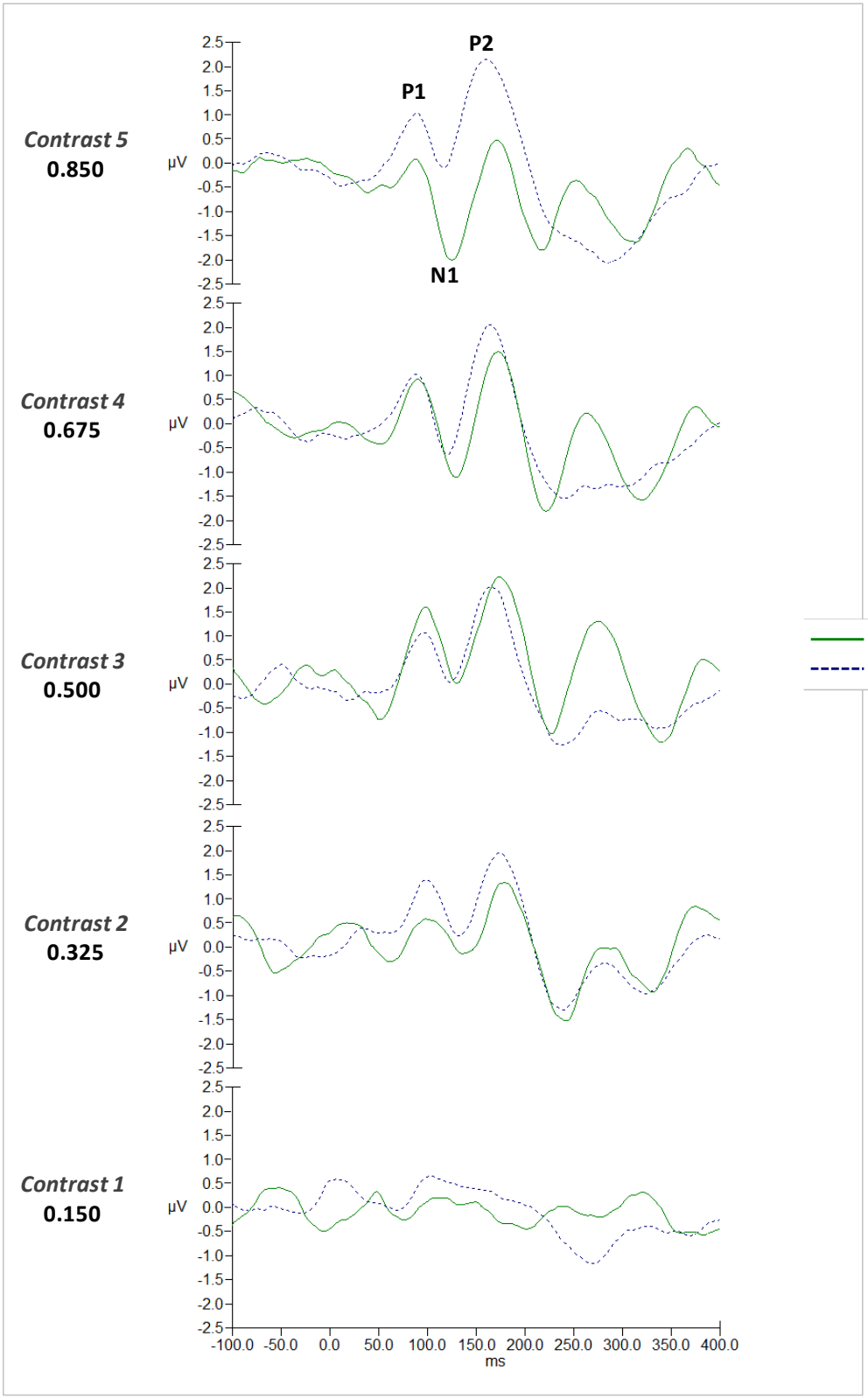

FIGURE 24. Grand averages of VEPs for koniocellular stimulation.

As in the parvocellular stimulation, koniocellular stimulation elicited transient VEPs as expected from temporal frequency of the stimuli (also 2 reversals per second), with similar characteristics. As before, the low temporal frequency allows the response to each stimulus modulation to reset to baseline before the next modulation (Boon et al., 2005). The grand averages of the VEPs of both groups obtained with S cone stimulation, showed two positive components, P1 and P2, and one negative component, N1, peaking around [70:110]ms, [130:200]ms, [100:150]ms, respectively, after the stimulus onset (**FIGURE 24**).

4.2.2. PEAK AMPLITUDE ANALYSIS

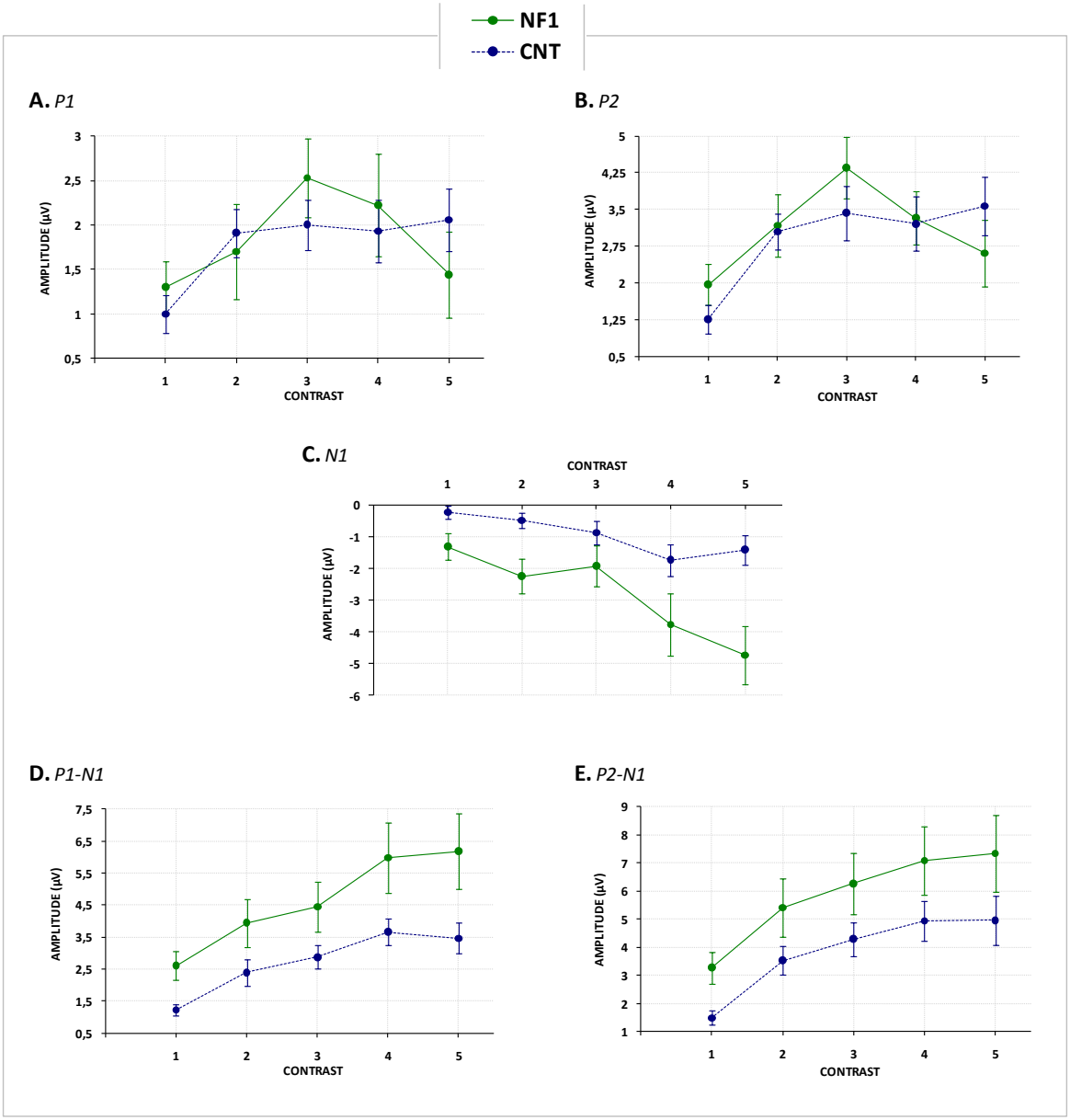

FIGURE 25. Average VEP peak amplitude as a function of contrast level for each group. **(A)** Mean amplitude of P1 – maximum amplitude in the time window of [70,110] ms; **(B)** Mean amplitude of P2 – maximum amplitude in the time window of [130,200] ms; **(C)** Mean amplitude of N1 – minimum amplitude in the time window of [100,150] ms; **(D)** Peak-to-peak amplitude: P1-N1; **(D)** Peak-to-peak amplitude: P2-N1.
Error bars represent ± SE.

TABLE 12. Statistical Analysis for koniocellular mean peak amplitude as a function of contrast.

	Effect of CONTRAST	Effect of GROUP	CONTRAST*GROUP interaction
P1	*F (4,128)=3.460* **p < 0.050***	*F (1,32)=0.024* p = 0.878	*F (4,128)=1.036* p = 0.391
P2	*F (4,128)=9.700* **p < 0.010****	*F (1,32)=0.093* p = 0.762	*F (4,128)=1.858* p = 0.122
N1	*F (2.171,69.481)=10.737* **p < 0.010****	*F (1,32)=8.877* **p < 0.010****	*F (2.171,69.481)=2.383* p = 0.095
P1-N1	*F (2.407,77.039)=14.125* **p < 0.010****	*F (1,32)=6.126* **p < 0.050***	*F (2.407,77.039)=0.788* p = 0.479
P2-N1	*F (2.254,72.120)=15.441* **p < 0.010****	*F (1,32)=3.841* p = 0.059	*F (2.254,72.120)=0.088* p = 0.934

The peak analysis for koniocellular stimulation showed a significant effect of contrast for all the components in analysis (**TABLE 12**), NF1 children having higher amplitudes than CNTs. Amplitudes of P1, P2, P1-N1 and P2-N1 seem to saturate for higher contrast levels (**FIGURE 25**).

Statistical analysis showed a significant effect of group only for N1 and P1-N1 (**TABLE 12**). This might suggest that in koniocellular VEPs, N1 is a relevant/characteristic component in this type of stimulation and its amplitude varies with the group. Therefore, the P1-N1 and P2-N1 effect of group may be linked to the N1 effect.

4.2.3. PEAK LATENCY ANALYSIS

Regarding the **FIGURE 24**, for contrast 1, as in parvocellular analysis, the peaks are not distinguishable from baseline. Therefore, it is not possible to accurately determine peak latency. Latencies should only be calculated from contrast 2 onwards.

So, for peak latency analysis, we examined only the values of the latencies of each peak for the contrasts from 2 to 5.

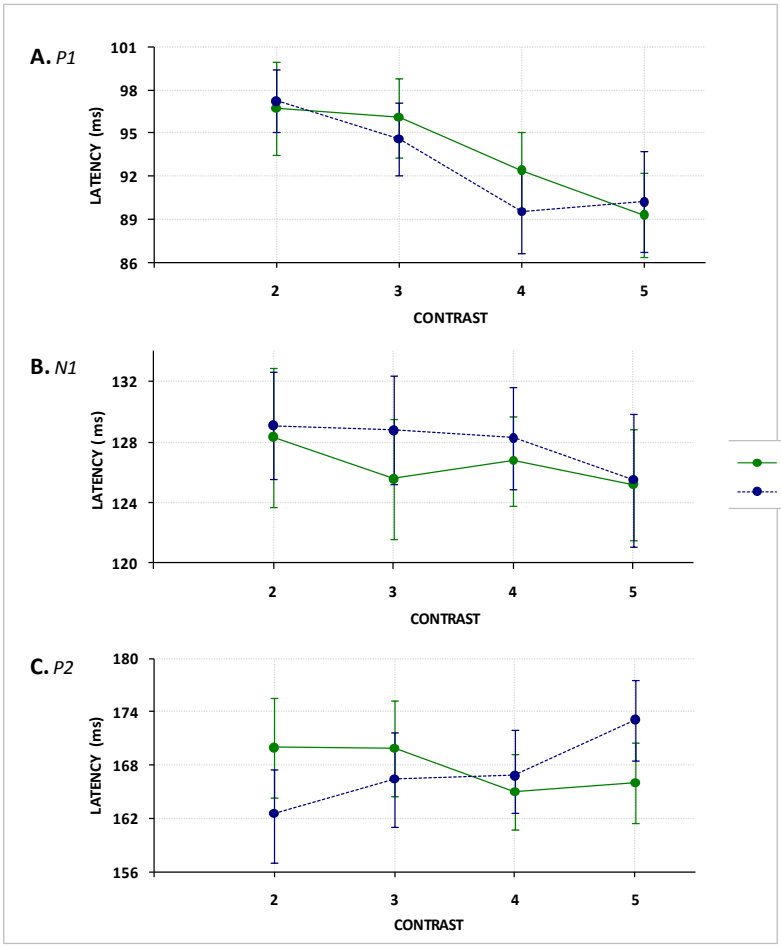

FIGURE 26. Mean peak latency for each group with the contrast. **(A)** Mean latency of P1 – maximum peak latency in the window of [70,110] ms; **(B)** Mean latency of N1 – minimum peak latency in the time window of [100,150] ms; **(C)** Mean latency of P2 – maximum peak latency in the time window of [130,200] ms.

Error bars represent ± SE.

TABLE 13. Statistical Analysis for koniocellular mean peak latency as a function of contrast.

	Effect of CONTRAST	Effect of GROUP	CONTRAST*GROUP interaction
P1	*F (3,96)=5.042* **p < 0.010****	*F (1,32)=0.057* p = 0.812	*F (3,96)=0.335* p = 0.800
N1	*F (1.898,60.739)=0.384* p = 0.672	*F (1,32)=0.151* p = 0.700	*F (1.898,60.739)=0.083* p = 0.912
P2	*F (3,96)=0.300* p = 0.825	*F (1,32)=0.011* p = 0.915	*F (3,96)=1.033* p = 0.382

There is only a significant effect of contrast in P1 latency (**TABLE 13**). With the enhancement of contrast, P1 peak that seems to be arise later in time (**FIGURE 26**).

4.2.4. SPECTRAL ANALYSIS

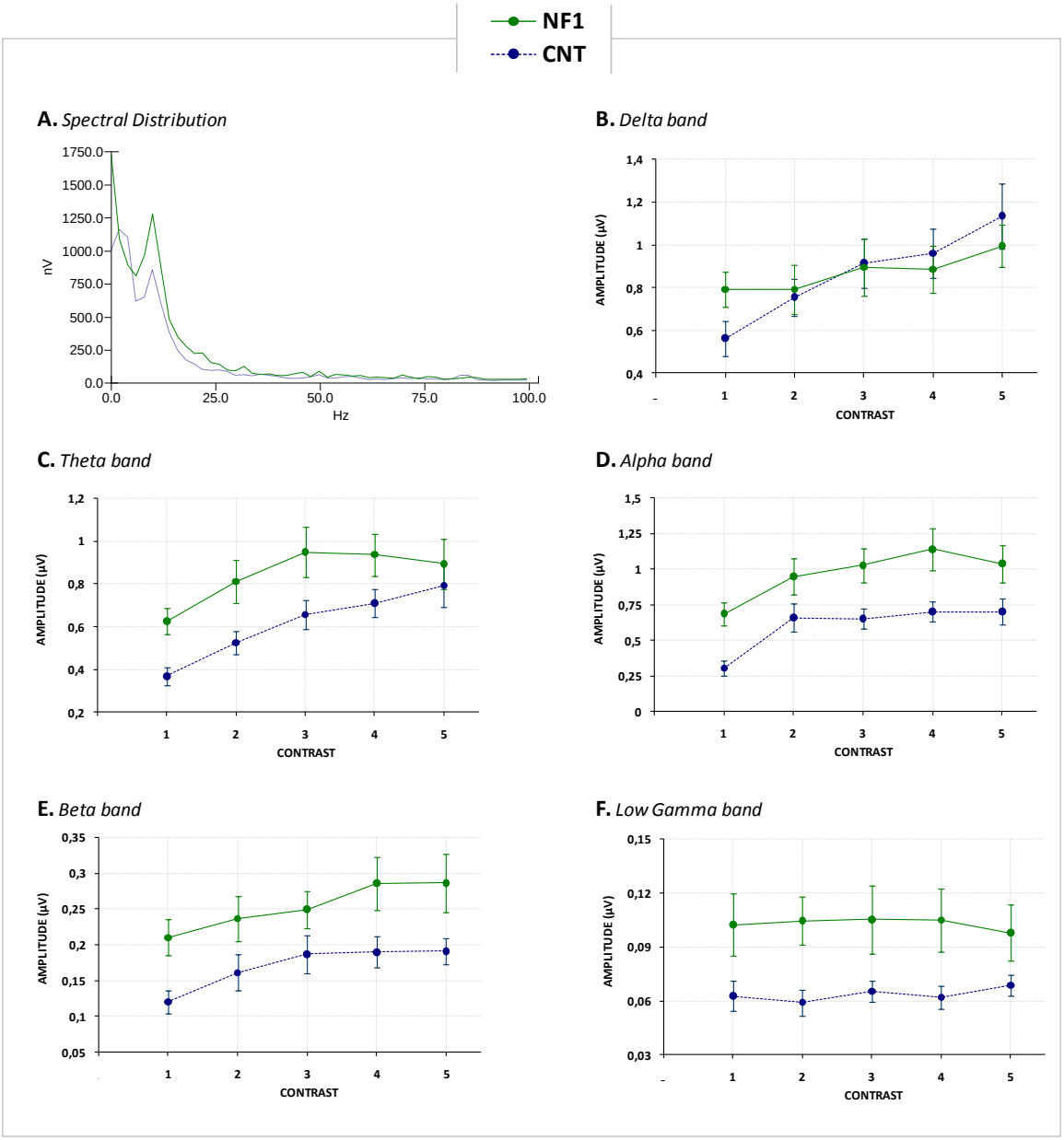

FIGURE 27. (A) Spectral distribution for each group. – Variation of the mean amplitude with the frequency of the waveform; Mean amplitude for each group with the contrast within each frequency band: **(B)** delta band [2-4]Hz; **(C)** theta band [4-8]Hz; **(D)** alpha band [8-12]Hz; **(E)** beta band [14-24]Hz; **(F)** low gamma band [24-40]Hz;

Error bars represent ± SE.

TABLE 14. Statistical Analysis for koniocellular mean amplitude as a function of contrast for each frequency band.

	Effect of CONTRAST	Effect of GROUP	CONTRAST*GROUP interaction
Delta	*F (4,128)=7.528* **p < 0.010****	*F (1,32)=0.002* p = 0.961	*F (4,128)=1.671* p = 0.161
Theta	*F (2.962,94.773)=11.745* **p < 0.010****	*F (1,32)=6.024* **p < 0.050***	*F (2.962,94.773)=0.838* p = 0.475
Alpha	*F (4,128)=14.345* **p < 0.010****	*F (1,32)=8.886* **p < 0.010****	*F (4,128)=0.391* p = 0.815
Beta	*F (2.875,92.004)=6.164* **p < 0.010****	*F (1,32)=6.460* **p < 0.050***	*F (2.875,92.004)=0.340* p = 0.788
Low Gamma	*F (4,128)=0.194* p = 0.941	*F (1,32)=5.206* **p < 0.050***	*F (4,128)=0.893* p = 0.470

Like in parvocellular stimulus, koniocellular stimulus has a temporal frequency and evoked reponse at 2Hz. Since delta band includes this frequency within its range, we need to take care in its analysis because it may lead to misleading conclusions. We can't disentangle the reversal oscillation rate of the koniocellular stimulation from the ongoing 2Hz rhythm. Therefore the delta band defined might be potentiated by the partial synchronization with the frequency of the stimulation.

There is a significant effect of contrast in the amplitude, for all the rhythms analyzed, except for low gamma band (**TABLE 14**). NF1 children showed higher amplitudes than CNTs (**FIGURE 27**).

Differently from parvocellular stimulation, the spectrum analysis indicate an effect of group for theta, beta and low gamma frequency bands, especially for alpha band, with p-value lower than 0.010 (**TABLE 14**), and NF1 amplitudes significantly higher than CNTs.

4.3. MAGNOCELLULAR STIMULATION

4.3.1. GRAND AVERAGES

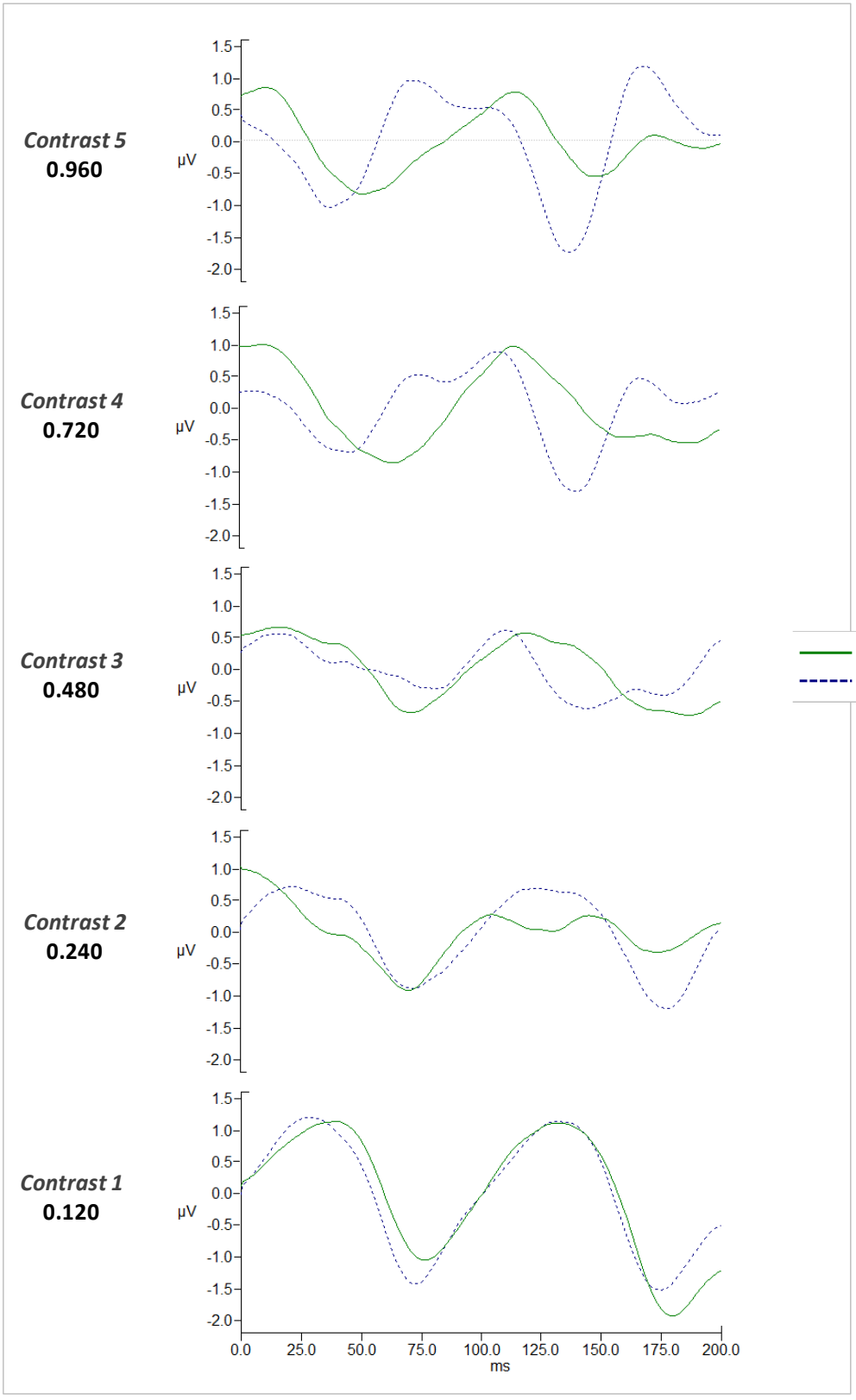

FIGURE 28. Grand averages of VEPs for magnocellular stimulation.

According to (Lee, 1996), to maximize the magnocellular contribution to the response of the achromatic stimulation, the stimuli used reversed at high frequency (10 reversals per second). The high frequency of the stimuli elicited steady state VEPs with a cycling frequency equal to the double of the cycling frequency of the stimulus (reversal rate of the stimulus). Differently from the chromatic evoked response, the achromatic stimulation elicits steady-state VEPs. The higher temporal frequency enables a summation of response such that the VEP produced is nearly sinusoidal with approximately constant amplitude and periodicity (Boon et al., 2005). The shape of the VEPs suggest the presence of two largely overlapping components (**FIGURE 28**).

4.3.2. MEAN AMPLITUDE

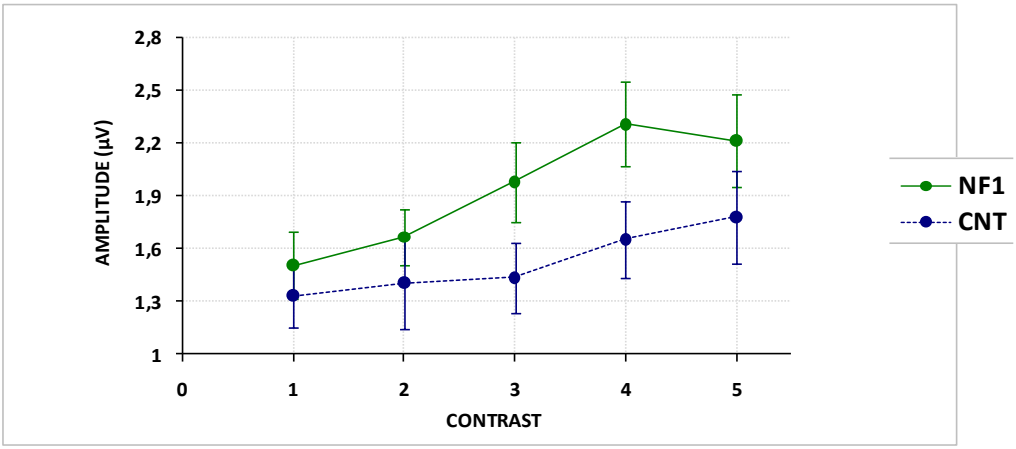

FIGURE 29. Mean amplitude of the rectified magnocellular evoked potential for each group as a function of contrast.

Error bars represent ± SE.

TABLE 15. Statistical analysis of mean amplitude of the magnocellular wave.

	Effect of CONTRAST	Effect of GROUP	CONTRAST*GROUP interaction
Mean Amplitude	*F (2.657,85.012)=7.361* **p < 0.010****	*F (1,32)=2.443* p = 0.357	*F (2.657,85.012)=1.080* p = 0.128

Since the two components overlap significantly (**FIGURE 28**), peaks do not necessarily represent the latency and amplitude of the underlying components (Luck, 2004). Therefore, for the analysis of the achromatic response, we did not separate the different components, instead, we measured the mean amplitude of the rectified wave over the period of one phase-reversed stimulus cycle. This measure can, that way, be a measure of strength of the signal evoked in the visual cortex (Luck, 2004). Repeated measures analysis of the mean amplitude showed a significant effect of

contrast (**FIGURE 29**), NF1 children having higher amplitudes than CNTs with a amplitude saturation for higher levels of contrast (**TABLE 15**). However, we did not observe any effect of group.

4.3.3. LATENCY ANALYSIS

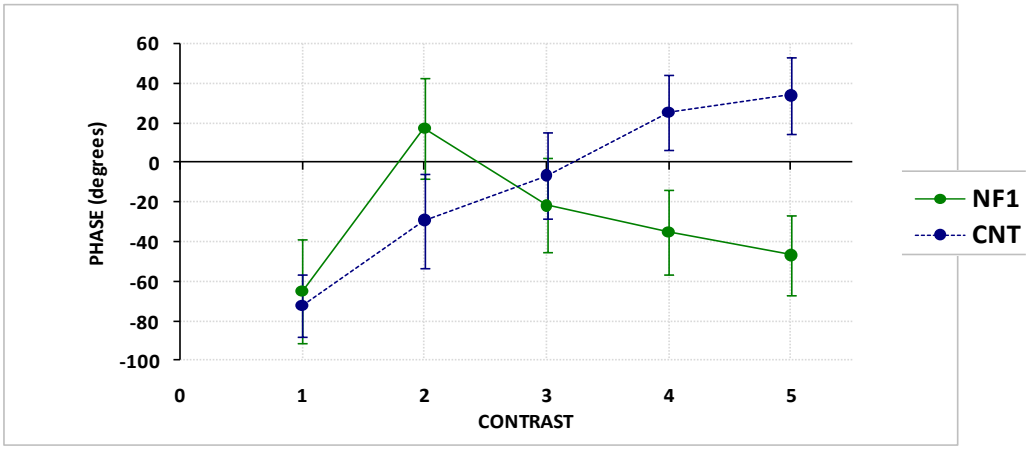

FIGURE 30. Mean phase of the magnocellular wave for each group as a function of contrast (at 10 Hz).

Error bars represent ± SE.

TABLE 16. Statistical analysis of the magnocellular wave phase.

	Effect of CONTRAST	Effect of GROUP	CONTRAST*GROUP interaction
Phase	*F (2.269,72.618)=3.965* **p < 0.050***	*F (1,32)=1.196* p = 0.282	*F (2.269,72.618)=3.465* **p < 0.050***

For the same reasons pointed out on magnocellular mean amplitude analysis, since there aren't defined peaks, we didn't perform latency analysis by the latency of the peaks. Instead, due to the shape of the wave (**FIGURE 28**), the latency analysis was based on the phase of the wave (phase at 10Hz, the frequency of the evoked response). The statistical analysis revealed an effect of contrast but not of group (**TABLE 16**). Rather, inspecting (**FIGURE 30**), we notice different behaviours of phase with contrast for each group. Indeed, statistical data show that there's a significant interaction of contrast with group (**TABLE 16**).

4.3.4. SPECTRAL ANALYSIS

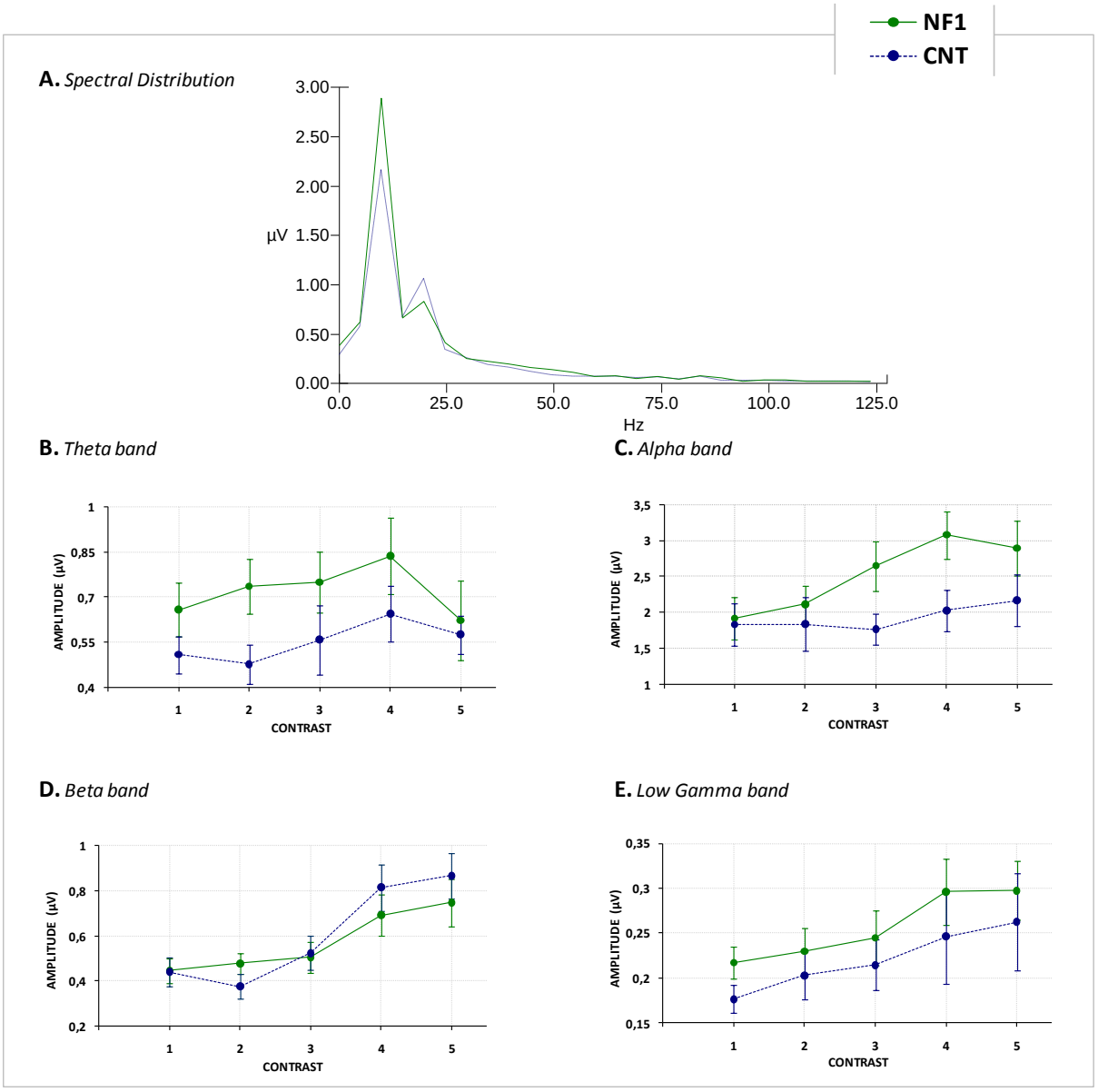

FIGURE 31. (A) Spectral distribution for each group. – Variation of the mean amplitude with the frequency of the waveform; Mean amplitude for each group with the contrast within each frequency band: **(B)** theta band [5]Hz; **(C)** alpha band [10]Hz; **(D)** beta band [15-20]Hz; **(E)** low gamma band [25-35]Hz;

Error bars represent ± SE.

TABLE 17. Statistical Analysis for magnocellular mean amplitude as a function of contrast for each frequency band.

	Effect of CONTRAST	Effect of GROUP	CONTRAST*GROUP interaction
Theta	*F (4,128)=1.132* p = 0.344	*F (1,32)=3.872* p = 0.058	*F (4,128)=0.419* p = 0.795
Alpha 10Hz	*F (2.383,76.251)=4.774* **p < 0.010****	*F (1,32)=2.700* p = 0.110	*F (2.383,76.251)=2.047* p = 0.128
Beta	*F (2.120,67.849)=23.526* **p < 0.010****	*F (1,32)=0.113* p = 0.739	*F (2.120,67.849)=1.633* p = 0.202
Low Gamma	*F (1.835,58.716)=5.810* **p < 0.010****	*F (1,32)=0.808* p = 0.376	*F (1.835,58.716)=0.095* p = 0.895

Since the temporal frequency of the stimulus is 5 Hz (10 Hz phase-reversal) and alpha band analysis is based on this frequency amplitudes, we need to take care in its analysis because the response evoked by the stimulus and alpha oscillations are overlapping at same oscillating frequency.

For all the rhythms analyzed (**FIGURE 31**) there is a very significant effect of contrast in the amplitude, except for theta band, which is, intriguingly the only one that has a very borderline effect of group (**TABLE 17**).

4.4. BEHAVIOURAL ANALYSIS – TASK PERFORMANCE AS A MEASURE OF ATTENTION DURING THE EXPERIMENTAL PROCEDURE

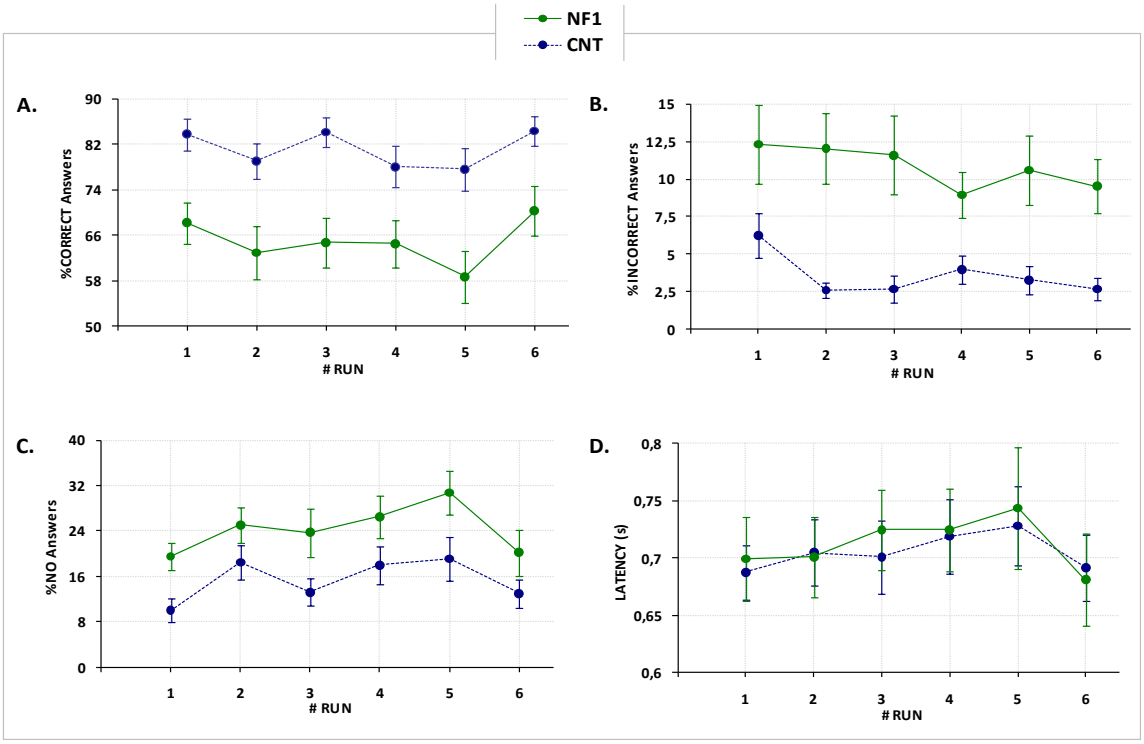

FIGURE 32. Behavioural analysis. **(A)** percentage of correct answers; **(B)** percentage of incorrect answers; **(C)** percentage of no answers; **(D)** latency of correct answers.
Error bars represent ± SE.

TABLE 18. Statistical analysis of behavioural responses.

	Effect of RUN	Effect of GROUP	RUN*GROUP interaction
% Correct Answers	*F (5,145)=3.846* **p < 0.010****	*F (1,29)=13.836* **p < 0.010****	*F (5,145)=0.665* p = 0.650
% Incorrect Answers	*F (5,145)=2.475* **p < 0.050***	*F (1,29)=17.056* **p < 0.010****	*F (5,145)=1.186* p = 0.319
% No Answers	*F (3.545,102.808)=5.228* **p < 0.010****	*F (1,29)=5.364* **p < 0.050***	*F (3.545,102.808)=0.363* p = 0.812
Latency	*F (3.482,100.987)=1.491* p = 0.216	*F (1,29)=0.005* p = 0.946	*F (3.482,100.987)=1.102* p = 0.356

To analyze the behavioural responses we calculated the percentage of each type of responses for each participant, for each run. There's no interaction between group and run, meaning that the effect of run is similar for both groups. The statistical analysis revealed significant effects of run and group on the percentage of the responses, either correct, incorrect or no answer. CNTs answer correctly more often than NF1s. NF1s also answer less times. Nonetheless, there's no group effect on latency suggesting that NF1 children take the same time as controls to respond correctly. The same velocity to answer may suggest the absence of motor problems. In general, these results suggest that NF1 children have more difficulty detecting the events, or in task comprehension. It is also possible that they pay less attention in the task or are less motivated to perform well.

4.5. STATISTICAL CORRELATIONS BETWEEN SEVERAL PARAMETERS FOR PARVOCELLULAR AND KONIOCELLULAR STIMULATION

4.5.1. ALPHA MEASUREMENTS CAN CORRELATE WITH THE EVOKED RESPONSE OF NF1 PATIENTS

TABLE 19. *Spearman's rho coefficient* and *p-value* for correlations of Parvo- and Koniocellular parameter means with the mean amplitude of alpha band for both groups.
*Extracted from (***TABLE 21**-**TABLE 24***) on the* 9. Appendix.D.

Spearman's rho		Alpha Mean Amplitude			
		Parvocellular Measures		Koniocellular Measures	
		CNT	NF1	CNT	NF1
P1 Mean Amplitude	*Cc*	,316	,473	,125	**,576***
	Sig. (2-tailed)	,216	,055	,633	**,016**
N1 Mean Amplitude	*Cc*	-,331	**-,495***	-,426	**-,591***
	Sig. (2-tailed)	,195	**,043**	,088	**,013**
P2 Mean Amplitude	*Cc*	**,797****	**,846****	**,775****	**,819****
	Sig. (2-tailed)	**,000**	**,000**	**,000**	**,000**
P1-N1 Mean Amplitude	*Cc*	**,556***	**,657****	,475	**,650****
	Sig. (2-tailed)	**,020**	**,004**	,054	**,005**
P2-N1 Mean Amplitude	*Cc*	**,873****	**,885****	**,892****	**,787****
	Sig. (2-tailed)	**,000**	**,000**	**,000**	**,000**
%Mean Correct Answers	*Cc*	-,054	**-,483***	,233	-,064
	Sig. (2-tailed)	,837	**,050**	,368	,808
%Mean No Answers	*Cc*	-,025	,112	-,278	-,155
	Sig. (2-tailed)	,926	,670	,279	,554
Age	*Cc*	**-,512***	**-,654****	-,341	-,469
	Sig. (2-tailed)	**,036**	**,004**	,181	,058

. Correlation is significant at the 0.05 level (2-tailed).
****. Correlation is significant at the 0.01 level (2-tailed).***
Cc = Correlation coefficient

There is a significant correlation between evoked alpha amplitude and evoked potential amplitude in both groups for two conditions (P1-N1 and P2-N1). This indicates that the measured peak amplitudes are related to the oscillatory activity (**TABLE 19**).

As we may notice from the statistical results on the **TABLE 19**, there's only a significant correlation between alpha mean amplitude and the percentage of correct answers for NF1 individuals and for parvocellular stimulation. However, excluding an NF1 case that seemed an outlier (by graphic inspection), annulled the correlation. Therefore we may conclude that there isn't a correlation between the alpha amplitude and the behaviour performance.

Still regarding the results presented on the **TABLE 19**, we notice a negative and significant correlation between the evoked alpha amplitude and the age of the individuals for both groups, but only on the parvocellular pathway. These results suggest a modulation of the evoked alpha amplitude on the parvocellular pathway with age, within the range of age of our participants, children and adolescents.

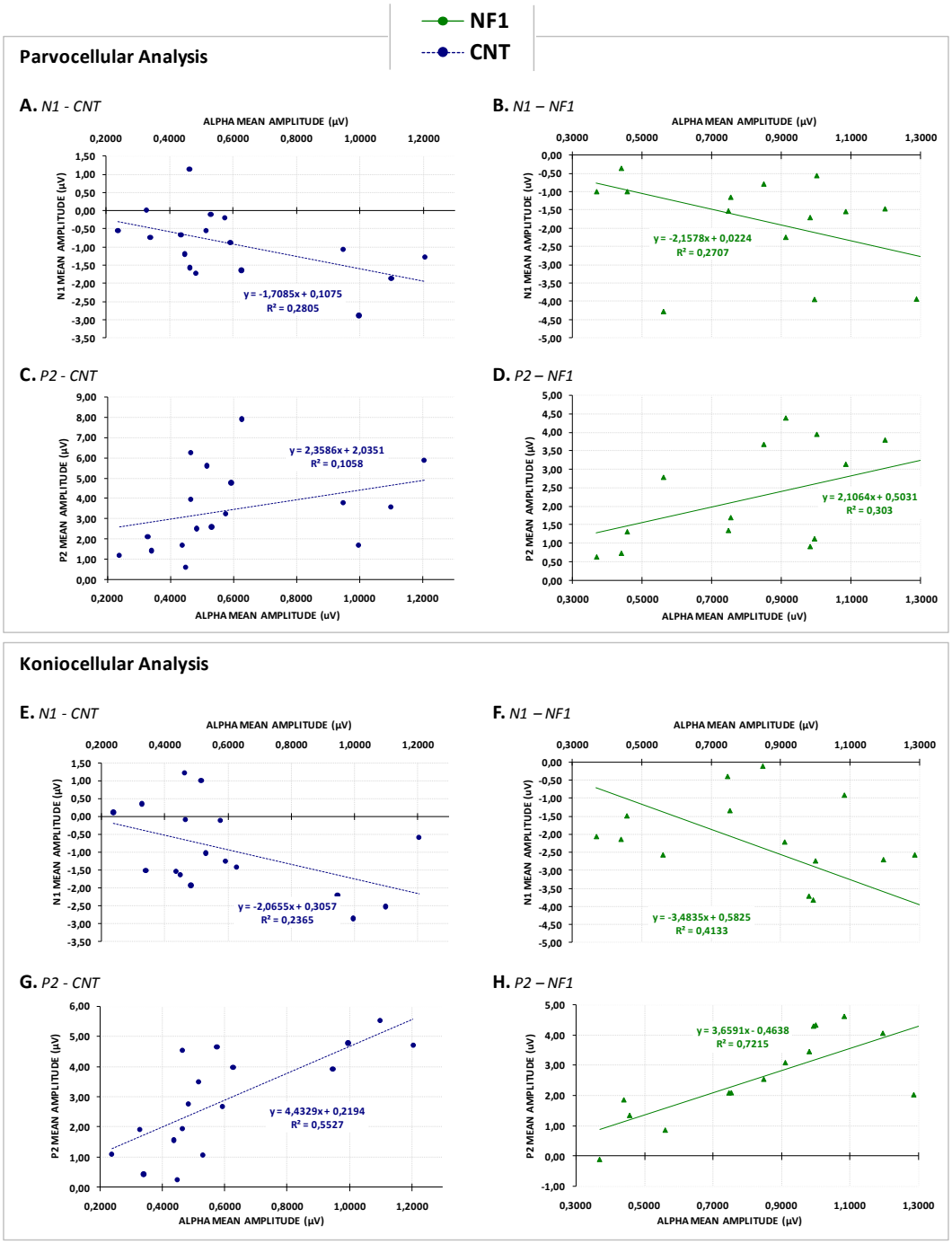

FIGURE 33. Scatter plots of the values of the alpha mean amplitude and the respective values of the N1 and P2 mean amplitudes for parvo- and koniocellular analysis. *Parvocellular Analysis*: **(A)** N1 amplitude for CNTs; **(B)** N1 amplitude for NF1 group; **(C)** P2 amplitude for CNTs; **(D)** P2 amplitude for NF1 group. *Koniocellular Analysis*: **(E)** N1 amplitude for CNTs; **(F)** N1 amplitude for NF1 group; **(G)** P2 amplitude for CNTs; **(H)** P2 amplitude for NF1 group.

For both parvo- and koniocellular stimulation we verify a strong and very significant correlation between P2 and alpha mean amplitude for both groups (**TABLE 19**, **FIGURE 33. C, D, G, H**). Interestingly, there is a significant correlation between N1 and alpha mean amplitude but only for

NF1 individuals (**TABLE 19**, **FIGURE 33. A, B, E, F**). This result meets the hypothesis of an overlapping of evoked alpha with the evoked response.

4.5.2. SELECTIVE AGE MODULATION OF PEAK AMPLITUDE OF THE EVOKED RESPONSE SUGGESTS DIFFERENT MATURATION FOR PARVO- AND KONIOCELLULAR PATHWAYS

TABLE 20. *Spearman's rho coefficient* and *p-value* for correlations of Parvo- and Koniocellular of the means of the peak amplitudes with the age for both groups.

*Extracted from (***TABLE 21**-**TABLE 24***) on the* 9. Appendix.D.

Spearman's rho		AGE					
		Parvocellular Measures		Koniocellular Measures		Magnocellular Measures	
		CNT	NF1	CNT	NF1	CNT	NF1
P1 Mean Amplitude	*Cc*	**-,493***	-,135	-,137	-,358	---	---
	Sig. (2-tailed)	**,045**	,606	,599	,158		
N1 Mean Amplitude	*Cc*	-,199	,239	-,267	-,048	---	---
	Sig. (2-tailed)	,445	,355	,300	,855		
P2 Mean Amplitude	*Cc*	**-,578***	-,458	-,272	-,314	---	---
	Sig. (2-tailed)	**,015**	,065	,291	,220		
P1-N1 Mean Amplitude	*Cc*	-,123	-,220	,025	-,013	---	---
	Sig. (2-tailed)	,639	,397	,926	,959		
P2-N1 Mean Amplitude	*Cc*	**-,490***	**-,529***	-,257	-,112	---	---
	Sig. (2-tailed)	**,046**	**,029**	,319	,670		
Mean Amplitude	*Cc*	---	---	---	---	**-,483***	-,042
	Sig. (2-tailed)					**,050**	,874

**. Correlation is significant at the 0.05 level (2-tailed).*

***. Correlation is significant at the 0.01 level (2-tailed).*

Cc = Correlation coefficient

We analysed the possible correlations between the peak amplitudes and the age of all participants for parvo- and koniocellular stimulation (**TABLE 20**). For magnocellular stimulation we analysed the possible correlations between the mean amplitude and the age of all participants. For koniocellular measures there's no correlation between age and any of the peaks, for both groups. For parvocellular measures, there's a significant correlation with age for P1, P2 and P2-N1, for CNTs. Although there's only a correlation with P2-N1 amplitude for NF1 children, we may say that the parvocellular pathway maturates within the age range of our participants. For magnocellular measures we observe a borderline and weak correlation of amplitude with age but only for controls. The different results for parvo- and konio- and magnocellular measures indicate a distinct group dependent maturation of the visual streams with age.

5. DISCUSSION

One possible direction to study and test the excess of inhibition in NF1 individuals is by taking advantage of the well established role of inhibitory neurotransmission in visual perception. Indeed, (Lund et al., 2003) reported that a balance between excitatory and inhibitory neurotransmission establishes the centre-surround antagonism and determine the receptive fields properties of visual neurons. Thus, centre-surround antagonism ensures the response of visual neurons to contrast and not to homogenous visual stimulation. Therefore, an alteration in inhibition will alter the perception of contrast. More inhibition leads to a decrease in the neuronal firing rate of the ganglion cells and other visual neurons.

One main finding of this work was the higher amplitude of the evoked potentials for NF1 children. This was an unexpected result since the main hypothesis of enhanced inhibition of the neuronal response to visual contrast in NF1 individuals would at first glance predict a decrease of the evoked potentials amplitude. This result, therefore, might be interpreted in contrary to what would be expected if NF1 was related to an increase in GABAergic transmission in the visual brain areas. However, our results also indicated that NF1 individuals showed brain oscillations with significantly higher amplitudes than controls, especially for the band centred on 10 Hz. Interestingly, enhanced amplitude of brain oscillations might be associated with enhanced inhibitory transmission. In turn, the increased amplitudes observed in the evoked responses might be a consequence of enhanced oscillatory activity and therefore an indirect consequence of enhanced inhibition.

- ***NF1 present higher levels of evoked alpha rhythm than controls, fitting the hypothesis of excess of inhibitory neurotransmission in NF1***

Rhythmic changes in the level of depolarization in the neuronal membrane potentials of a group of neurons are reflected in brain oscillations. Therefore, these naturally occurring oscillations reflect phases of low versus high excitability, regulating the transmission, and influencing the processing of early-stage visual information (Klimesch et al., 2007;Lorincz et al., 2009). The predominant oscillation in the visual cortex is the alpha rhythm. By performing the FFT of the VEPs, we were able to determine the evoked alpha, the ongoing alpha time-locked with stimulus presentation. The analysis of the alpha rhythm indicated that its amplitude is modulated by the stimulus contrast and it is significantly higher for NF1 children. Cortical alpha is believed to be modulated by thalamo-cortico-thalamic networks, dictated by rhythmic fluctuations of GABAergic neurons of both thalamus and cortex (Klimesch et al., 2007). There are several pharmacological studies indicating that brain rhythms are affected by the administration of benzodiazepines, drugs

that enhance GABAergic neurotransmission. (Alexander et al., 2004) reported reductions in alpha power following lorazepam administration. By contrast, (Hall et al., 2010) describe an increase in the intrinsic baseline alpha after diazepam administration. These paradoxical observations are probably a consequence of dose variations, or/and specificity issues since these drugs lack an overall specificity for GABA-A subunits. Nonetheless, it is consensual that GABAergic modulation is directly related to alpha oscillations. As discussed before, we hypothesise that NF1 children present enhanced inhibitory neurotransmission due to the excessive GABA levels, triggered by an up regulation of Ras (for more details see "1.1. Cognitive deficits in Neurofibromatosis type-1"). Since our study showed that NF1 individuals have higher alpha amplitude, our results are compatible with abnormal GABAergic transmission that might be responsible for the impairment of the visual processing and the cognitive deficits related to NF1.

- ***NF1 children have lower performances in the visuo-motor task, unrelated to motor deficits***

Higher amplitude of alpha rhythm has been associated to an idling of visual cortical areas, being attenuated by attention, particularly visual attention (Niedermeyer and Lopes da Silva, 1999). The JLO test examines visuospatial abilities, working memory, visuo-attentional and visuo-motor skills. NF1 children have lower performance in JLO test (Hachon et al., 2010). Therefore, it is possible that higher alpha levels be related to participant's performance.

In our study, the visuo-motor task involved detection of luminance changes in the central fixation square. The participants were asked to press one of two buttons depending if luminance increases or decreases. NF1 children revealed a problem detecting luminance changes and remembering which button to press suggesting visuo-motor attentional deficits and learning or memory difficulties.

Previous studies on motor abilities have shown that 20 to 30% of the NF1 children have impairments in fine motor coordination and lower motor speed, specific to motor function and independent of cognitive functioning (Hachon et al., 2010). The NF1s had more difficulty in detecting the change of luminance of the fixation square, but, in correct responses, had similar velocity of response. Therefore we think that the basis of NF1 lower performance, in our task, was not due to slow motor skills. Rather, they may fail more to answer due to problems in detecting visual stimulus.

- ***The amplitudes of the evoked responses is higher for NF1 children than controls, possibly due to alpha phase-reset***

The morphology of our VEPs were in agreement to previous reports (Boon et al., 2005). VEP studies revealed that the activation of retinocortical processing streams of the visual system is modulated by stimulus contrast. In spite of the intercellular heterogeneity, previous studies reported a similar CRF that applies to the overwhelming majority of neurons. As contrast increases from zero, nearly all neurons in early visual cortex increase their activity monotonically with contrast: the response increases in an accelerating fashion, remains dynamic over some limited range of contrasts, and then saturates (Albrecht et al., 2002;Ress and Heeger, 2003). In our study, we observed an evoked response modulated by the contrast level, for all pathways analysed. The contrast-response functions elicited by stimulation of each retino-cortical pathway are consistent to previous studies. As expected, there was a general and gradual increase of the amplitude of the evoked potentials with the contrast for both groups of participants that started to saturate at a certain contrast level. In fact, the shapes of the CRFs for the three pathways are in agreement with the previous studies, with CRFs expansive at low contrasts and compressive at high contrasts. This behaviour can be explained by a facilitation mechanism at low contrasts and masking mechanism at high contrasts (Boynton et al., 1999).

Several studies point to inhibitory neurotransmission playing an important role in visual perception. There are evidences of excessive inhibition in NF1 individuals (Cui et al., 2008;Staley and Anderson, 2009). Since the balance between the excitatory and inhibitory signals regulates the nervous impulse in response to a stimuli, our initial hypothesis was that the evoked potentials elicited by visual stimulation on the NF1 children would have lower amplitude in relation to the CNTs. Instead, our data revealed higher amplitudes for NF1, and especially significant in chromatic stimulation. Recently, it has been discussed and promoted a new theory – *the phase-reset theory* – that postulates that phase resetting of oscillations is a process actively involved in the generation of the VEP. Based on this theory, the higher amplitudes seen in NF1 children might be due to the alpha phase resetting when a stimulus is presented.

- ***Higher amplitudes observed for NF1 children might be due to a phase resetting of ongoing alpha prior the visual stimulation***

The most common method employed to measure brain's visual event-related electrical activity is the VEP. However, the basis of the VEPs is still controversial and has been an issue of discussion due to the gap between electrophysiological observations and the underlying neurophysiological processes. Contrary to the typical impression that stimulus-evoked activity arises

from a static, flat activity baseline, VEP is typically much smaller in magnitude than the ongoing spontaneous EEG signal (Makeig et al., 2004a;Risner et al., 2009). Scalp VEPs are derived by averaging a large number of responses time-locked to the stimulus presentation following a partial synchronization of neuronal potentials. The standard theory postulates that VEP is a phenomenon independent of the ongoing EEG activity. Nevertheless, some authors state that the VEPs are generated by one of two theories. One describes VEP as a linear summation of ongoing and evoked activity (evoked or additive theory). The other postulates that VEP is generated by alpha rhythm phase resetting (oscillatory or phase-reset theory) (Min et al., 2007;Becker et al., 2008). Many studies support the VEP as a consequence of phase resetting of the spontaneous alpha rhythm over an additive process (Hanslmayr et al., 2007;Klimesch et al., 2007;Hanslmayr et al., 2007). The alpha phase resetting theory consists on the unbalance of the phase distribution of the ongoing EEG rhythms (namely the alpha) following event/stimuli. Prior the stimulation, the EEG phase has a uniform distribution. A "*simple addition of an ERP of fixed polarity and phase to each trial*", or "*a transient perturbation of the phase of synchronized local field activity within cortical EEG source areas*", creates an imbalance (Makeig et al., 2004a). Therefore, the stimulation unbalances the phase distribution to one unique value. Therefore the signal becomes completely 'phase-locked' to the event (Hanslmayr et al., 2007;Makeig et al., 2004b).

Inspecting the parvo- and koniocellular grand averages VEPs for both groups, the evoked response seems to be superposed by an oscillatory response nearly at 10 Hz. This superimposition is more pronounced in koniocellular stimulation, and more accentuated on NF1 group. The alpha rhythm was defined in the frequency range of 8 to 12 Hz. Furthermore, we observed the higher levels of alpha on the NF1 group. We also performed the Spearman correlation test between the mean alpha amplitude and the peak amplitude measurements for parvo- and koniocellular pathways. The test revealed a significant correlation between evoked alpha and the VEP amplitudes, further corroborating our hypothesis.

Together, these results suggest that it is possible that the higher amplitudes observed for NF1 VEPs to be a consequence of the higher levels of the ongoing alpha rather than a higher neuronal firing rate elicited by the visual stimulus.

- ***Parvocellular stream cells show different maturation in relation to koniocellular stream cells***

Since it is known that chromatic sensitivity develops during childhood peaking around adolescence (Boon et al., 2007), we were curious to see how the amplitudes of the VEPs behaved with the age of our participants. Previous studies show a decrease of the evoked potentials with age (Crognale, 2002). For the koniocellular stimulation the peak amplitudes of the VEPs didn't correlate with age. For the parvocellular response, we see a negative correlation with peak amplitudes. Indeed there's a correlation of age with P2-N1, stronger for NF1 group. Since we suggested that alpha phase reset is involved on the VEP generation, we analyzed the correlations between alpha mean amplitude and the age of the participants. Supporting the theory of phase resetting, we obtained similar results. There's a significant negative correlation between alpha amplitude and age but only for parvocellular measures, stronger for NF1 children. Altogether we may assume a distinct maturation of the konio- over the parvocellular pathway. Therefore, the higher evoked potentials in NF1 might be associated to a developmental delay .

We also analyzed the changes of magnocellular VEPs mean amplitudes with age. Previous studies reported that this pathway reaches highly stability after about 2-3 months an appears adult-like by 1 year of age (Crognale, 2002). So, we didn't expect any correlation. However, we the analysis showed a correlation for CNTs, suggesting an additional maturation step for this pathway.

- ***The velocity of transmission of the visual information is similar for NF1 and control children***

The latency of the VEPs determines the retinocortical time, i.e., the transit time between the activation of retinocortical structures and the arrival of the signal in the visual cortex, expressed in milliseconds. Therefore, the latency of VEPs reflects the functioning of the optic nerve (Celesia and Kaufman, 1985;Wright and Spiegel, 2003). There's no significant difference between CNT and NF1 children. In addition to the EEG recording, the participants were subjected to ophthalmologic tests including the measure of visual acuity which didn't reveal any evidence of visual deficits related to optic gliomas. Furthermore, it was also performed a MRI (Magnetic Resonance Imaging) test to all NF1s. The MRI results didn't show the presence of optic gliomas. Therefore, as expected, the optic nerve conduction integrity is not compromised.

6. SUMMARY / CONCLUSIONS

The confirmation that a disease mechanism identified in the animal model of NF1, excessive GABAergic neurotransmission, is valid for the human disease and therefore adequate to therapeutic intervention will, in my opinion, have a strong impact in the clinical community because it will open the doors to new therapeutic trials. Consequently, the drug and treatment development will become facilitated allowing the improvement of the quality of life of these patients.

EEG recordings of NF1 children presented visually evoked brain oscillations with significantly higher amplitude than controls over the posterior side of the brain, and with an increase of VEP amplitude with contrast level for both groups. NF1 children showed particularly higher amplitudes in the alpha frequency band, as revealed by a statistically significant effect group for all the three visual streams. Alpha rhythm (8-13 Hz) has been related to conditions of physical relaxation and relatively mental inactivity. Therefore, abnormally high alpha amplitude might indicate problems with cortical engagement in visual processing. Furthermore, as GABAergic transmission plays a very important role in the generation of brain oscillations, these results are consistent with abnormally high levels of GABAergic neurotransmission in the NF1 brain. So, this results suggest that as in the animal model NF1 individuals might present enhancement in inhibition that could be associated to the deficits in synaptic plasticity that possibly underlie the learning disabilities related with neurofibromatosis 1.

7. REPERCUSSIONS

Verifying that the disease mechanism identified in the animal model of NF1, excessive GABAergic neurotransmission, is valid for the human disease and therefore adequate to therapeutic intervention will, in my opinion, exert big influence in the clinical community opening new doors to new therapeutic trials. Consequently, the drug and treatment development will become facilitated allowing the improvement of the quality of life of these patients.

Moreover, there are several animal models of other developmental disorders related to behavioural problems, such as Down syndrome and Autism, also associated to abnormal inhibition in the central nervous system (Tabuchi et al., 2007;Fernandez et al., 2007). So, the tests and the NF1 model study might be useful to determine physiologic abnormalities in other disorders.

8. FUTURE WORK

In our study we suggested that the phase-resetting of the ongoing alpha rhythm would be the basis of the higher amplitudes verified for NF1 children. However it is only a theory. The significant differences of evoked alpha amplitudes between groups were a very intriguing result. It would be very interesting to develop more deeply the alpha phase-reset theory as an explanatory model concerning the NF1 disorder.

I suggest performing a visual feature detection task, similar to the one used by (Hanslmayr et al., 2007). The basic idea consists in the measure of the ongoing alpha activity prior to stimulus onset, the study of the alpha phase modulation and the proof that it is a nonadditive process (to confirm the evoked model).

In addition, it would be also interesting to test a new behavioural task. The first aim of the button press task was only to keep the attention of the participants on the centre of the screen during the runs. Therefore, alternative tasks assessing behavioural performance should be considered. Allied to the alpha phase-reset model testing, in the future it would be interesting to perform a task directed to the behavioural analysis that gives additional scores that can be more adequate to correlate with the alpha variations.

9. APPENDIX

A. TCL SCRIPTS

A.1. NF1 parvocellular analysis.tcl

```
set path "C:\\Documents and Settings\\Proprietário-de-HP\\Os meus
documentos\\NF1_Otília\\NF1_EEG data\\Children\\[redacted]\\parvo"
set filename "[redacted]Parvo"

OPENFILE "$path\\$filename.cnt"
FILTER BANDPASS ZEROPHASESHIFT 0.5 12 100 12 0 0 0 N "$path\\$filename filtered.cnt"
CLOSEFILE  "$path\\$filename.cnt"

OPENFILE "$path\\$filename filtered.cnt"

CREATESORT sortname

sortname -TypeEnabled YES -TypeCriteria "1-30"
EPOCH PORT "" -100 400 N Y Y N N  "sortname" "$path\\$filename.eeg"
CLOSEFILE "$path\\$filename filtered.cnt"

#REDUCTION NUMBER OF POINTS TO POWER OF 2
OPENFILE  "$path\\$filename.eeg"
SPLINEFIT 512  "$path\\$filename 512p.eeg"
CLOSEFILE "$path\\$filename.eeg"

OPENFILE "$path\\$filename 512p.eeg"

BASECOR PRE 0 0 Y Y "$path\\$filename BLC.eeg"
CLOSEFILE  "$path\\$filename 512p.eeg"

OPENFILE "$path\\$filename BLC.eeg"

ARTREJ CRITERIA Y 0 0 N -50 50 Y Y
SAVEAS "$path\\$filename BLC AR.eeg"
CLOSEFILE  "$path\\$filename BLC.eeg"

# create averages
OPENFILE "$path\\$filename BLC AR.eeg"

set stimuli {"1,2,11,12,21,22" "3,4,13,14,23,24" "5,6,15,16,25,26" "7,8,17,18,27,28"
"9,10,19,20,29,30"}

foreach element $stimuli {
CREATESORT sortname2
sortname2 -TypeEnabled YES -TypeCriteria "$element"

AVERAGE T Y N "" 0 0 0 "sortname2" "$path\\$filename $element.avg"
}
CLOSEFILE "$path\\$filename BLC AR.eeg"
```

A.2. NF1 parvocellular peak analysis.tcl

```
set path "C:\\Documents and Settings\\Proprietário-de-HP\\Os meus
documentos\\NF1_Otília\\NF1_EEG data\\Children\\[redacted]\\parvo"
set filename "[redacted]Parvo"

set stimuli {"1,2,11,12,21,22" "3,4,13,14,23,24" "5,6,15,16,25,26" "7,8,17,18,27,28"
"9,10,19,20,29,30"}

foreach element $stimuli {

OPENFILE "$path\\$filename $element.avg"
```

```
LDR "C:\\Documents and Settings\\Proprietário-de-HP\\Os meus
documentos\\NF1_Otília\\NF1_EEG data\\LDR_files\\LDR_avgChannels.ldr" "$path\\LDR
$filename$element.avg"
CLOSEFILE "$path\\$filename $element.avg"

OPENFILE "$path\\LDR $filename$element.avg"
PEAKDETECTION_EX P1 Y 50 90 MAX N x Y Y BOTH RED {PZ P1 P2 POZ PO4 PO3 OZ O1 O2}
PEAKDETECTION_EX P2 Y 100 170 MAX N x Y Y BOTH RED {PZ P1 P2 POZ PO4 PO3 OZ O1 O2}
PEAKDETECTION_EX N1 Y 60 120 MIN N x Y Y BOTH RED {PZ P1 P2 POZ PO4 PO3 OZ O1 O2}

SAVEPEAK "$path\\LDR $filename$element.dat" -SubstituteBad "Bad Electrodes"
RESETFORPEAKDETECTION

CLOSEFILE "$path\\LDR $filename$element.avg"
}
```

A.3. NF1 parvocellular analysis spectrum LDR.tcl

```
set path "C:\\Documents and Settings\\Proprietário-de-HP\\Os meus
documentos\\NF1_Otília\\NF1_EEG data\\Children\\[redacted]\\parvo"
set filename "[redacted]Parvo"

set stimuli {"1,2,11,12,21,22" "3,4,13,14,23,24" "5,6,15,16,25,26" "7,8,17,18,27,28"
"9,10,19,20,29,30"}

foreach element $stimuli {

OPENFILE "$path\\LDR $filename$element.avg"
SPECTRUM PHASE 0 COS 10 "$path\\LDR phase $filename $element.avg"
SPECTRUM MAGNITUDE AMPLITUDE COS 10 "$path\\LDR amplitude $filename $element.avg"
CLOSEFILE "$path\\LDR $filename$element.avg"

OPENFILE "$path\\LDR phase $filename $element.avg"
EXPORTAVG "C:\\Documents and Settings\\Proprietário-de-HP\\Os meus
documentos\\NF1_Otília\\NF1_EEG
data\\Children\\PARVO\\ParvoFreqAnalysis\\LDR_freq\\LDR_phase\\LDR phase $filename
$element.dat" POINTS N Y N N Y N N
CLOSEFILE "$path\\LDR phase $filename $element.avg"

OPENFILE "$path\\LDR amplitude $filename $element.avg"
EXPORTAVG "C:\\Documents and Settings\\Proprietário-de-HP\\Os meus
documentos\\NF1_Otília\\NF1_EEG
data\\Children\\PARVO\\ParvoFreqAnalysis\\LDR_freq\\LDR_amplitude\\LDR amplitude $filename
$element.dat" POINTS N Y N N Y N N
CLOSEFILE "$path\\LDR amplitude $filename $element.avg"
}
```

A.4. NF1 koniocellular analysis.tcl

```
set path "C:\\Documents and Settings\\Proprietário-de-HP\\Os meus
documentos\\NF1_Otília\\NF1_EEG data\\Children\\[redacted]\\konio"
set filename "[redacted]Konio"

OPENFILE "$path\\$filename.cnt"
FILTER BANDPASS ZEROPHASESHIFT 0.5 12 100 12 0 0 0 N "$path\\$filename filtered.cnt"
CLOSEFILE  "$path\\$filename.cnt"

OPENFILE "$path\\$filename filtered.cnt"

CREATESORT sortname
sortname -TypeEnabled YES -TypeCriteria "1-30"
EPOCH PORT "" -100 400 N Y Y N N  "sortname" "$path\\$filename.eeg"
CLOSEFILE "$path\\$filename filtered.cnt"

#REDUCTION NUMBER OF POINTS TO POWER OF 2
OPENFILE  "$path\\$filename.eeg"
SPLINEFIT 512  "$path\\$filename 512p.eeg"
CLOSEFILE "$path\\$filename.eeg"
```

```
OPENFILE "$path\\$filename 512p.eeg"

BASECOR PRE 0 0 Y Y "$path\\$filename BLC.eeg"
CLOSEFILE  "$path\\$filename 512p.eeg"

OPENFILE "$path\\$filename BLC.eeg"

ARTREJ CRITERIA Y 0 0 N -50 50 Y Y
SAVEAS "$path\\$filename BLC AR.eeg"
CLOSEFILE  "$path\\$filename BLC.eeg"

# create averages
OPENFILE "$path\\$filename BLC AR.eeg"

set stimuli {"1,2,11,12,21,22" "3,4,13,14,23,24" "5,6,15,16,25,26" "7,8,17,18,27,28"
"9,10,19,20,29,30"}

foreach element $stimuli {
CREATESORT sortname2
sortname2 -TypeEnabled YES -TypeCriteria "$element"

AVERAGE T Y N "" 0 0 0 "sortname2" "$path\\$filename $element.avg"
}
CLOSEFILE "$path\\$filename BLC AR.eeg"
```

A.5. NF1 koniocellular peak analysis.tcl

```
set path "C:\\Documents and Settings\\Proprietário-de-HP\\Os meus
documentos\\NF1_Otília\\NF1_EEG data\\Children\\[redacted]\\konio"
set filename "[redacted]Konio"

set stimuli {"1,2,11,12,21,22" "3,4,13,14,23,24" "5,6,15,16,25,26" "7,8,17,18,27,28"
"9,10,19,20,29,30"}

foreach element $stimuli {

OPENFILE "$path\\$filename $element.avg"
LDR "C:\\Documents and Settings\\Proprietário-de-HP\\Os meus
documentos\\NF1_Otília\\NF1_EEG data\\LDR_files\\LDR_avgChannels.ldr" "$path\\LDR
$filename$element.avg"
CLOSEFILE "$path\\$filename $element.avg"

OPENFILE "$path\\LDR $filename$element.avg"
PEAKDETECTION_EX P1 Y 70 110 MAX N x Y Y BOTH RED {PZ P1 P2 POZ PO4 PO3 OZ O1 O2}
PEAKDETECTION_EX P2 Y 130 200 MAX N x Y Y BOTH RED {PZ P1 P2 POZ PO4 PO3 OZ O1 O2}
PEAKDETECTION_EX N1 Y 100 150 MIN N x Y Y BOTH RED {PZ P1 P2 POZ PO4 PO3 OZ O1 O2}

SAVEPEAK "$path\\LDR $filename$element.dat" -SubstituteBad "Bad Electrodes"
RESETFORPEAKDETECTION
CLOSEFILE "$path\\LDR $filename$element.avg"
}
```

A.6. NF1 koniocellular analysis spectrum LDR.tcl

```
set path "C:\\Documents and Settings\\Proprietário-de-HP\\Os meus
documentos\\NF1_Otília\\NF1_EEG data\\Children\\[redacted]\\konio"
set filename "[redacted]Konio"

set stimuli {"1,2,11,12,21,22" "3,4,13,14,23,24" "5,6,15,16,25,26" "7,8,17,18,27,28"
"9,10,19,20,29,30"}

foreach element $stimuli {

OPENFILE "$path\\LDR $filename$element.avg"
SPECTRUM PHASE 0 COS 10 "$path\\LDR phase $filename $element.avg"
SPECTRUM MAGNITUDE AMPLITUDE COS 10 "$path\\LDR amplitude $filename $element.avg"
CLOSEFILE "$path\\LDR $filename$element.avg"

OPENFILE "$path\\LDR phase $filename $element.avg"
EXPORTAVG "C:\\Documents and Settings\\Proprietário-de-HP\\Os meus
documentos\\NF1_Otília\\NF1_EEG
data\\Children\\KONIO\\KonioFreqAnalysis\\LDR_freq\\phase\\LDR phase $filename
$element.dat" POINTS N Y N N Y N N
```

```
CLOSEFILE "$path\\LDR phase $filename $element.avg"

OPENFILE "$path\\LDR amplitude $filename $element.avg"
EXPORTAVG "C:\\Documents and Settings\\Proprietário-de-HP\\Os meus
documentos\\NF1_Otília\\NF1_EEG
data\\Children\\KONIO\\KonioFreqAnalysis\\LDR_freq\\amplitude\\LDR amplitude $filename
$element.dat" POINTS N Y N N Y N N
CLOSEFILE "$path\\LDR amplitude $filename $element.avg"
}
```

A.7. NF1 magnocellular analysis filter100.tcl

```
set path "C:\\Documents and Settings\\Proprietário-de-HP\\Os meus
documentos\\NF1_Otília\\NF1_EEG data\\Children\\[redacted]\\magno"
set filename "[redacted]Magno"

OPENFILE "$path\\$filename.cnt"
FILTER BANDPASS ZEROPHASESHIFT 1 12 100 12 0 0 0 N "$path\\$filename filtered.cnt"
CLOSEFILE "$path\\$filename.cnt"

OPENFILE "$path\\$filename filtered.cnt"
CREATESORT allstimuli
allstimuli -TypeEnabled YES -TypeCriteria "1, 3, 5, 7, 9, 11, 13, 15, 17, 19, 21, 23, 25,
27, 29"
EPOCH PORT "" 0 200 N Y Y N N "allstimuli" "$path\\$filename filtered.eeg"
CLOSEFILE "$path\\$filename filtered.cnt"

#REDUCTION NUMBER OF POINTS TO POWER OF 2
OPENFILE "$path\\$filename filtered.eeg"
SPLINEFIT 256  "$path\\$filename filtered 256P.eeg"
CLOSEFILE "$path\\$filename filtered.eeg"

OPENFILE "$path\\$filename filtered 256P.eeg"
BASECOR E 0 0 N N "$path\\$filename filtered BLC.eeg"
CLOSEFILE "$path\\$filename filtered 256P.eeg"
OPENFILE  "$path\\$filename filtered BLC.eeg"
SETCHANATTRIBUTE "All" -Art Y
ARTREJ CRITERIA Y 0 0 N -50 50 Y Y
SAVEAS "$path\\$filename filtered BLC AR.eeg"
CLOSEFILE "$path\\$filename filtered BLC.eeg"

#CREATE AVERAGES
OPENFILE "$path\\$filename filtered BLC AR.eeg"

set oddnumbers {"1,11,21" "3,13,23" "5,15,25" "7,17,27" "9,19,29"}
foreach element "$oddnumbers" {
CREATESORT oddstim
oddstim -TypeEnabled YES -TypeCriteria "$element"
AVERAGE T Y N "" 0 0 0 "oddstim" "$path\\$filename $element.avg"
}
CLOSEFILE "$path\\$filename filtered BLC AR.eeg"
```

A.8. NF1 magnocellular analysis area report.tcl

```
set path "C:\\Documents and Settings\\Proprietário-de-HP\\Os meus
documentos\\NF1_Otília\\NF1_EEG data\\Children\\[redacted]\\magno"
set filename "[redacted]Magno"

set oddnumbers {"1,11,21" "3,13,23" "5,15,25" "7,17,27" "9,19,29"}
foreach element "$oddnumbers" {

OPENFILE "$path\\$filename $element.avg"
LDR "C:\\Documents and Settings\\Proprietário-de-HP\\Os meus
documentos\\NF1_Otília\\NF1_EEG data\\LDR_files\\LDR_avgChannels.ldr" "$path\\LDR
$filename$element.avg"
CLOSEFILE "$path\\$filename $element.avg"

OPENFILE "$path\\LDR $filename$element.avg"
EXTRACT {P1 PZ P2 PO3 POZ PO4 O1 OZ O2} "C:\\Documents and Settings\\Proprietário-de-HP\\Os
meus documentos\\NF1_Otília\\NF1_EEG data\\Children\\MAGNO\\LDR_eeg\\LDR $filename occ
$element.eeg"
CLOSEFILE "$path\\LDR $filename$element.avg"
```

```
OPENFILE "C:\\Documents and Settings\\Proprietário-de-HP\\Os meus
documentos\\NF1_Otília\\NF1_EEG data\\Children\\MAGNO\\LDR_eeg\\LDR $filename occ
$element.eeg"
AREAREPORT "C:\\Documents and Settings\\Proprietário-de-HP\\Os meus
documentos\\NF1_Otília\\NF1_EEG data\\Children\\MAGNO\\LDR\\LDR $filename $element
meanamp.dat" MEAN Y Y 0 0
CLOSEFILE "C:\\Documents and Settings\\Proprietário-de-HP\\Os meus
documentos\\NF1_Otília\\NF1_EEG data\\Children\\MAGNO\\LDR_eeg\\LDR $filename occ
$element.eeg"
}
```

A.9. NF1 magnocellular analysis spectrum LDR.tcl

```
set path "C:\\Documents and Settings\\Proprietário-de-HP\\Os meus
documentos\\NF1_Otília\\NF1_EEG data\\Children\\[redacted]\\magno"
set filename "[redacted]Magno"

set oddnumbers {"1,11,21" "3,13,23" "5,15,25" "7,17,27" "9,19,29"}

foreach element "$oddnumbers" {

OPENFILE "$path\\LDR $filename$element.avg"
SPECTRUM PHASE 0 COS 10 "$path\\LDR phase$filename $element.avg"
SPECTRUM MAGNITUDE AMPLITUDE COS 10 "$path\\LDR amplitude$filename $element.avg"
CLOSEFILE "$path\\LDR $filename$element.avg"

OPENFILE "$path\\LDR phase$filename $element.avg"
EXPORTAVG "$path\\LDR phase$filename $element.dat" POINTS N Y N N Y N N
CLOSEFILE "$path\\LDR phase$filename $element.avg"

OPENFILE "$path\\LDR amplitude$filename $element.avg"
EXPORTAVG "$path\\LDR amplitude$filename $element.dat" POINTS N Y N N Y N N
CLOSEFILE "$path\\LDR amplitude$filename $element.avg"
}
```

B. MATLAB SCRIPTS

B.1. Peak_Analysis.m

```
%%
% Peak Analysis
%
% Written by Otilia dAlmeida _ 08 Jan 2010
%
% For each contrast, the program selects the electrodes being used on the
% experiment and calculates, the mean of the mean amplitudes for each
% channel and latencies.

%% Get the data from excel
[file1, PathName] = uigetfile('*.dat','Select the mean amplitude file - CONTRAST 1');
cont1 = importdata(file1);
[file2, PathName] = uigetfile('*.dat','Select the mean amplitude file - CONTRAST 2');
cont2 = importdata(file2);
[file3, PathName] = uigetfile('*.dat','Select the mean amplitude file - CONTRAST 3');
cont3 = importdata(file3);
[file4, PathName] = uigetfile('*.dat','Select the mean amplitude file - CONTRAST 4');
cont4 = importdata(file4);
[file5, PathName] = uigetfile('*.dat','Select the mean amplitude file - CONTRAST 5');
cont5 = importdata(file5);

table.channel_peak=cont1.textdata(2:end,3:4);
dim=size(table.channel_peak);
num_channels=dim(1);
table.amplitude=zeros(num_channels,5);
table.latencies=zeros(num_channels,5);
i=1;

while (i<num_channels+1)

    table.latencies(i,1)=cont1.data(i,1);
    table.amplitude(i,1)=cont1.data(i,2);
    table.latencies(i,2)=cont2.data(i,1);
    table.amplitude(i,2)=cont2.data(i,2);
    table.latencies(i,3)=cont3.data(i,1);
    table.amplitude(i,3)=cont3.data(i,2);
    table.latencies(i,4)=cont4.data(i,1);
    table.amplitude(i,4)=cont4.data(i,2);
    table.latencies(i,5)=cont5.data(i,1);
    table.amplitude(i,5)=cont5.data(i,2);
    i=i+1;

end
```

B.2. Mean_Amplitude.m

```
%%
% Mean Amplitudes Analysis
%
% Written by Otilia dAlmeida _ 08 Jan 2010
%
% For each contrast, the program selects the 9 electrodes being used on the
% experiment and calculates the mean of the mean amplitudes for each
% channel.


%% Get the data from excel
[file1, PathName] = uigetfile('*.dat','Select the mean amplitude file - CONTRAST 1');
cont1 = importdata(file1);
[file2, PathName] = uigetfile('*.dat','Select the mean amplitude file - CONTRAST 2');
cont2 = importdata(file2);
[file3, PathName] = uigetfile('*.dat','Select the mean amplitude file - CONTRAST 3');
cont3 = importdata(file3);
[file4, PathName] = uigetfile('*.dat','Select the mean amplitude file - CONTRAST 4');
cont4 = importdata(file4);
[file5, PathName] = uigetfile('*.dat','Select the mean amplitude file - CONTRAST 5');
cont5 = importdata(file5);
```

```
table.channel=cont1.textdata(2:10,2);
table.values=zeros(9,5);
i=1;

while (i<10)

    table.values(i,1)=cont1.data(i,1);
    table.values(i,2)=cont2.data(i,1);
    table.values(i,3)=cont3.data(i,1);
    table.values(i,4)=cont4.data(i,1);
    table.values(i,5)=cont5.data(i,1);
    i=i+1;

end
```

B.3. Behaviour Analysis.m

```
%%
% Behavioural Outputs (STIM) Analysis

% Written by Otilia dAlmeida
% BehaviourMagno.m adaptation

% Modified 31 March 2010
% Modified 21 April 2010


%% Get the data from excel
[FileName, PathName] = uigetfile('*.xls','Select xls-output behaviour file');
file = xlsread(FileName);
dim=size(file);


%% Response stimulus line
sl=[];                                  % records response stimulus lines
i =1;
while i<=dim(1)
    if (file(i,2)>10 && file(i,2)<31)
        sl=[sl,i];
        j=5;                            % j=5 (konio, parvo); j=15 (magno)
    else
        j=1;
    end
    i=i+j;
end
sl=[sl,dim(1)];

%% Variables definition
repeated=0;
noans=0;
wnum=0;
correct=0;
right_lat=[];
wrong_lat=[];

%%
p=1;
while p<size(sl,2)
        l=sl(p);
    while l<sl(p+1)

         l=l+1;
        if (file(l,3)==8 || file(l,3)==1)
            if (file(l,6)-file(sl(p),6)>=0.150 && file(l,6)-file(sl(p),6)<3)
                if (((file(sl(p),2) > 10 && file(sl(p),2) < 21) && file(l,3)==8) || ((
file(sl(p),2)>21 && file(sl(p),2)<=30) && file(l,3)==1))
                    correct=correct+1;
                    right_lat=[right_lat,file(l,6)-file(sl(p),6)];
                    l=sl(p+1);
                elseif (((file(sl(p),2) > 10 && file(sl(p),2) < 21) && file(l,3)==1) || ((
file(sl(p),2)>21 && file(sl(p),2)<=30) && file(l,3)==8))
                    wnum=wnum+1;
                    wrong_lat=[wrong_lat,file(l,6)-file(sl(p),6)];
                    l=sl(p+1);
```

```
                end
            end
        end
    end
p=p+1;
end

noans=(p-1)-(correct+wnum);
pcorrect=(correct/(p-1))*100;
pwnum=(wnum/(p-1))*100;
pnoans=(noans/(p-1))*100;

%%
Statistics = struct('File',FileName, 'correct_perc', pcorrect ,'correct_responses',
correct, 'wrong_perc', pwnum,'wrong_number', wnum,...
    'no_ans_perc', pnoans, 'no_answer', noans)

Mean_RT = struct('right_ans',mean(right_lat),'wrong_ans',mean(wrong_lat))
```

C. EEG CAP

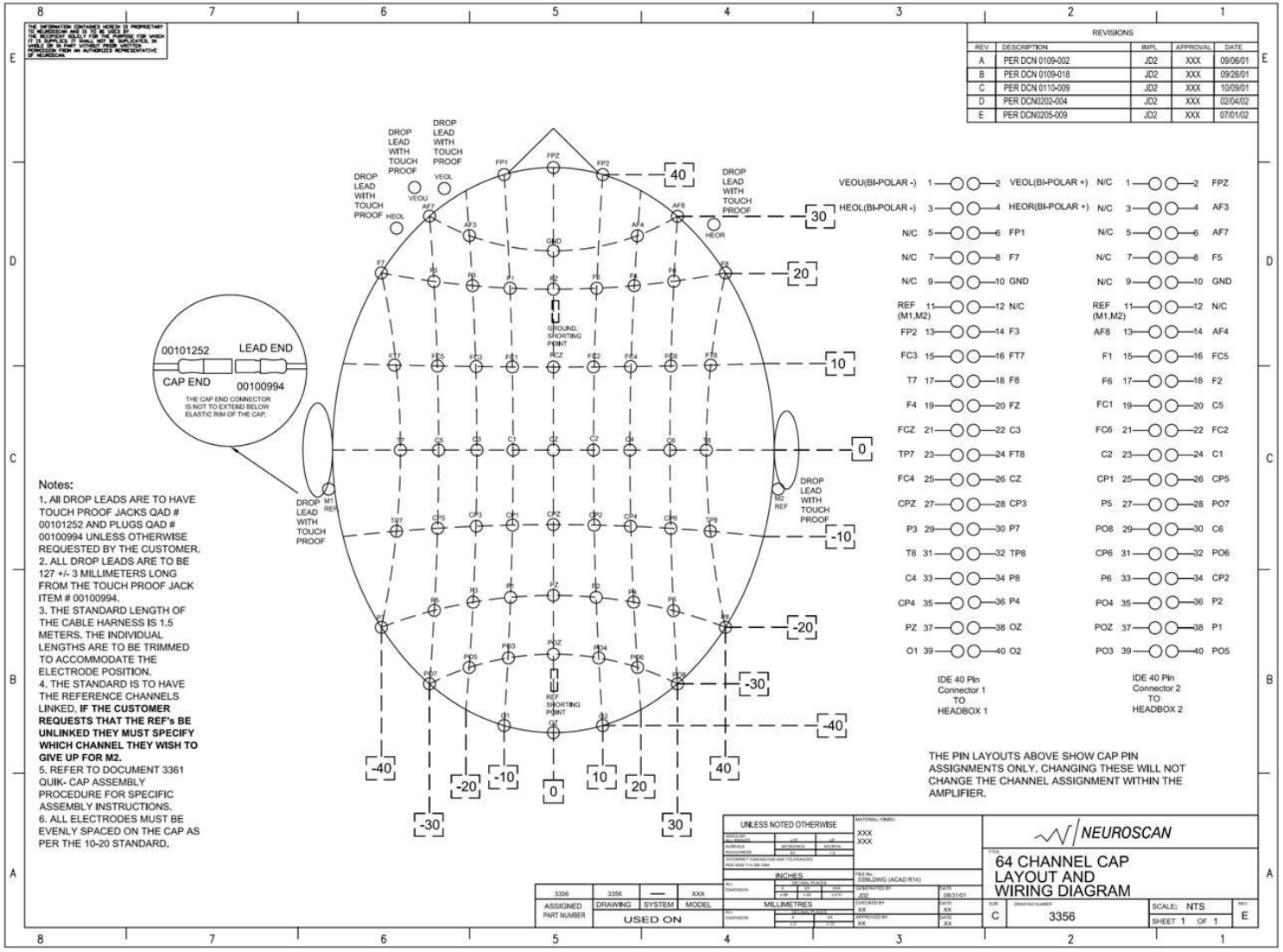

FIGURE 34. 64-Channel Quik-Cap layout and wiring diagram by NeuroScan, USA.

D. STATISTICAL CORRELATIONS BETWEEN SEVERAL PARAMETERS FOR PARVOCELLULAR AND KONIOCELLULAR STIMULATION

D.1. PARVOCELLULAR DATA CORRELATIONS

TABLE 21. *Spearman's rho coefficient* and *p-value* for correlations of Parvocellular parameter means analyzed for the Control group (17 subjects).

Group = Control (N=17)		P1 Mean Amplitude	N1 Mean Amplitude	P2 Mean Amplitude	P1-N1 Mean Amplitude	P2-N1 Mean Amplitude	Delta Mean Amplitude	Theta Mean Amplitude	Alpha Mean Amplitude	Beta Mean Amplitude	Low Gamma Mean Amplitude	%Mean Correct Answers	%Mean No Answers	Age
Spearman's rho														
P1 Mean Amplitude	*Cc*	1,000	,108	,301	**,510***	,208	,397	,360	,316	**,564***	,279	,186	-,326	**-,493***
	Sig. (2-tailed)	.	,680	,240	**,037**	,422	,115	,155	,216	**,018**	,277	,474	,202	**,045**
N1 Mean Amplitude	*Cc*		1,000	-,017	**-,755****	-,358	,118	-,105	-,331	**-,505***	-,419	,181	-,248	-,199
	Sig. (2-tailed)		.	,948	**,000**	,158	,653	,687	,195	**,039**	,094	,486	,338	,445
P2 Mean Amplitude	*Cc*			1,000	,321	**,912****	**,801****	**,836****	**,797****	**,623****	,412	,049	-,115	**-,578***
	Sig. (2-tailed)			.	,209	**,000**	**,000**	**,000**	**,000**	**,008**	,101	,852	,660	**,015**
P1-N1 Mean Amplitude	*Cc*				1,000	**,527***	,140	,331	**,556***	**,843****	**,583***	-,093	,039	-,123
	Sig. (2-tailed)				.	**,030**	,593	,195	**,020**	**,000**	**,014**	,722	,881	,639
P2-N1 Mean Amplitude	*Cc*					1,000	**,721****	**,833****	**,873****	**,696****	**,547***	-,012	-,022	**-,490***
	Sig. (2-tailed)					.	**,001**	**,000**	**,000**	**,002**	**,023**	,963	,933	**,046**
Delta Mean Amplitude	*Cc*						1,000	**,875****	**,743****	,395	,294	,113	-,162	**-,699****
	Sig. (2-tailed)						.	**,000**	**,001**	,117	,252	,667	,535	**,002**
Theta Mean Amplitude	*Cc*							1,000	**,828****	**,493***	,453	,179	-,216	**-,767****
	Sig. (2-tailed)							.	**,000**	**,045**	,068	,492	,406	**,000**
Alpha Mean Amplitude	*Cc*								1,000	**,679****	**,623****	-,054	-,025	**-,512***
	Sig. (2-tailed)								.	**,003**	**,008**	,837	,926	**,036**
Beta Mean Amplitude	*Cc*									1,000	**,699****	,069	-,150	-,272
	Sig. (2-tailed)									.	**,002**	,794	,567	,291
Low Gamma Mean Amplitude	*Cc*										1,000	,419	-,466	-,176
	Sig. (2-tailed)										.	,094	,060	,498
%Mean Correct Answers	*Cc*											1,000	**-,951****	-,047
	Sig. (2-tailed)											.	**,000**	,859
%Mean No Answers	*Cc*												1,000	,174
	Sig. (2-tailed)												.	,504
Age	*Cc*													1,000
	Sig. (2-tailed)													.

**. Correlation is significant at the 0.05 level (2-tailed).*

***. Correlation is significant at the 0.01 level (2-tailed).*

Cc = Correlation coefficient

TABLE 22. *Spearman's rho coefficient* and *p-value* for correlations of Parvocellular parameter means for the NF1 group (17 subjects).

	Group = NF1 (N=17)		P1 Mean Amplitude	N1 Mean Amplitude	P2 Mean Amplitude	P1-N1 Mean Amplitude	P2-N1 Mean Amplitude	Delta Mean Amplitude	Theta Mean Amplitude	Alpha Mean Amplitude	Beta Mean Amplitude	Low Gamma Mean Amplitude	%Mean Correct Answers	%Mean No Answers	Age
Spearman's rho	P1 Mean Amplitude	*Cc*	1,000	-,071	,350	**,637****	,299	,375	,255	,473	**,517***	,304	-,407	,262	-,135
		Sig. (2-tailed)	.	,786	,168	**,006**	,244	,138	,323	,055	**,034**	,236	,105	,309	,606
	N1 Mean Amplitude	*Cc*		1,000	-,279	**-,708****	**-,713****	-,414	-,466	**-,495***	**-,578***	**-,703****	**,588***	-,109	,239
		Sig. (2-tailed)		.	,277	**,001**	**,001**	,098	,060	**,043**	**,015**	**,002**	**,013**	,677	,355
	P2 Mean Amplitude	*Cc*			1,000	,458	**,821****	**,623****	**,723****	**,846****	**,775****	**,390**	-,120	-,186	-,458
		Sig. (2-tailed)			.	,064	**,000**	**,008**	**,001**	**,000**	**,000**	**,122**	,646	,474	,065
	P1-N1 Mean Amplitude	*Cc*				1,000	**,733****	**,625****	**,512***	**,657****	**,775****	**,806****	**-,608****	,137	-,220
		Sig. (2-tailed)				.	**,001**	**,007**	**,036**	**,004**	**,000**	**,000**	**,010**	,599	,397
	P2-N1 Mean Amplitude	*Cc*					1,000	**,689****	**,762****	**,885****	**,843****	**,716****	-,400	-,096	**-,529***
		Sig. (2-tailed)					.	**,002**	**,000**	**,000**	**,000**	**,001**	,112	,715	**,029**
	Delta Mean Amplitude	*Cc*						1,000	**,890****	**,600***	**,740****	**,669****	-,118	-,300	-,294
		Sig. (2-tailed)						.	**,000**	**,011**	**,001**	**,003**	,653	,241	,251
	Theta Mean Amplitude	*Cc*							1,000	**,689****	**,721****	**,578***	-,123	-,292	-,279
		Sig. (2-tailed)							.	**,002**	**,001**	**,015**	,639	,256	,279
	Alpha Mean Amplitude	*Cc*								1,000	**,804****	**,551***	**-,483***	,112	**-,654****
		Sig. (2-tailed)								.	**,000**	**,022**	**,050**	,670	**,004**
	Beta Mean Amplitude	*Cc*									1,000	**,757****	-,373	-,066	-,454
		Sig. (2-tailed)									.	**,000**	,141	,801	,067
	Low Gamma Mean Amplitude	*Cc*										1,000	**-,527***	,118	-,317
		Sig. (2-tailed)										.	**,030**	,653	,216
	%Mean Correct Answers	*Cc*											1,000	**-,730****	,458
		Sig. (2-tailed)											.	**,001**	,065
	%Mean No Answers	*Cc*												1,000	-,249
		Sig. (2-tailed)												.	,335
	Age	*Cc*													1,000
		Sig. (2-tailed)													.

**. Correlation is significant at the 0.05 level (2-tailed).*

***. Correlation is significant at the 0.01 level (2-tailed).*

Cc = Correlation coefficient

D.2. KONIOCELLULAR DATA CORRELATIONS

TABLE 23. *Spearman's rho coefficient* and *p-value* for correlations of Koniocellular parameter means analyzed for the Control group (17 subjects).

Group = Control (N=17)		P1 Mean Amplitude	N1 Mean Amplitude	P2 Mean Amplitude	P1-N1 Mean Amplitude	P2-N1 Mean Amplitude	Delta Mean Amplitude	Theta Mean Amplitude	Alpha Mean Amplitude	Beta Mean Amplitude	Low Gamma Mean Amplitude	%Mean Correct Answers	%Mean No Answers	Age
Spearman's rho	**P1 Mean Amplitude**	*Cc*	1,000	,208	**,539***	,444	,333	,299	,248	,125	,451	,174	,025	-,104	-,137
		Sig. (2-tailed)	.	,422	**,026**	,074	,191	,244	,338	,633	,069	,504	,926	,691	,599
	N1 Mean Amplitude	*Cc*		1,000	-,147	**-,748****	**-,549***	,368	-,037	-,426	-,417	-,407	,103	-,105	-,267
		Sig. (2-tailed)		.	,573	**,001**	**,022**	,147	,889	,088	,096	,105	,694	,687	,300
	P2 Mean Amplitude	*Cc*			1,000	,463	**,858****	**,571***	**,745****	**,775****	**,824****	**,581***	,118	-,201	-,272
		Sig. (2-tailed)			.	,061	**,000**	**,017**	**,001**	**,000**	**,000**	**,014**	,653	,439	,291
	P1-N1 Mean Amplitude	*Cc*				1,000	**,723****	-,118	,196	,475	**,681****	,461	-,074	,033	,025
		Sig. (2-tailed)				.	**,001**	,653	,451	,054	**,003**	,063	,779	,900	,926
	P2-N1 Mean Amplitude	*Cc*					1,000	,426	**,711****	**,892****	**,853****	**,652****	,142	-,213	-,257
		Sig. (2-tailed)					.	,088	**,001**	**,000**	**,000**	**,005**	,586	,411	,319
	Delta Mean Amplitude	*Cc*						1,000	**,821****	**,598***	,363	,260	,277	-,309	**-,610****
		Sig. (2-tailed)						.	**,000**	**,011**	,152	,314	,282	,227	**,009**
	Theta Mean Amplitude	*Cc*							1,000	**,799****	**,605***	**,591***	,203	-,240	**-,669****
		Sig. (2-tailed)							.	**,000**	**,010**	**,013**	,434	,353	**,003**
	Alpha Mean Amplitude	*Cc*								1,000	**,721****	**,605***	,233	-,278	-,341
		Sig. (2-tailed)								.	**,001**	**,010**	,368	,279	,181
	Beta Mean Amplitude	*Cc*									1,000	**,752****	,225	-,251	-,189
		Sig. (2-tailed)									.	**,000**	,384	,330	,468
	Low Gamma Mean Amplitude	*Cc*										1,000	**,493***	-,464	-,208
		Sig. (2-tailed)										.	**,045**	,061	,422
	%Mean Correct Answers	*Cc*											1,000	**-,976****	-,157
		Sig. (2-tailed)											.	**,000**	,548
	%Mean No Answers	*Cc*												1,000	,136
		Sig. (2-tailed)												.	,602
	Age	*Cc*													1,000
		Sig. (2-tailed)													.

**. Correlation is significant at the 0.05 level (2-tailed).*

***. Correlation is significant at the 0.01 level (2-tailed).*

Cc = Correlation coefficient

TABLE 24. *Spearman's rho coefficient* and *p-value* for correlations of Koniocellular parameter means analyzed for the NF1 group (17 subjects).

Group = NF1 (N=17)		P1 Mean Amplitude	N1 Mean Amplitude	P2 Mean Amplitude	P1-N1 Mean Amplitude	P2-N1 Mean Amplitude	Delta Mean Amplitude	Theta Mean Amplitude	Alpha Mean Amplitude	Beta Mean Amplitude	Low Gamma Mean Amplitude	%Mean Correct Answers	%Mean No Answers	Age
Spearman's rho														
P1 Mean Amplitude	*Cc*	1,000	**-,534***	,449	**,755****	**,537***	**,559***	,240	**,576***	**,605***	**,522***	,034	-,269	-,358
	Sig. (2-tailed)	.	**,027**	,071	**,000**	**,026**	**,020**	,353	**,016**	**,010**	**,032**	,896	,297	,158
N1 Mean Amplitude	*Cc*		1,000	**-,532***	**-,919****	**-,850****	**-,583***	-,414	**-,591***	**-,740****	**-,544***	,115	,153	-,048
	Sig. (2-tailed)		.	**,028**	**,000**	**,000**	**,014**	,098	**,013**	**,001**	**,024**	,660	,557	,855
P2 Mean Amplitude	*Cc*			1,000	**,569***	**,858****	**,551***	**,723****	**,819****	**,647****	,272	,115	-,224	-,314
	Sig. (2-tailed)			.	**,017**	**,000**	**,022**	**,001**	**,000**	**,005**	,291	,660	,387	,220
P1-N1 Mean Amplitude	*Cc*				1,000	**,828****	**,610****	,387	**,650****	**,767****	**,500***	-,118	-,168	-,013
	Sig. (2-tailed)				.	**,000**	**,009**	,125	**,005**	**,000**	**,041**	,653	,519	,959
P2-N1 Mean Amplitude	*Cc*					1,000	**,586***	**,615****	**,787****	**,779****	,436	,022	-,185	-,112
	Sig. (2-tailed)					.	**,013**	**,009**	**,000**	**,000**	,080	,933	,477	,670
Delta Mean Amplitude	*Cc*						1,000	**,755****	**,723****	**,770****	**,642****	-,206	-,202	-,475
	Sig. (2-tailed)						.	**,000**	**,001**	**,000**	**,005**	,428	,436	,054
Theta Mean Amplitude	*Cc*							1,000	**,797****	**,767****	**,517***	-,228	-,033	-,437
	Sig. (2-tailed)							.	**,000**	**,000**	**,034**	,379	,900	,080
Alpha Mean Amplitude	*Cc*								1,000	**,804****	,475	-,064	-,155	-,469
	Sig. (2-tailed)								.	**,000**	,054	,808	,554	,058
Beta Mean Amplitude	*Cc*									1,000	**,723****	-,328	,049	-,331
	Sig. (2-tailed)									.	**,001**	,198	,852	,194
Low Gamma Mean Amplitude	*Cc*										1,000	-,294	,060	-,350
	Sig. (2-tailed)										.	,252	,819	,169
%Mean Correct Answers	*Cc*											1,000	**-,841****	,296
	Sig. (2-tailed)											.	**,000**	,249
%Mean No Answers	*Cc*												1,000	-,072
	Sig. (2-tailed)												.	,784
Age	*Cc*													1,000
	Sig. (2-tailed)													.

**. Correlation is significant at the 0.05 level (2-tailed).*

***. Correlation is significant at the 0.01 level (2-tailed).*

Cc = Correlation coefficient

10. REFERENCES

Albrecht DG, Hamilton DB (1982) Striate cortex of monkey and cat: contrast response function. J Neurophysiol 48:217-237.

Albrecht DG, Geisler WS, Frazor RA, Crane AM (2002) Visual Cortex Neurons of Monkeys and Cats: Temporal Dynamics of the Contrast Response Function. J Neurophysiol 88:888-913.

Alexander AF, Andrew AF, Reetta K, Eero P, Risto JI, Seppo K (2004) The interplay of lorazepam-induced brain oscillations: microstructural electromagnetic study. pp 674-690.

American Clinical Neurophysiology Society (ACNS) (2006) Guideline 5: Guidelines for Standard Electrode Position Nomenclature. Journal of Clinical Neurophysiology 23.

Becker R, Ritter P, Villringer A (2008) Influence of ongoing alpha rhythm on the visual evoked potential. NeuroImage 39:707-716.

Blin O, Mestre D, Paut O, Vercher JL, Audebert C (1993) GABA-ergic control of visual perception in heathy volunteers: effects of midazolam, a benzodiazepine, on spatio-temporal contrast sensitivity. Br J Clin Pharmac 36:117-124.

Boon MY, Suttle CM, Dain SJ (2007) Transient VEP and psychophysical chromatic contrast thresholds in children and adults. Vision Research 47:2124-2133.

Boon MY, Suttle CM, Henry B (2005) Estimating chromatic contrast thresholds from the transient visual evoked potential. Vision Research 45:2367-2383.

Boyd KP, Korf BR, Theos A (2009) Neurofibromatosis type 1. Journal of the American Academy of Dermatology 61:1-14.

Boynton MY, Demb JB, Glover GH, Heeger DJ (1999) Neuronal basis of contrast discrimination. Vision Research 39:257-269.

Brainard DH, Pelli DG, Robson T (2002) Display characterization. (Hornak J, ed), pp 172-188. Wiley.

Brainard DH, Stockman A (2010) Colorimetry. In: OSA Handbook of Optics (Bass M, ed), pp 10.1-10.56. New York: McGraw-Hill.

Celesia GG, Kaufman D (1985) Pattern ERGs and visual evoked potentials in maculopathies and optic nerve diseases. Invest Ophthalmol Vis Sci 26:726-735.

Cichowski K, Jacks T (2001) NF1 Tumor Suppressor Gene Function: Narrowing the GAP. Cell 104:593-604.

Clements-Stephens AM, Rimrodt SL, Gaur P, Cutting LE (2008) Visuospatial processing in children with neurofibromatosis type 1. Neuropsychologia 46:690-697.

Cole GR, Hine T (1992) Computations of cone contrasts for color vision research. Behaviour Research Methods, Instruments and Computers 24:22-27.

Cole GR, Hine T, McIlhagga W (1993) Detection mechanisms in L-, M-, and S-cone contrast space. J Opt Soc Am A 10:38-51.

Costa RM, Federov NB, Kogan JH, Murphy GG, Stern J, Ohno M, Kucherlapati R, Jacks T, Silva AJ (2002) Mechanism for the learning deficits in a mouse model of neurofibromatosis type 1. Nature 415:526-530.

Costa RM, Silva AJ (2002) Review Article : Molecular and Cellular Mechanisms Underlying the Cognitive Deficits Associated With Neurofibromatosis 1. Journal of Child Neurology 17:622-626.

Crognale MA (2002) Development, maturation, and aging of chromatic visual pathways: VEP results. Journal of Vision 2.

Cui Y, Costa RM, Murphy GG, Elgersma Y, Zhu Y, Gutmann DH, Parada LF, Mody I, Silva AJ (2008) Neurofibromin Regulation of ERK Signaling Modulates GABA Release and Learning. Cell 135:549-560.

Daston MM, Scrable H, Nordlund M, Sturbaum AK, Nissen LM, Ratner N (1992) The protein product of the neurofibromatosis type 1 gene is expressed at highest abundance in neurons, Schawn cells, and oligodendrocytes. Neuron 8:415-428.

Derrington AM, Krauskopf J, Lennie P (1984) Chromatic mechanisms in lateral geniculate nucleus of macaque. The Journal of Physiology 357:241-265.

Fernandez F, Morishita W, Zuniga E, Nguyen J, Blank M, Malenka RC, Garner CC (2007) Pharmacotherapy for cognitive impairment in a mouse model of Down syndrome. Nat Neurosci 10:411-413.

Giersch A, Speeg-Schatz C, Tondre M, Gottenkiene S (2006) Impairment of contrast sensitivity in long-term lorazepam users. Psychopharmacology 186:594-600.

Hachon C, Iannuzzi S, Chaix Y (2010) Behavioural and cognitive phenotypes in children with neurofibromatosis type 1 (NF1): The link with the neurobiological level. Brain and Development In Press, Corrected Proof.

Hall SD, Barnes GR, Furlong PL, Seri S, Hillebrand A (2010) Neuronal network pharmacodynamics of GABAergic modulation in the human cortex determined using pharmaco-magnetoencephalography. Human Brain Mapping 31:581-594.

Hanslmayr S, Klimesch W, Sauseng P, Gruber W, Doppelmayr M, Freunberger R, Pecherstorfer T, Birbaumer N (2007) Alpha Phase Reset Contributes to the Generation of ERPs. Cereb Cortex 17:1-8.

Harris J, Phillipson O (1995) Effects of lorazepam on human contrast sensitivity. Psychopharmacology 117:379-384.

Hendry SHC, Reid RC (2000) The Koniocellular Pathway in Primate Vision. Annual Review of Neuroscience 23:127-153.

Ho IS, Hannan F, Guo HF, Hakker I, Zhong Y (2007) Distinct Functional Domains of Neurofibromatosis Type 1 Regulate Immediate versus Long-Term Memory Formation. J Neurosci 27:6852-6857.

Hyman SL, Shores A, North KN (2005) The nature and frequency of cognitive deficits in children with neurofibromatosis type 1. Neurology 65:1037-1044.

Kandel ER, Schwartz JH, Jessell TM (1995) Essentials of Neural Science and Behavior. McGraw-Hill Professional.

Kandel ER, Schwartz JH, Jessell TM (2000) Principles of Neural Science. New York: McGraw-Hill Medical.

Kapadia MK, Westheimer G, Gilbert CD (2000) Spatial Distribution of Contextual Interactions in Primary Visual Cortex and in Visual Perception. J Neurophysiol 84:2048-2062.

Klimesch W, Sauseng P, Hanslmayr S (2007) EEG alpha oscillations: The inhibition-timing hypothesis. Brain Research Reviews 53:63-88.

Krauskopf J, Williams DR, Heeley DW (1982) Cardinal directions of color space. Vision Research 22:1123-1231.

Kulikowski JJ, McKeefry DJ, Robson AG (1997) Selective stimulation of colour mechanisms: an empirical perspective. Spatial Vision 10:379-402.

Kumar AS (2004) Neurofibromatosis Type 1: Involvement of NF1 Mutations in Nervous System Tumours and Learning and Cognitive Dysfunction in this Disorder. Journal on Developmental Disabilities 11:41-62.

Lee BB (1996) Receptive field structure in the primate retina. Vision Research 36:631-644.

Levine TM, Materek A, Abel J, O'Donnell M, Cutting LE (2006) Cognitive Profile of Neurofibromatosis Type 1. Seminars in Pediatric Neurology 13:8-20.

Lorincz ML, Kékesi KA, Juhász G, Crunelli V, Hughes SW (2009) Temporal Framing of Thalamic Relay-Mode Firing by Phasic Inhibition during the Alpha Rhythm. Neuron 63:683-696.

Luck SJ (2004) Ten simple rules for designing ERP experiments. In: Event-Releted Potentials: A Methods Handbook (Handy TC, ed), pp 17-32. Cambridge,MA: MIT Press.

Luck SJ (2005) An Introduction to the Event-Related Potential Technique. MIT Press.

Lund JS, Angelucci A, Bressloff PC (2003) Anatomical Substrates for Functional Columns in Macaque Monkey Primary Visual Cortex. Cereb Cortex 13:15-24.

MacLeod DI, Boynton RM (1979) Chromaticity diagram showing cone excitation by stimuli of equal luminance. J Opt Soc Am 69:1183-1186.

Makeig S, Debener S, Onton J, Delorme A (2004a) Mining event-related brain dynamics. Trends in Cognitive Sciences 8:204-210.

Makeig S, Debener S, Onton J, Delorme A (2004b) Mining event-related brain dynamics. Trends in Cognitive Sciences 8:204-210.

Malmivuo J, Plonsey R (1995) Bioelectromagnetism: Principles and Applications of Bioelectric and Biomagnetic Fields. New York: Oxford University Press.

Merigan WH, Maunsell JHR (1993) How Parallel are the Primate Visual Pathways? Annual Review of Neuroscience 16:369-402.

Min BK, Busch NA, Debener S, Kranczioch C, Hanslmayr S, Engel AK, Herrmann CS (2007) The best of both worlds: Phase-reset of human EEG alpha activity and additive power contribute to ERP generation. International Journal of Psychophysiology 65:58-68.

Mitrushina MN, Boone KB, Razani J, D'Elia LF (2005) Handbook of normative data for neuropsychological assessment. New York, US: Oxford University Press.

Mullen K, Dumoulin S, McMahon K, de Zubicaray G, Hess R (2007) Selectivity of human retinotopic visual cortex to S-cone-opponent, L/M-cone-opponent and achromatic stimulation. Eur J Neurosci 25:491-502.

Niedermeyer E, Lopes da Silva FH (1999) The normal EEG of the waking adult. In: Electroencephalography: basic principles, clinical applications and related fields pp 149-173. Baltimore MD: Lippincott Williams & Wilkins.

NINDS (2010) National Institute of Neurological Disorders and Stroke - Neurofibromatosis.

Odom JV, Bach M, Brigell M, Holder G, McCulloch DL, Tormene AP, Vaegan (2010) ISCEV standard for clinical visual evoked potentials (2009 update). Documenta Ophthalmologica 120:111-119.

Ress D, Heeger DJ (2003) Neuronal correlates of perception in early visual cortex. Nat Neurosci 6:414-420.

Ribeiro MJ, Castelo-Branco M (2010) Psychophysical channels and ERP population responses in human visual cortex: Area summation across chromatic and achromatic pathways. Vision Research 50:1283-1291.

Risner ML, Aura CJ, Black JE, Gawne TJ (2009) The Visual Evoked Potential is independent of surface alpha rhythm phase. NeuroImage 45:463-469.

Robert JB, Adam RC, Stuart JJ, Christopher RB (2009) EEG differences in children between eyes-closed and eyes-open resting conditions. pp 1806-1811.

Sankeralli MJ, Mullen KT (1996) Estimation of the L-, M-, and S-cone weights of the postreceptoral detection mechanisms. J Opt Soc Am A 13:906-915.

Sankeralli MJ, Mullen KT (1997) Postreceptoral chromatic detection mechanisms revealed by noise masking in three-dimensional cone contrast space. J Opt Soc Am A 14:2633-2646.

Schrimsher GW, Billingsley RL, Slopis JM, Moore III BD (2003) Visual-spatial performance deficits in children with neurofibromatosis type-1. American Journal of Medical Genetics 120A:326-330.

Shilyansky C, Lee YS, Silva AJ (2010) Molecular and Cellular Mechanisms of Learning Disabilities: A Focus on NF1. Annual Review of Neuroscience 33:221-243.

Silva AJ, Frankland PW, Marowitz Z, Friedman E, Lazlo G, Cioffi D, Jacks T, Bourtchuladze14 R (1997) A mouse model for the learning and memory deficits associated with neurofibromatosis type I. Nat Genet 15:281-284.

Sincich LC, Park KF, Wohlgemuth MJ, Horton JC (2004) Bypassing V1: a direct geniculate input to area MT. Nat Neurosci 7:1123-1128.

Staley KJ, Anderson AE (2009) Hyperactive interneurons impair learning in a neurofibromatosis model. Nat Neurosci 12:8-10.

Stockman A, Sharpe LT (2000) The spectral sensitivities of the middle- and long-wavelength-sensitive cones derived from measurements in observers of known genotype. Vision Research 40:1711-1737.

Tabuchi K, Blundell J, Etherton MR, Hammer RE, Liu X, Powell CM, Sudhof TC (2007) A Neuroligin-3 Mutation Implicated in Autism Increases Inhibitory Synaptic Transmission in Mice. Science 318:71-76.

Taylor MJ, Baldeweg T (2002) Application of EEG, ERP and intracranial recordings to the investigation of cognitive functions in children. Developmental Science 5:318-334.

Taylor MJ, McCulloch DL (1992) Visual Evoked Potentials in Infants and Children. Journal of Clinical Neurophysiology 9.

Teplan M (2002) Fundamentals of EEG Measurement. Measurement Science Review 2:1-11.

Tobimatsu S, Tomoda H, Kato M (1995) Parvocellular and magnocellular contributions to visual evoked potentials in humans: stimulation with chromatic and achromatic gratings and apparent motion. Journal of the Neurological Sciences 134:73-82.

Vanni S, Henriksson L, Viikari M, James AC (2006) Retinotopic distribution of chromatic responses in human primary visual cortex. Eur J Neurosci 24:1821-1831.

Wandell BA, Poirson AB, Newsome WT, Baseler HA, Boynton GM, Huk A, Gandhi S, Sharpe LT (1999) Color signals in human motion-selective cortex. Neuron 24:901-909.

Whiting PJ (2006) GABA-A receptors: a viable target for novel anxiolytics? Current Opinion in Pharmacology 6:24-29.

Wright KW, Spiegel PH (2003) Pediatric ophthalmology and strabismus. Springer.

Xu X, Ichida JM, Allison JD, Boyd JD, Bonds AB, Casagrande VA (2001) A comparison of koniocellular, magnocellular and parvocellular receptive field properties in the lateral geniculate nucleus of the owl monkey (Aotus trivirgatus). The Journal of Physiology 531:203-218.

[Online source] NINDS (2010) National Institute of Neurological Disorders and Stroke - Neurofibromatosis. http://www.ninds.nih.gov/disorders/neurofibromatosis/neurofibromatosis.htm & http://www.ninds.nih.gov/disorders/neurofibromatosis/detail_neurofibromatosis.htm [Access date: 13-05-2010]

[Online source] Pinson S (2002) Neurofibromatosis type I. http://www.orpha.net/data/patho/GB/uk-NF1.pdf [Access date: 21-06-2010]

[Online source] http://www.sharp-sighted.org/ [Access date: 17-08-2010]